TARGETING OF THE CARDIAC VOLTAGE-GATED SODIUM CHANNEL 1.5 REQUIRES AN ANKYRIN-G-DEPENDENT PATHWAY

By

John Stewart Lowe

Dissertation

Submitted to the Faculty of the

Graduate School of Vanderbilt University

in partial fulfillment of the requirements

for the degree of

DOCTOR OF PHILOSOPHY

in

Pathology

December, 2008

Nashville, Tennessee

Approved:

Professor Peter J. Mohler

Professor Larry Swift

Professor Sabina Kupershmidt

Professor Richard Hoover

Professor Pampee Young

PATHOLOGY

TARGETING OF THE CARDIAC VOLTAGE-GATED SODIUM CHANNEL 1.5 REQUIRES AN ANKYRIN-G-DEPENDENT PATHWAY

JOHN STEWART LOWE

Dissertation under the direction of Professor Peter J. Mohler

The focus of this project is determining if an ankyrin-G-based pathway controls the membrane expression of the voltage-gated sodium channel 1.5 ($Na_v1.5$) in cardiomyocytes. Disruption of the normal localization of $Na_v1.5$ can lead to a fatal cardiac arrhythmia termed Brugada Syndrome and has been linked to myopathic cardiac disease.

This project defines that an ankyrin-G-based pathway controls the expression, localization, and function of $Na_v1.5$ at the cardiomyocyte plasma membrane. These studies were accomplished by developing a primary cell culture system where ankyrin-G could be reduced and selectively restored to define if $Na_v1.5$ targeting was truly dependent on a direct interaction with an ankyrin-G-based mechanism. Moreover, these studies have identified the residues on ankyrin-G necessary for the interaction of $Na_v1.5$ and ankyrin-G. Together, these findings provide critical clues in understanding the molecular mechanism of $Na_v1.5$ targeting in the cardiomyocyte and have developed exciting new tools for studying the targeting pathway.

To my lovely wife Cheryl for her incredible support and counsel in both bad and good times, and our beloved family for their motivation

ACKNOWLEDGEMENTS

This work would not have been possible without the financial support from the Vanderbilt Training Grant in Mechanisms of Vascular Disease (5T32HL007751-15) and a project specific grant titled Dysfunction in Ankyrin-based Pathways and Human Arrhythmia (5R01HL083422-03). I am especially grateful for the invaluable guidance, mentoring, and friendship from my preceptor Dr. Peter J. Mohler and my dissertation committee chairman Dr. Richard Hoover who have been guardians of my academic and research development. My training would not have been possible without the continued support of Dr. Sam Santoro, Chair of the Department of Physiology, and Dr. Larry Swift, Chair of Investigational Pathology who have provided important guidance in my research training.

My dissertation committee is made of first class scientists who are also good people. Dr. Pampee Young, Dr. Sabina Kupershmidt, and Dr. David Bader have provided advice and guidance pivotal for the success of my project and for my development as a scientist. I am honored and truly appreciative for their individual contributions to my project and my professional development. I am also very grateful to all of the amazing people that I have had the pleasure to work with in the pursuit of my project and in collaborative endeavors.

I also want to thank my mother Meriam for her wisdom, love and encouragement. I am also grateful to Ed and Charlie for their unerring support and inspiration. Finally, I would like to thank my wife Cheryl for her

understanding, support, love, and counsel throughout my pre-doctoral work for I know that I could not have made it through my training and whatever tests are to come without her.

TABLE OF CONTENTS

Page

LIST OF FIGURES

LIST OF ABBREVIATIONS

ANK ankyrin repeat

AP action potential

ARF adenosine di-phosphate ribosylation factor

Bves blood vessel epicardial substance

Ca^{2+} calcium ion (bi-valent)

hAnkG human ankyrin-G

K^+ potassium ion

rAnkG rat ankyrin-G

Na^+ sodium ion

NA numerical aperture

NHERF1 Na^+/H^+ exchange regulatory factor-1

I_{Na} sodium current

I_{CaL} L-type (Long) calcium current

I_{to} transient outward current

I_{Kr} rapid delayed-rectifier potassium current

I_{Ks} slow delayed-rectifier potassium current

shRNA short hairpin ribonucleic acid

TTX tetrodotoxin

CHAPTER I

THE ELECTRICAL BASIS OF CARDIAC FUNCTION

The human heart beats approximately two billion times during the course of an average human lifetime (Dobson, 2003). The precisely coordinated contraction and relaxation events of each heart beat are controlled by complex molecular mechanisms (Roden et al., 2002). Disruption of the rhythmic activity of the heart (arrhythmia) may result in the drop of oxygenated blood to the brain and peripheral tissues (Rubart and Zipes, 2005). In fact, half a million fatalities a year are associated with an arrhythmic event (Yu and Catterall, 2003). Therefore, understanding the mechanisms underlying potentially fatal cardiac arrhythmias is critical for the treatment and diagnosis of human disease.

Currents from ion channels and transporters combine to form the electrical signals that control cardiac rhythm. These electrical signals are called action potentials. Heart rhythm is controlled by the coordinated propagation of action potentials through specialized electrically-excitable cardiac cells and tissues (Ackerman and Clapham, 1997; Bers, 2001a; Roden et al., 2002). Chapter 1 will introduce the mechanisms governing ion channel and transporter function for action potential development. Additionally, Chapter 1 will discuss how ion channel dysfunction may result in human cardiovascular disease. Finally, this chapter will provide special emphasis on the role of voltage-gated Na^+ channels in cardiac function and disease.

Cardiac structure and action potentials

The mammalian heart has four chambers. Bilateral atria accept blood from peripheral (right atria) and pulmonary (left atria) tissues, whereas the bilateral ventricles pump blood out into the pulmonary (right) and peripheral (left) tissues (Figure 1A). This highly coordinated pumping action of the heart supplies blood to all tissues. Blood carries oxygen and nutrients to sustain the metabolic needs of all cells. The coordinated pumping activity of the heart is controlled by the transmission of action potentials between specialized cardiac cell types.

Action potentials spread through diverse cardiac cell types via tightly controlled electrical pathways (Bers, 2001; Roden et al., 2002). Specifically, the heart contains a number of specialized electrically-excitable cell types including sinoatrial node myocytes, atrial myocytes, atrioventricular node myocytes, His-Purkinje fibers, and ventricular myocytes (Figure 1) (Schram et al., 2002). Each heartbeat initiates in the sinoatrial node via an impulse fired from the rhythmic cycles of depolarization controlled by pacemaker currents (I_f) (Figure 1) (Schram et al., 2002). The initial sinoatrial node stimulus is then transmitted to the atria. Atrial myocytes subsequently trigger action potentials that spread throughout the atria, which pause briefly in the atrioventricular node (Figure 1A) (Schram et al., 2002). During this pause, the atria load the ventricles with blood (Schram et al., 2002). The atrioventricular node then transmits an action potential through the His-Purkinje system and the ventricular myocardium, resulting in the coordinated

pumping of blood to the lungs and peripheral tissues (Figure 1A) (Schram et al., 2002). Action potential shape and velocity of propagation through sinoatrial and atrioventricular tissue is unique from other cardiac excitable tissues (Figure 1B) (Schram et al., 2002). These unique electrical properties allow the coordinated depolarization and thus contraction of the entire myocardium.

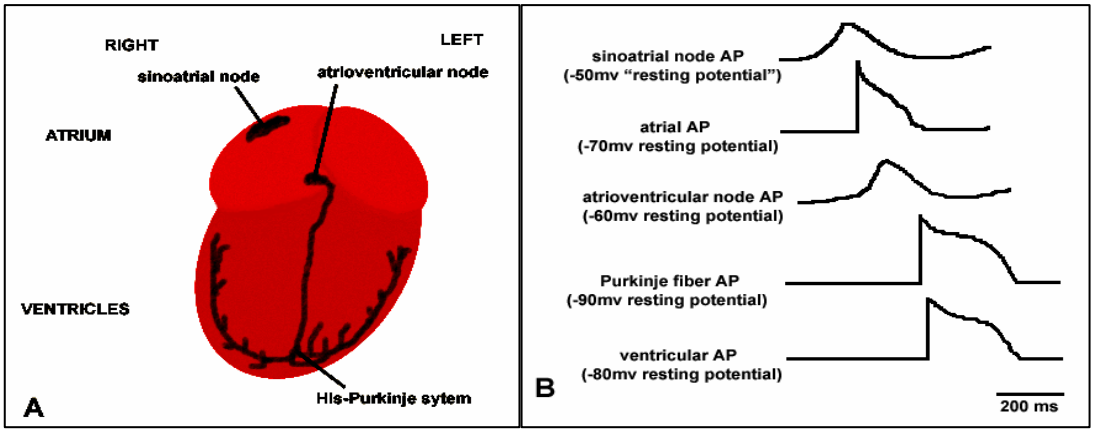
RIGHT
LEFT
sinoatrial node
atrioventricular node
ATRIUM
VENTRICLES
His-Purkinje sytem
A
sinoatrial node AP
(-50mv "resting potential")
atrial AP
(-70mv resting potential)
atrioventricular node AP
(-60mv resting potential)
Purkinje fiber AP
(-90mv resting potential)
ventricular AP
(-80mv resting potential)
B
200 ms

Figure 1.

Figure 1. Basic heart structures and action potential components. A. The working myocardium is composed of bilateral atria and ventricles. The heartbeat is coordinated by the initiation of an electrical impulse (action potential) in the sinoatrial node, conduction through the atria to the atrioventricular node, and then conduction through the His-Purkinje system into the ventricles. B. Action potential morphology and velocity varies between the different cell types of the heart. This figure was adapted from Schram et al. *Circulation Research* 2002 (Schram et al., 2002).

The ventricular action potential

Ventricular action potentials have five phases (Figure 2). Phase 0 is controlled by the rapid activation/inactivation of the primary cardiac voltage-gated Na^+ channel ($Na_v1.5$) that drives the upstroke of the action potential (Figure 2) (Nerbonne and Kass, 2005; Schram et al., 2002). Near the end of phase 0, a transient outward current (I_{to}) offsets the inward sodium current with a repolarizing current that results in the phase 1 "notch" (Figure 2) (Nerbonne and Kass, 2005; Schram et al., 2002). Phase 2 correlates with the action potential plateau that is the result of a balance between inward (Ca^{2+}) and outward (K^+) currents (Nerbonne and Kass, 2005; Schram et al., 2002). Phase 3 is a repolarizing phase controlled by the inactivation of $I_{Ca,L}$ and the increased activity of I_{Ks} and I_{Kr} (delayed-rectifier K^+ channels) (Schram et al., 2002). I_{Ks} and I_{Kr} are voltage-gated K^+ channel currents that are activated as the membrane voltage repolarizes after Phase 2. Phase 4 marks the return to resting potential that is maintained by I_{K1} in ventricular tissue (Figure 2).

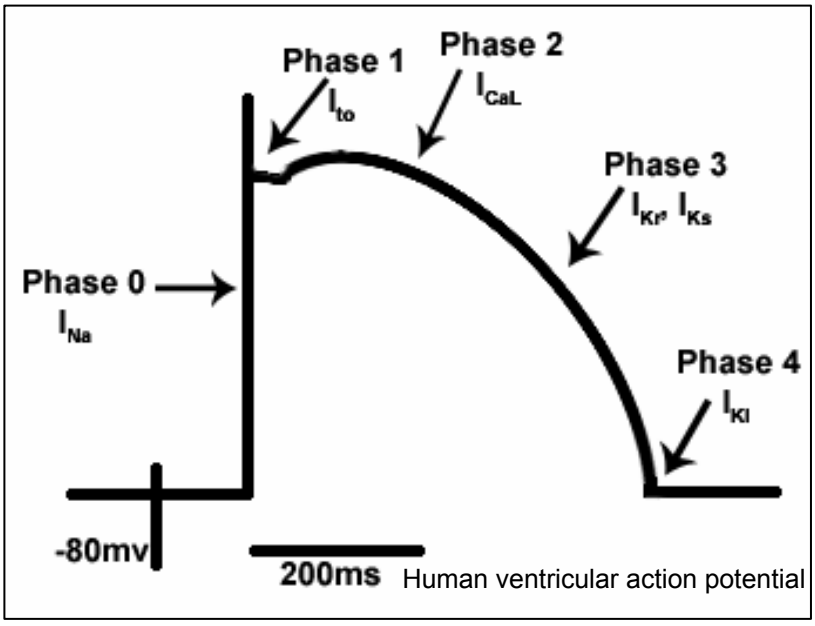
Phase 1
I_{to}
Phase 2
I_{CaL}
Phase 3
I_{Kr}, I_{Ks}
Phase 0
I_{Na}
Phase 4
I_{Kl}
-80mv
200ms
Human ventricular action potential

Figure 2.

Figure 2. Human ventricular action potential. The five phases (arrows) of the cardiac action potential are controlled by the activation and inactivation of several ion channels and transporters. The predominant currents that regulate each phase are listed (Figure 2). This figure was modified from Schram et al. *Circulation Research* 2002 (Schram et al., 2002).

The primary ion channel currents that control the cardiac action potential are complemented by the activity of additional channels, pumps, and transporters including the Na^+/Ca^{2+} exchanger, the Na^+/K^+ ATPase, the SR/ER Ca^{2+} ATPase (SERCA2a), the ryanodine receptor, the inositol 1,4,5, trisphosphate (IP3) receptor, and the plasma membrane Ca^{2+} ATPase (PMCA) (Lehnart et al., 2007; Priori and Napolitano, 2005).

Human cardiac channel diseases ("Cardiac Channelopathies")

Dysfunction in ion channels or transporters may result in human diseases termed "channelopathies". These cardiac "channelopathies" may be inherited, or acquired in response to drug interactions (Lees-Miller et al., 2000; Lehnart et al., 2007; Mitcheson et al., 2000). For example, a number of pharmaceutical compounds have been linked to increased risk of sudden cardiac death by altering the function of cardiac ion channels (Lehnart et al., 2007; Priori and Napolitano, 2005; Priori et al., 2001b).

Alternatively, human carriers of specific ion channel gene gain- or loss-of-function variants may display cardiac channelopathies and risk for arrhythmia (Keating et al., 1991). To date, variants in nine different genes including *KCNQ1* (LQT1; encodes KVLQT1, I_{Ks} potassium channel alpha-subunit) (Wang et al., 1996), *HERG* (LQT2; encodes human ether-a-go-go-related gene, I_{Kr} potassium channel alpha-subunit) (Curran et al., 1995), *SCN5A* (LQT3; encodes $Na_v1.5$, voltage-gated Na^+ channel alpha-subunit) , *KCNE1* (LQT5; encodes MinK, beta-

subunit for I_{Ks} potassium) (Splawski et al., 2000), *KCNE2* (LQT6; encodes MiRP, beta-subunit for I_{Kr} potassium channel) (Splawski et al., 2000), *KCNJ2* (Anderson syndrome 1; encodes Kir2.1, potassium channel responsible for I_{K1} current) (Plaster et al., 2001), *RyR2* (CPVT1; encodes ryanodine receptor calcium-release channel) (Priori et al., 2001b), and *CACNA1C* (Timothy Syndrome; encodes the cardiac voltage-gated Ca^{2+} channel, $Ca_v1.2$) have been implicated in human arrhythmia (Splawski et al., 2004).

Human Na^+ channelopathies

Na_v channel variants that may alter biophysical function have been linked to Brugada syndrome, sick sinus syndrome, type 3 long QT syndrome, and atrial fibrillation (Balser, 2001). Human *SCN5A* gain-of-function variants may result in prolongation of the cardiac action potential and type 3 long QT (LQT3) syndrome (Priori et al., 2002). LQT3 syndrome is a potentially fatal cardiac arrhythmia, and the third most common form of long QT syndrome (Clancy et al., 2002; Moss et al., 1995). LQT3 $Na_v1.5$ variants may result in defects in channel inactivation gating that lead to a small persistent Na^+ current and increases the potential for early after-depolarizations (triggers of ventricular fibrillation) (Roden et al., 2002; Schram et al., 2002). The persistent LQT3 Na^+ current offsets the outward currents of K^+ channels in phase 2 of the cardiac action potential that leads to a prolonged QT interval on electrocardiogram (Figure 2) (Balser, 2001; Priori et al., 2002a; Roden et al., 2002). More than forty-three LQT3 variants have been

identified to date (Roden et al., 2002; Schram et al., 2002). The electrocardiogram of LQT3 patients may have a distinct T-wave that is excessively far-away from the QRS complex compared to unaffected controls (Moss et al., 1995; Zareba, 2006). The persistent Na^+ current predisposes affected LQT3 patients with the possibility of ventricular tachycardia during sleep or periods of rest (Priori et al., 2001a).

In contrast, $Na_v1.5$ variants leading to $Na_v1.5$ loss-of-current may result in Brugada syndrome (Brugada and Brugada, 1995; Brugada and Brugada, 1992). Gating defects in Brugada Syndrome variant channels can result in reduced $Na_v1.5$ current (Brugada et al., 1998; Priori et al., 2002b). The reduced Na^+ current due to Brugada Syndrome variants can result in ventricular arrhythmias during periods of stress or exercise (Brugada et al., 1998; Priori et al., 2002b). Patients with Brugada syndrome may present with periods of syncope or in the worst case, sudden death (Roden et al., 2002). Due to the difference in $Na_v1.5$ expression in the ventricular wall, the electrocardiogram of Brugada Syndrome patients has an elevated ST fragment (Catterall et al., 2005; Roden et al., 2002). The elevated ST fragment and T-wave inversions seen in Brugada syndrome patient electrocardiograms are commonly seen in patients with significant structural heart defects and are thought to be due to conduction defects (Antzelevitch et al., 2005). However, Brugada syndrome patients are free of structural heart abnormalities (Antzelevitch et al., 2005). Interestingly, disrupted $Na_v1.5$ expression is also one of the proposed mechanisms of disease for patients with Brugada syndrome (Priori et al., 2002).

Voltage-gated Na^+ channels

The ultra-rapid entry of sodium into the ventricular myocyte through $Na_v1.5$ causes a rapid change in the membrane potential that facilitates the activation and inactivation of other ion currents (Schram et al., 2002). The velocity and amplitude of $Na_v1.5$-dependent current overcomes the propensity of the cell to remain at rest (Bers, 2002; Hille, 2001). In heart, the upstroke of the action potential is critical to reach the depolarized state that allows the activation of calcium-induced calcium-release (CICR) that drives the contraction of cardiac myofilaments (Bers, 2002).

Voltage-gated Na^+ channels are composed of pore-forming alpha-subunits and accessory beta-subunits (Yu and Catterall, 2003). There are nine voltage-gated Na^+ channel alpha-subunits ($Na_v1.1$-1.9) (Yu and Catterall, 2003). The primary cardiac voltage-gated Na^+ channel alpha-subunit is $Na_v1.5$ (Roden et al., 2002). There are four Na_v beta-subunits (beta1-beta4) that may complex with alpha-subunits (Figure 3) (Yu and Catterall, 2003). Human $Na_v1.5$ is a glycosylated polypeptide comprised of 2016 amino acids with a predicted molecular mass of 260 kilodaltons (Balser, 2001; Yu and Catterall, 2003). $Na_v1.5$ contains four homologous domains (DI-DIV), each comprised of six transmembrane alpha-helices (S1-S6) that are linked by cytosolic and extracellular loops (Figure 3) (Yu and Catterall, 2003). Cytosolic amino- and carboxy-termini as well as inter-domain and inter-segment linkers comprise the cytosolic components of $Na_v1.5$ (Balser, 2001; Yu and Catterall, 2003). Inter-

segment linkers including the pore-lining S5-S6 linkers make up the extracellular components of $Na_v1.5$ (Balser, 2001; Yu and Catterall, 2003). The extracellular and cytosolic loops connecting the transmembrane segments are critical for several processes including membrane localization, intermolecular interactions, and channel-gating activities (Balser, 2001; Yu and Catterall, 2003). For example, the DIII-DIV linker is critical for inactivation of the channel (Balser, 2001; Yu and Catterall, 2003). Specific ion channel pore structures may be particularly sensitive to pharmacological substrates or even natural toxins (Lange et al., 2006a). For example, several Na_v channels are sensitive to the natural toxin tetrodotoxin (TTX) found in the *Tetrodontidae* family of fish (used to make the Japanese delicacy Fugu) (Yu and Catterall, 2003). Specifically, multiple Na_v channels are blocked by nanomolar concentrations of TTX (Yu and Catterall, 2003). Interestingly, unlike other voltage-gated Na_v channels, $Na_v1.5$ is blocked by TTX at 1-10μM (Balser, 2001; Yu and Catterall, 2003). This difference in TTX-sensitivity between Na_v isoforms is primarily attributed to a single amino acid (cysteine 373) in $Na_v1.5$ transmembrane segment S6 (Balser, 2001; Yu and Catterall, 2003). The unique TTX-sensitivity of $Na_v1.5$ has proved valuable for differentiating $Na_v1.5$ activity from other neuronal-type $Na_v1.X$ isoforms (Balser, 2001; Yu and Catterall, 2003). Voltage-gated Na_v channel structure plays a key role for channel biophysical regulation. For example, positively-charged arginine residues in the S4 (transmembrane segment-4) segments of each transmembrane domain comprise the $Na_v1.5$ voltage-sensor (Balser, 2001; Yu and Catterall, 2003). Specifically, these highly charged residues are arranged so

that upon membrane depolarization the S4 segments move through the lipid bilayer (Balser, 2001; Yu and Catterall, 2003). This motion causes a change in $Na_v1.5$ protein configuration and allows the permeation of Na^+ (Balser, 2001). The structural properties of Na^+ channel alpha-subunits together with the activity of modulatory molecules and accessory subunits regulate alpha-subunit gating properties (Balser, 2001). Na_v channel beta-subunits have a single transmembrane pass motif with an extracellular amino-terminus and a cytosolic carboxy-terminus (Figure 3) (Isom et al., 1995; Malhotra et al., 2001; Malhotra et al., 2000). The extracellular motif of beta-subunits has similar characteristics to cell adhesion molecules, and is the site for covalent binding of beta2 and beta4 subunits to neuronal Na_v isoforms (Figure 3) (Isom et al., 1995; Malhotra et al., 2001; Malhotra et al., 2000). The cytosolic domains of beta1- and beta3-subunits contain a phosphorylation site hypothesized to be critical for interaction with cytoplasmic proteins (Malhotra et al., 2004). The role of the beta-subunits in heart will be further discussed in Chapter 3.

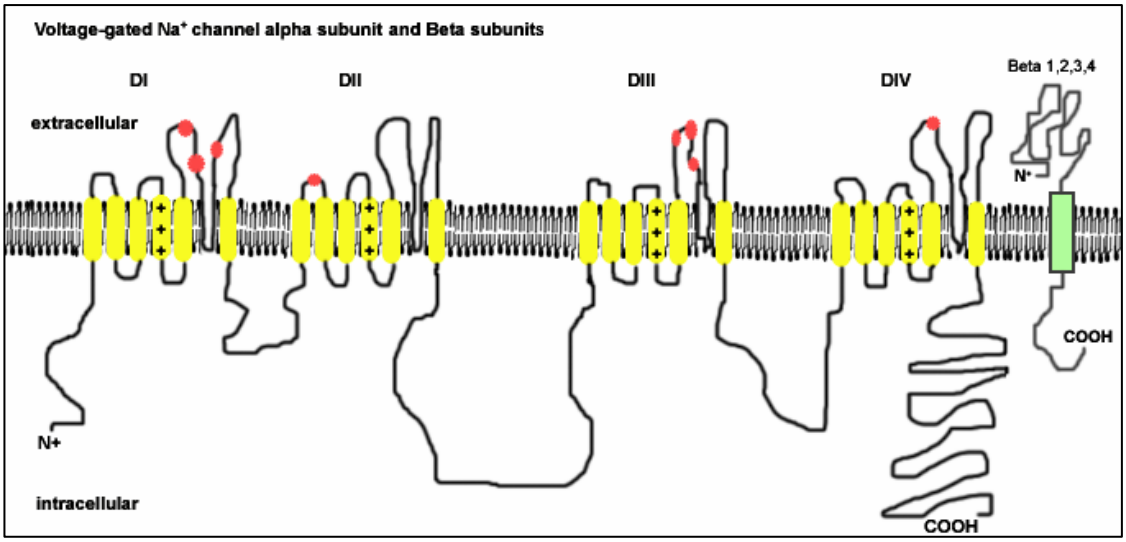
Voltage-gated Na+ channel alpha subunit and Beta subunits
DI
DII
DIII
DIV
Beta 1,2,3,4
extracellular
N+
COOH
N+
intracellular
COOH

Figure 3.

Figure 3. Voltage-gated Na^+ channel alpha-subunit and accessory beta-subunit. Voltage-gated Na^+ channel alpha-subunits are comprised of four six-transmembrane domains with amino- and carboxy- termini. Alpha-subunits are glycosylated at several sites (red circles) (Roden et al., 2002). Accessory beta-subunits have a cytosolic carboxy-terminus and an extracellular amino-terminus with immunoglobulin-like folds. This figure was modified from Roden et al. *Annual Review of Physiology* 2002 (Roden et al., 2002).

In addition to the channel pore-forming structure, additional transcriptional, post-transcriptional, and post-translational modifications and interactions modulate Na_v channel function. These include $Na_v1.5$ mRNA splicing, phosphorylation, intermolecular interactions, glycosylation, trafficking, and neurohumoral regulation (Cusdin et al., 2008; Delisle et al., 2004; Herfst et al., 2004). The mechanisms that control the specific functional properties of $Na_v1.5$ (and other cardiac ion channels) remain an active area of research.

$Na_v1.5$ activity in non-cardiac tissues

In addition to its role in regulation of cardiac function, recent findings illustrate that $Na_v1.5$ has a number of unexpected non-cardiac functions. Specifically, $Na_v1.5$ has been identified in smooth muscle cells of the uterus, endocytic macrophages, limbic regions of the brain, and the gastrointestinal tract (Abriel, 2007). In uterine smooth muscle, $Na_v1.5$ is important for regular and sustained contraction (Seda et al., 2007). Specifically, $Na_v1.5$ current initiates smooth muscle contraction by promoting calcium-induced calcium-release (Seda et al., 2007). Recently, the unique expression of $Na_v1.5$ in the endocytic vesicles of primary monocyte-derived macrophages was discovered (Carrithers et al., 2007). $Na_v1.5$ is proposed to promote phagocytosis of bacteria and acidification of endocytic vesicles by proton flux (Carrithers et al., 2007). In the limbic region of the brain (display high $Na_v1.5$ expression) human probands with *SCN5A* variants display reduced GABAergic activity, and a high propensity for

schizophrenia (Roberts, 2006). In the gastrointestinal tract, $Na_v1.5$ is expressed in intestinal smooth muscle and the interstitial cell of Cajal, a specialized set of cells required for intestinal smooth muscle contraction (Strege et al., 2003). Interestingly, a recent study found patients with *SCN5A* variants with displayed increased likelihood for episodes of intestinal pain (Locke, 2006). The cause of pain is hypothesized to result from prolonged contraction of intestinal smooth muscle cells due to persistent (increased) $Na_v1.5$ current (Locke, 2006).

Genetically-engineered $Na_v1.5$ animal models

Studies of $Na_v1.5$ knockout and transgenic animals demonstrate the importance of $Na_v1.5$ (Papadatos et al., 2002). $Na_v1.5$ null ($Na_v1.5^{-/-}$) mice fail to develop beyond embryonic day 11, and have an irregular electrocardiogram (Papadatos et al., 2002; Royer et al., 2005). Sections from $Na_v1.5^{-/-}$ hearts show severe ventricular developmental defects (Papadatos et al., 2002). $Na_v1.5$ heterozygous ($Na_v1.5^{+/-}$) mice display impaired action potential conduction velocity between the atria and ventricles (Papadatos et al., 2002). Moreover, $Na_v1.5^{+/-}$ mice are highly susceptible to the onset of fibrosis and development of conduction defects (Papadatos et al., 2002; Royer et al., 2005). In fact, $Na_v1.5^{+/-}$ mice phenocopy human disease termed Lev-Lenègre (a progressive human cardiac conduction disorder caused by *SCN5A* variants) (Royer et al., 2005).

Interestingly, in studies using a transgenic mouse model of $Na_v1.5$ overexpression (ten times the amount of $Na_v1.5$ total protein), cardiomyocytes

from transgenic animals are electrophysiologically indistinguishable from wild-type mice (Zhang et al., 2007). These data suggest there are potential mechanisms that maintain the amount of $Na_v1.5$ active at the membrane surface. One potential hypothesis is that there could be a finite amount of space available for $Na_v1.5$ to fill at the membrane surface. Alternatively, the excess $Na_v1.5$ remains inactive or fails to achieve the state of maturation necessary to be functionally expressed at the membrane surface.

Alternative mechanisms of channelopathies

Recent findings have identified a new class of inherited cardiac arrhythmia based not on gene variants that may affect channel biophysics, but based instead on mutations that cause dysfunction in cellular pathways required for the proper localization of ion channels and transporters within the cardiomyocyte (Lehnart et al., 2007). Several non-ion channel or ion channel subunit genes have been linked to cardiac channelopathies including; ankyrin-B (*ANK2)* , caveolin-3 (*CAV3)* (Cronk et al., 2007; Vatta et al., 2006; Yarbrough et al., 2002), glycerol phosphate-3-dehydrogenase 1-like protein (*GPD1L*) (London et al., 2007; Van Norstrand et al., 2007), and calsequestrin (*CASQ2*) (Chopra et al., 2007). These new findings will be discussed in detail in Chapter 3.

CHAPTER II

EXCITATION-CONTRACTION COUPLING AND CARDIOMYOCYTE STRUCTURAL ORGANIZATION

Cardiomyocyte structural organization

The proper expression, localization, and distribution of ion channels and transporters at subcellular and tissue-specific levels are critical for excitation-contraction coupling (Schram et al., 2002). The plasma membrane of myocytes is referred to as the sarcolemma (Lange et al., 2006b). Contained within the muscle cell sarcolemma are a number of structural components that support the activity of the contractile machinery (Lange et al., 2006b). Muscle fibers, also called myofibrils, are composed of serially-connected structures that contain the myosin/actin contractile machinery (Lange et al., 2006b). These structures are called sarcomeres (Lange et al., 2006b). The border of each sarcomere is marked by a Z-disc (Lange et al., 2006b). The Z-disc provides structural support for each sarcomere and acts as the anchor point for the actin-based thin filaments (Figure 4) (Lange et al., 2006b). The Z-discs appear as an electron dense region on electron micrographs of myocytes (Figure 4) (Danowski et al., 1992; Lange et al., 2006b). Each Z-disc is surrounded by a lighter appearing region containing the actin-based thin filaments (Danowski et al., 1992; Lange et al., 2006b). The Z-disc and the light region on both sides of each Z-disc is

referred to as the I-band (Figure 4, lower panel) (Danowski et al., 1992; Lange et al., 2006b). Areas of contact between the sarcomere and the extracellular matrix are interspersed between Z-disc and act as points of force transmission between myocytes (Figure 4 upper panel) (Danowski et al., 1992; Lange et al., 2006a). These specialized areas surrounding the Z-disc are referred to as the costameres (Danowski et al., 1992).

The M-band or M-line is the point where the myosin-based thick filaments are cross-linked by a protein complex (Figure 4) (Agarkova and Perriard, 2005). On either side of the M-band, myosin-based thick filaments extend from the center of the sarcomere toward the Z-discs (Figure 4) (Agarkova and Perriard, 2005). The region of the sarcomere containing the M-line and the thick filaments of myosin is referred to as the A-band (Figure 4, lower panel) (Agarkova and Perriard, 2005). Together, the components of the sarcomere provide the structural framework for actin-myosin mediated contraction and relaxation (Agarkova and Perriard, 2005).

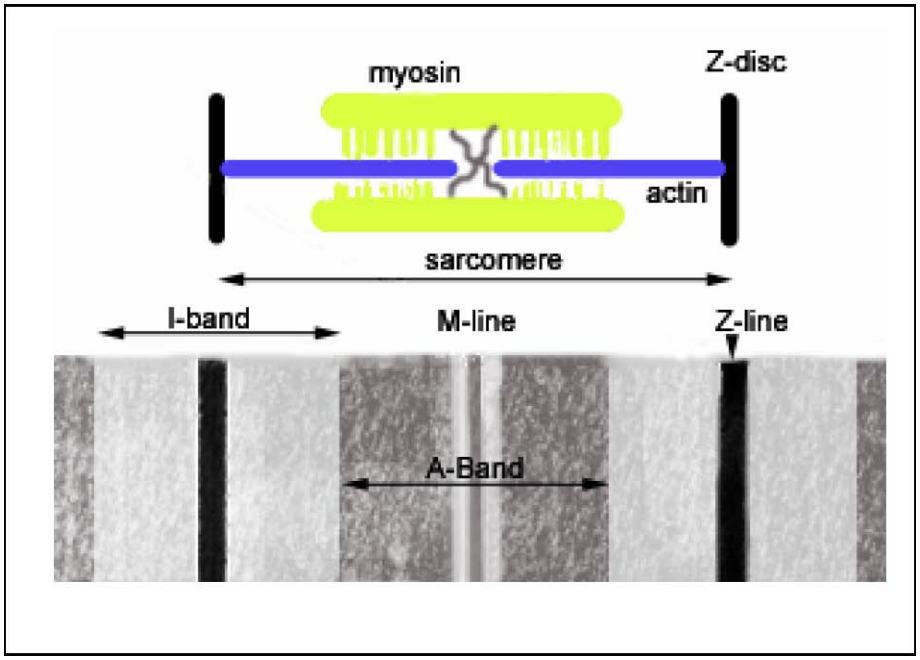

Figure 4.

Figure 4. Sarcomere organization. Upper panel representation of myosin-rich thick filaments cross-linked at M-band. Actin-based thin filaments are attached to Z-disc. Lower panel electron micrograph of sarcomere marked with Z-line, M-band, I-band, and A-band. Figure from Agarkova et al. (Liu et al., 2003).

Sarcolemmal organization

Sarcolemma

The sarcolemmal membrane envelopes the intracellular content of the myocyte (Bers and Despa, 2006; Nerbonne and Kass, 2005; Roden et al., 2002). Moreover, the sarcolemmal membrane forms an electrically-insulated surface between intracellular and extracellular ion concentration gradients (Bers and Despa, 2006; Nerbonne and Kass, 2005; Roden et al., 2002). Ion pumps, channels, and transporters maintain the "resting" ion concentration gradients and respond to stimuli upon excitation (Bers and Despa, 2006; Nerbonne and Kass, 2005; Roden et al., 2002). The sarcolemmal surface is populated with several ion channels (discussed in Chapter 1) and transporters including the Na^+/Ca^{2+} exchanger (NCX), the Na^+/K^+ ATPase (NKA), the plasma membrane Ca^{2+} ATPase (PMCA), and the Na^+/H^+ exchanger (NHE) (Bers and Despa, 2006; Nerbonne and Kass, 2005; Roden et al., 2002). The ion transporters NHE and NKA reduce the cytosolic Na^+ content in response to the clearance of Ca^{2+} by NCX (1 Ca^{2+} ion out for 3 Na^+ ions in) (Bers and Despa, 2006; Nerbonne and Kass, 2005; Roden et al., 2002).

Transverse-tubule network

Specialized invaginations of the sarcolemmal membrane make up the transverse-tubule (T-tubule) membrane network (Agarkova and Perriard, 2005; Brette and Orchard, 2003; Lange et al., 2006a). The T-tubule membrane

network has both transverse and thinner axial projections that project into the myocyte cell body (Figure 5) (Agarkova and Perriard, 2005; Brette and Orchard, 2003; Lange et al., 2006a). The T-tubules are populated with ion channels and transporters that are strategically juxtaposed to calcium release proteins of the sarcoplasmic reticulum (Agarkova and Perriard, 2005; Brette and Orchard, 2003; Lange et al., 2006a). The larger diameter terminal opening of the T-tubules are localized along the Z-line (Agarkova and Perriard, 2005; Brette and Orchard, 2003; Lange et al., 2006a). The difference in diameter of the opening and distal branches of the T-tubule system provides temporal regulation of the excitation-contraction cycle of the myocyte due to limited diffusion of ions in distal portions of the T-tubules (Agarkova and Perriard, 2005; Brette and Orchard, 2003; Lange et al., 2006a). A specialized intracellular calcium storage and release system called the sarcoplasmic reticulum (described below) is located adjacent to sarcolemmal membrane domains (Agarkova and Perriard, 2005; Brette and Orchard, 2003; Lange et al., 2006a).

Intercalated disc

Cardiomyocytes have a unique sarcolemmal membrane structure at their terminal ends called intercalated discs (ID) (Figure 5) (Awad et al., 2008; Perriard et al., 2003). The intercalated discs provide intracellular and intercellular (adherens junctions) structural stability to the longitudinally-oriented contractile proteins (desmosomes) and the membrane elements of cardiomyocytes (Awad et al., 2008; Perriard et al., 2003). The adherens junction proteins form contact points between cells at the intercalated discs (Awad et al., 2008; Perriard et al.,

2003). The adherens junctions are comprised of N-cadherin transmembrane proteins and cytosolic binding partners, alpha-catenin, beta-catenin, plakoglobin, and spectrin which attach the myofibrillary proteins (Awad et al., 2008; Perriard et al., 2003).

The desmosome provides structural stability between cell membranes and contractile proteins of adjacent cells, and has suggested roles in Ca^{2+} homeostasis and apoptotic signaling (Awad et al., 2008; Perriard et al., 2003). Desmosomes are comprised of desmocollin and desmoglein transmembrane proteins and plakoglobin and desmoplakin cytosolic proteins (Awad et al., 2008; Perriard et al., 2003). These desmosomal cadherins help establish intercalated disc domains and provide stability to the desmin-rich intermediate filaments that cross-link the myofibrillary proteins (Awad et al., 2008; Perriard et al., 2003). Intercalated discs are also sites of cell-cell ion transport through gap junctions (Figure 5) (Awad et al., 2008; Perriard et al., 2003).

The primary gap junction protein in ventricular myocytes is connexin-43 which forms a hexa-meric pore between the membrane of two adjoining cells (Petty and Lo, 2002). The gap junctions, along with ion channels including $Na_v1.5$, are localized to the intercalated discs and allow ion conduction between adjacent cells (Figure 5) (Petty and Lo, 2002). Disruption of the gap junction proteins and intercalated discs are evidenced in patients with cardiomyopathic disease (Petty and Lo, 2002).

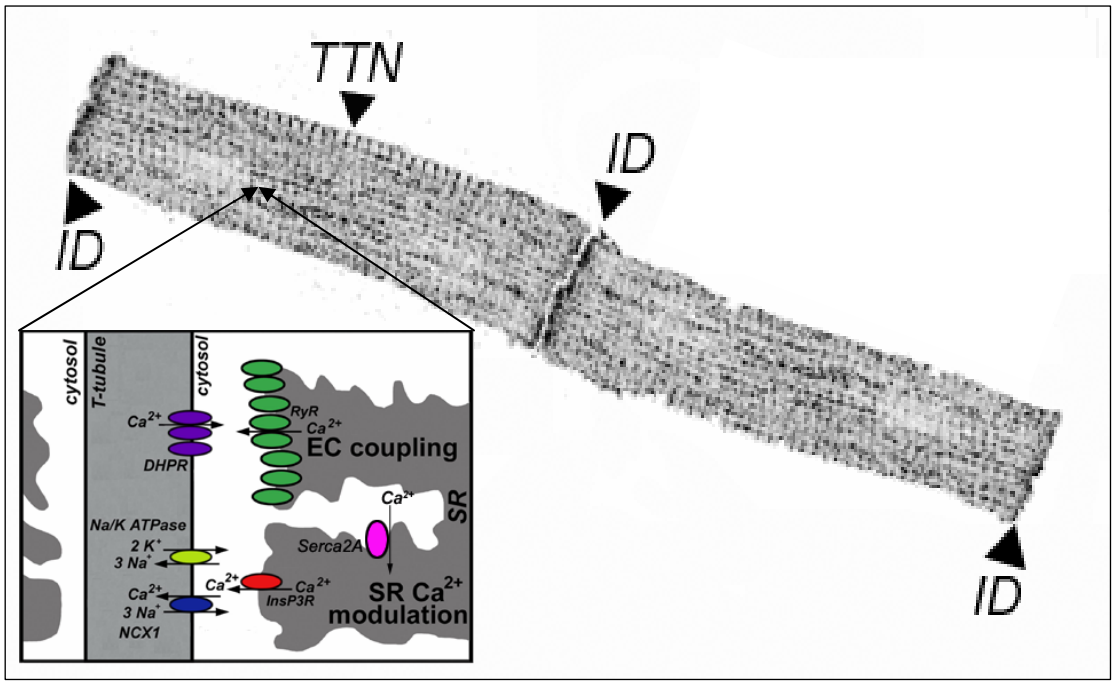
TTN
ID
ID
ID
cytosol
T-tubule
cytosol
Ca2+
DHPR
RyR
Ca 2+
EC coupling
Ca2+
SR
Na/K ATPase
2 K+
3 Na+
Serca2A
Ca2+
Ca2+
3 Na+
NCX1
Ca2+
Ca 2+
InsP3R
SR Ca2+
modulation

Figure 5.

Figure 5. Intercalated disc and transverse-tubule network membrane domains. *Inverted grayscale confocal image of two coupled adult rat cardiomyocytes*. Intercalated discs (ID) provide a mechanical and electrical junction between cardiomyocytes. The transverse-tubule network (TTN and inset) is comprised of specialized sarcolemmal invaginations that facilitate the coordinated contraction along the length of cardiomyocytes. (Inset) Clusters of ion channels (DHPR) and transporters (Na^+/Ca^{2+} exchanger, Na^+/K^+ ATPase, RyR, $InsP_3$, SERCA 2A) expressed at sarcolemmal and sarcoplasmic membranes are placed proximally to regulate intracellular Ca^{2+} stores (adapted from Mohler et al. *PloS* 2005) (Mohler et al., 2005a).

Sarcoplasmic reticulum

The sarcoplasmic reticulum (SR) is a specialized intracellular organelle unique to myocytes (Figure 5, inset; grey membrane compartment). The SR is the site of intracellular Ca^{2+} storage (10 times the content in the cytosol) in the cardiomyocyte (Bers and Despa, 2006). The SR is populated with specialized calcium release channels including the ryanodine receptor (RyR) and the inositol 1,4,5, trisphosphate receptor (*IP3R*) (Figure 5, inset) (Bers and Despa, 2006). The SR membrane also contains Ca^{2+} uptake transporters including the sarcoplasmic/endoplasmic reticulum calcium ATPase transporter and the SERCA2a inhibitory regulator phospholamban (not pictured) (Figure 5, inset) (Bers and Despa, 2006). Phosphorylation of phospholamban removes the inhibition (reduced affinity for Ca^{2+}) on SERCA2a and allows Ca^{2+} to be loaded into the SR and cleared from the cytosol (Bers and Despa, 2006). Maintenance of the intracellular ion content is critical for normal physiological activity and in prevention of disease (Bers and Despa, 2006).

Excitation-contraction coupling

As described above, the vertebrate cardiomyocyte contains a number of structural, electrical, and signaling components. These components collaborate to modulate the functional activity of the myocyte. This process, that translates

electrical stimulation with mechanical force to generate cellular contraction, relaxation, and thus cardiac function is termed excitation-contraction coupling.

Excitation-contraction coupling is initiated by the rapid entry of Na^+ into the cardiomyocyte at phase 0 (Figure 2) through $Na_v1.5$. This initial event drives the depolarization of the myocyte, and triggers the activation of voltage-gated Ca^{2+} channels ($Ca_v1.2$) along the T-tubule membrane network (Ohtsuki and Morimoto, 2008). $Ca_v1.2$ channels are closely juxtaposed to specialized calcium-release channels on the SR termed ryanodine receptors (RyR) (Ohtsuki and Morimoto, 2008). This specialized juxtaposition of external and internal membranes is referred to as the "dyad" (Ohtsuki and Morimoto, 2008). Cellular depolarization causes calcium-influx through $Ca_v1.2$ resulting in an increase in local cytosolic Ca^{2+} (10-20 μM) within the dyad (Endoh, 2006; Ohtsuki and Morimoto, 2008). This elevation in local Ca^{2+} subsequently triggers calcium-induced calcium-release from internal SR stores via the RyR (Endoh, 2006; Ohtsuki and Morimoto, 2008). Once cytosolic Ca^{2+} reaches a threshold of 10^{-6} – 10^{-5} M, Ca^{2+} binds and activates troponin-C, resulting in the inhibitory release of actin/tropomyosin-based thin filaments by troponin-I (Endoh, 2006; Ohtsuki and Morimoto, 2008). Following release from troponin-I, thin-filaments form cross-bridges with myosin-based thick filaments and generate force due to filaments sliding over each other to shorten the sarcomere (Endoh, 2006; Ohtsuki and Morimoto, 2008). Following contraction, the activation of Na^+/Ca^{2+} exchanger, SERCA2a, and plasma membrane Ca^{2+} ATPase (PMCA) Ca^{2+} efflux pathways restore cytosolic Ca^{2+} concentrations to pre-contraction levels (Endoh, 2006;

Ohtsuki and Morimoto, 2008). Once cytosolic $[Ca^{2+}]_i$ are restored to diastolic levels, cross-bridge formation, and the affinity of troponin-C for Ca^{2+} is reduced resulting in sarcomere filamentary relaxation (Endoh, 2006; Ohtsuki and Morimoto, 2008).

CHAPTER III

VOLTAGE-GATED SODIUM CHANNEL-ASSOCIATED PROTEIN ACTIVITY AND MEMBRANE BIOGENESIS

Regulation of Na_v channel expression

Control of Na_v channel expression is an intricate process that requires a series of incompletely understood transcriptional, translational, and post-translational mechanisms (Abriel, 2007; Herfst et al., 2004). Transcription is tightly controlled by the association of transcription factors and mechanisms that modify the accessibility of DNA (Abriel, 2007; Cusdin et al., 2008; Herfst et al., 2004). Newly translated $Na_v1.5$ is inserted into the ER under the guidance of specific signal sequences that bind signal recognition particles that target the nascent protein to receptors on the ER (Abriel, 2007; Cusdin et al., 2008; Herfst et al., 2004). Once nascent $Na_v1.5$ is inserted into the ER there are several chaperone molecules that are thought to associate and provide quality control and guidance for folding and maturation of the protein (Delisle et al., 2004). The membrane topology of $Na_v1.5$ is critically important because the multi-transmembrane pass motifs are interspersed with specific cytoplasmic and extracellular functional elements (Delisle et al., 2004). Once inserted into the ER, $Na_v1.5$ is core glycosylated as cellular quality control machinery ensures that the protein is properly folded (Delisle et al., 2004). Misfolded proteins that fail quality control measures are marked for degradation by proteasomal or lysosomal machinery (Delisle et al., 2004). Proper protein folding is thought to

mask ER retention motifs which allow the nascent $Na_v1.5$ to be trafficked through the ER-Golgi intermediate compartment to the Golgi (Cusdin et al., 2008). Once $Na_v1.5$ is in the Golgi, several rounds of glycosylation drive the maturation of the protein (Cusdin et al., 2008). The matured $Na_v1.5$ is then sent to the Trans-Golgi network for sorting and determination of the final destination of the protein (Cusdin et al., 2008; Delisle et al., 2004). The molecular chaperones and cytosolic signal sequences on $Na_v1.5$ and molecules that complex with these motifs are thought to guide the efflux of $Na_v1.5$ to the proper intracellular destination, however the specific mechanisms that control ion channel and transporter traffic to the membrane remain unresolved (Cusdin et al., 2008; Delisle et al., 2004). $Na_v1.5$ and other excitable-cell proteins that reach the sarcolemmal membrane are assembled into respective complexes and are often anchored to specific membrane domains (Cusdin et al., 2008). Integral membrane proteins are often recycled or turned over by the endosomal proteins that can signal the proteins for degradation or recycling back to the membrane (Abriel and Kass, 2005). Several molecules are suggested to interact with $Na_v1.5$ and modulate channel biophysical activity or membrane expression (Abriel, 2007; Abriel and Kass, 2005).

Proposed interacting/targeting proteins

Recent studies have suggested that $Na_v1.5$ interacts with diverse molecules to modulate membrane trafficking (Cusdin et al., 2008). Molecules

with proposed importance for localization of ion channels have been suggested to interact with $Na_v1.5$ including Na_v beta-subunits (*SCN1B-SCN4B*) (Isom et al., 1995; Malhotra et al., 2001; Malhotra et al., 2000; Malhotra et al., 2002; Malhotra et al., 2004; Yu and Catterall, 2003), syntrophins (*SNTA1, SNTB1, SNTB2*) (Gavillet et al., 2006b; Ou et al., 2003), and Nedd-4-like ubiquitin ligase (*NEDD4-2*) (Rougier et al., 2004; van Bemmelen et al., 2004). Additionally, molecules with poorly defined or unknown physiological function have also been suggested to change the membrane expression of $Na_v1.5$ including glycerol phosphate-3-dehydrogenase 1-like protein (*GPD1L*) (London et al., 2007b; Van Norstrand et al., 2007a), and ran guanine nucleotide release factor (*MOG1*) (Wu et al., 2008). The following section will review these proposed interacting molecules and their potential roles in regulating $Na_v1.5$ membrane targeting.

The contribution of Na_v beta-subunits to modify channel gating kinetics and localization of $Na_v1.5$ has conflicting reports in the literature from studies in different cell types (Maier et al., 2004). All four Na_v beta-subunit genes (*SCN1B-SCN4B*) are reported to be expressed in heart (Maier et al., 2004; Meadows and Isom, 2005). Na_vbeta-2, Na_vbeta-1, and Na_vbeta-4 subunits are reported to be expressed at the intercalated disc and Na_vbeta-1 and Na_vbeta-3 along the T-tubules (Maier et al., 2004). The phosphorylation state of Na_vbeta-subunit isoforms (1 and 3) is reported to be important for association with ankyrin proteins (Malhotra et al., 2004). Na_vbeta-1 at the intercalated disc is phosphorylated and cannot interact with ankyrin-G (Malhotra et al., 2004). In contrast, Na_vbeta-1 along the T-tubules is non-phosphorylated and is suggested

to interact with similar ankyrin-B (Malhotra et al., 2004). The Na_vbeta-1 subunits at the intercalated disc are suggested to stabilize the intercalated disc by complexing with N-cadherin and connexin 43 (Lopez-Santiago et al., 2007). However, studies of cardiomyocytes from Na_vbeta-1-knockout mice show that reduction of Na_vbeta-1 subunit expression does not reduce expression or membrane stability of $Na_v1.5$, connexin 43, or N-cadherin (Lopez-Santiago et al., 2007). Interestingly, the expression and activity of $Na_v1.5$ is increased in Na_vbeta-1 knockout cardiomyocytes, however it is noteworthy that the knockout mice have severe neurological defects (Lopez-Santiago et al., 2007). These data show that despite the similarities in Na_v channel trafficking in neurons and cardiomyocytes, the specific channel isoform and cellular context is critical when studying trafficking mechanisms (Chen et al., 2002). Cardiomyocytes from a knockout model of Na_vbeta-2 display no discernable phenotype in the activity or expression of $Na_v1.5$ in the heart, but the activity and expression of neuronal Na_v channels was disrupted in the brain (Chen et al., 2002). The functions of Na_vbeta-3 and Na_vbeta-4 have not been demonstrated *in vivo* however *SCN4B* variants (gene that encodes Na_vbeta-4) are linked with a family of LQT3 patients (Kahlig et al., 2006). Recent studies have identified variants in *SCN1B* (encodes Na_vbeta-1) that have been linked to both neuronal (epilepsy) and cardiac (Brugada syndrome) arrhythmic disease (Watanabe et al., 2008). However, due to the contradicting information from studies using different cell systems and the lack of animal models for all Na_vbeta-subunits, the specific role of Na_vbeta-subunits remains unresolved in heart. Chapter 6 will revisit and propose future

experiments to address the role for Na_vbeta subunits and ankyrins with respect to Na_v channel targeting in the heart.

Co-immunoprecipitation experiments showed the association of $Na_v1.5$ and alpha- and beta-Syntrophins (*SNTA1, SNTB1, SNTB2*) (Gavillet et al., 2006a; Ueda et al., 2008). Alpha- and beta-syntrophins are hypothesized to provide a link between the dystrophin complex and the PDZ-binding domain in the carboxy-terminus of $Na_v1.5$ (Gavillet et al., 2006a; Ueda et al., 2008). Removal of the PDZ-binding domain blocked the interaction of $Na_v1.5$ and the dystrophin complex (Gavillet et al., 2006b). These experiments were conducted in the context of a dystrophin-deficient mouse and showed a significant reduction in $Na_v1.5$ protein expression (immunoblot) and surface current density (Gavillet et al., 2006b). However these studies failed to show the specific contribution of the syntrophin isoforms for $Na_v1.5$ localization or physiological function. Future studies are needed to define the physiological relevance of syntrophin isoforms for $Na_v1.5$ activity and localization.

Nedd4-like ubiquitin ligase (*NEDD4-2*) is a member of the E3 protein-ubiquitin ligase family of enzymes that bind and ubiquitinate target proteins at specific sites (PY-motif, PPXY) that mark proteins for degradation by the proteasome (Rougier et al., 2004; van Bemmelen et al., 2004). The carboxy-terminus of $Na_v1.5$ contains a PY-motif known to bind E3 protein-ubiquitin ligases like Nedd4-2 (Rougier et al., 2004; van Bemmelen et al., 2004). Heterologous cells expressing $Na_v1.5$ down-regulate I_{Na} upon overexpression of Nedd4-2 (Rougier et al., 2004; van Bemmelen et al., 2004). There is also biochemical

evidence that $Na_v1.5$ is ubiquitinated *in vivo* (Rougier et al., 2004; van Bemmelen et al., 2004). However these studies fail to represent the extent of $Na_v1.5$ internalization and degradation due to Nedd4-2 activity and the physiological importance of the Nedd4-2-based pathway.

Glycerol phosphate-3-dehydrogenase 1-like protein (*GPD1L)* is a protein of unknown function that has been linked to Brugada Syndrome and sudden infant death syndrome using mutational analyses (London et al., 2007b; Van Norstrand et al., 2007a). *GPD1L* variants expressed in heterologous cells (HEK293 and COS-7) or in transduced neonatal mouse cardiomyocytes result in reduction of sodium current density (London et al., 2007b; Van Norstrand et al., 2007a). However, the specific physiological effect of GPD1L transduction is undefined as well as the primary function of the protein (London et al., 2007b; Van Norstrand et al., 2007a). Trafficking studies in heterologous cells suggest that GPD1L may effect the proper cellular localization of $Na_v1.5$ (London et al., 2007b; Van Norstrand et al., 2007a). However, the physiological function of GPD1L remains unresolved. Moreover, determining the physiological function and potential Nav1.5 trafficking role of GPD1L would benefit from the development of a transgenic animal model or other reduction/reconstitution strategies.

Ran-guanine nucleotide release factor (*MOG1*) was identified as an interacting partner of $Na_v1.5$, using the DII-DIII linker of $Na_v1.5$, in yeast two-hybrid analyses (Wu et al., 2008). Subsequent *in vitro* binding analyses and co-immunoprecipitation experiments demonstrated that MOG1 and $Na_v1.5$ associate

(Wu et al., 2008). Overexpression of MOG1 resulted in a gain in I_{Na} density in both HEK293 cells co-expressing $Na_v1.5$ and neonatal cardiomyocytes (Wu et al., 2008). The authors also failed to provide any data demonstrating the physical expression of increased $Na_v1.5$ at the membrane (Wu et al., 2008). Biochemical analyses of HEK293 cells overexpressing $Na_v1.5$ and MOG1 had increased $Na_v1.5$ in the membrane fraction of lysates (Wu et al., 2008). These results are interesting, however they would benefit from further analyses in more physiological contexts such as primary cardiomyocytes (Wu et al., 2008) . Moreover, the specific mechanism that MOG1 may play on $Na_v1.5$ activity (increase in surface expression or channel gating) and the primary biochemical function of MOG1 remain unknown. These studies would benefit from the development of a transgenic animal model or other reduction/reconstitution system to determine the function of MOG1.

In summary, although several proteins interact with $Na_v1.5$ and possibly modify membrane targeting, the specific mechanisms and contributions of the interaction partner proteins to these processes remain unclear.

Proposed interacting/modulatory proteins

Several proteins have been discovered to interact and possibly modulate the biophysical activity of $Na_v1.5$ (Abriel, 2007). Calmodulin (*CALM1*) interacts with the carboxy-terminus of $Na_v1.5$ and has been linked to the regulation of other ion channels (Kim et al., 2004; Maltsev et al., 2008; Shah et al., 2006; Tan

et al., 2002; Wingo et al., 2004). The primary cardiac caveolin-family member, caveolin-3 (*CAV3*) is reported to interact with $Na_v1.5$ (Cronk et al., 2007; Vatta et al., 2006; Yarbrough et al., 2002). Fibroblast growth factor homologous factor 1B (*FHF1B)* has also been suggested to interact with $Na_v1.5$ (Liu et al., 2003). Several signaling proteins including, protein tyrosine phosphatase, non-receptor type 3 (*PTPH1)* (Jespersen et al., 2006), Src-family protein tyrosine kinase, Fyn (*FYN*) (Ahern et al., 2005), and tyrosine 3-monooxygenase/tryptophan 5-monooxygenase activation protein (*14-3-3)* (Allouis et al., 2006).

Calmodulin (*CALM1*) binds an IQ motif on the carboxy-terminal tail of $Na_v1.5$ (Shah et al., 2006; Wingo et al., 2004). Data from structural analyses and heterologous co-expression studies suggest that calmodulin interacts with the inactivation gating structures of $Na_v1.5$ and modify channel availability in response to Ca^{2+} (Shah et al., 2006; Wingo et al., 2004). The results from these studies have been conflicting regarding the specific form and state of inactivation affected, or not, by calmodulin (Maltsev et al., 2008; Tan et al., 2002). Recent studies in failing dog heart, and in TSA201 cells, show that the presence of Ca^{2+} and excess calmodulin results in a hyperpolarizing shift in the steady-state inactivation curve of $Na_v1.5$ (Maltsev et al., 2008; Tan et al., 2002). The authors suggest that the presence of Ca^{2+} and excess calmodulin increases the slow component of inactivation (Maltsev et al., 2008; Shah et al., 2006; Wingo et al., 2004). However, conflicting data has been described in rabbit cardiomyocytes and other heterologous cell systems (Wagner et al., 2006). Therefore, the exact role that calmodulin plays in regulating $Na_v1.5$ remains a topic of debate.

Furthermore, the specific molecular mechanism, Ca^{2+} binding state (bound or unbound), and the conformation of the inactivation gating structure required for calmodulin to bind $Na_v1.5$ remain unresolved.

Caveolin-3 (*CAV3*) is the primary form of caveolin in striated muscle cells (Westermann et al., 2005). *CAV3* variants have been linked to both LQT3 and sudden infant death syndrome (Cronk et al., 2007; Vatta et al., 2006). Caveolin-3 knockout mice do not have a significant difference with respect to $Na_v1.5$ phenotype, however the mice develop severe cardiomyopathy (Park et al., 2002). One study showed that $Na_v1.5$ was enriched in the caveolin-3-rich detergent-free density centrifugation membrane fraction (Yarbrough et al., 2002). However, it is important to note that whether caveolin-3 directly interacts with $Na_v1.5$ has yet to be experimentally determined. Co-expression studies of *CAV3* and $Na_v1.5$ in heterologous cells resulted in persistent I_{Na} (Cronk et al., 2007; Vatta et al., 2006). Further analyses in myocytes suggest that $Na_v1.5$ rich caveolae increase I_{Na} density in response to beta-adrenergic signaling through the G-protein $G_S$alpha (Palygin et al., 2008). Moreover, the physiological-state where caveolin-3-linked $Na_v1.5$ current modulation is required is yet to be determined.

Fibroblast growth factor homologous factor 1B (*FHF1B)* associates with the carboxy-terminus of $Na_v1.5$ as revealed by yeast two-hybrid analysis and co-immunoprecipitation from heterologous cell lysates over-expressing human $Na_v1.5$ fusion protein (Liu et al., 2003). HEK293 cells expressing $Na_v1.5$ and FHF1B did not have any change in activation however, there was a -9mV (hyperpolarizing) shift in inactivation (Liu et al., 2003). Heterologous co-

expression of a LQT3 (*SCN5A*) variant D1790G, blocked this electrophysiological affect and the *in vitro* binding of FHF1B (Liu et al., 2003). However, the physiological importance of FHF1B activity has not yet been demonstrated. Moreover, the nature of the interaction of FHF1B and $Na_v1.5$ is poorly understood. Additionally, there are no diseases currently linked to variants in *FHF1B.* Therefore, the physiological importance of FHF1B in regulating $Na_v1.5$ remains unknown.

Protein tyrosine phosphatase, non-receptor type 3 (*PTPH1)* is proposed to interact with $Na_v1.5$ as suggested by *in vitro* binding and pull-down analyses (Jespersen et al., 2006). The carboxy-terminus of $Na_v1.5$ has a PDZ-binding domain motif that was shown to be critical for interaction with PTPH1 in this study (Jespersen et al., 2006). Co-expression studies of PTPH1 with $Na_v1.5$ in HEK293 cells causes a hyperpolarizing shift in steady-state inactivation however, there is no affect on channel activation (Jespersen et al., 2006). Experiments with PTPH1 were complemented by the use of constitutively active Fyn, a protein tyrosine kinase (Jespersen et al., 2006). Co-expression studies incorporating constitutively active Fyn suggest that phosphorylation changes the stability of the inactivation gate, and shifts inactivation to more positive potentials (Ahern et al., 2005). However the physiological importance of the contrasting activities of PTPH1 and protein tyrosine kinase Fyn has not yet been demonstrated.

Tyrosine 3-monooxygenase/tryptophan 5-monooxygenase activation protein (*14-3-3)* was identified as an interacting protein using the cytoplasmic interdomain linker (DI-DII) of $Na_v1.5$ in a yeast two-hybrid screen (Allouis et al.,

2006). 14-3-3η was effectively co-immunoprecipitated with $Na_v1.5$ from heterologous cells expressing $Na_v1.5$ and mouse heart lysates (Allouis et al., 2006). Co-expression experiments demonstrated that 14-3-3η caused a hyperpolarizing shift in inactivation and increased the time for recovery from inactivation (Allouis et al., 2006). These studies suggest that 14-3-3η can modify the availability of $Na_v1.5$ and the kinetics of channel activity (Allouis et al., 2006). However, the physiological importance or effect of 14-3-3η with regard to $Na_v1.5$ activity is yet to be determined and requires the development of transgenic animal models to deductively address these questions.

The complex regulatory mechanisms that control the biophysical activity and membrane targeting of $Na_v1.5$ are the focus of research in several labs around the world. Further investigation of these potential interaction proteins will provide important clues in understanding these complex regulatory mechanisms. Interestingly, ankyrin family proteins have been linked to the membrane activity of other channels and transporters as well as $Na_v1.5$. The ankyrin family of proteins will be discussed in Chapter IV.

CHAPTER IV

ANKYRINS AND DISEASE

Ankyrins are a family of multivalent membrane-adaptor proteins first identified in the erythrocyte over twenty five years ago as a link between the anion exchanger and the spectrin-based cytoskeleton. Since their initial discovery, ankyrin function has been linked to protein targeting and membrane domain organization in a variety of cell-types including erythrocytes, neurons, epithelial cells, and cardiomyocytes. Recent findings demonstrate that dysfunction in ankyrin-based cellular pathways in heart may lead to human ventricular tachycardia and sudden cardiac death.

Specifically, mutations in ankyrin-based cellular pathways potentially lead to two cardiac arrhythmia syndromes including ‘ankyrin-B syndrome’, an atypical long QT syndrome (previously referred to as type 4 long QT syndrome) and Brugada syndrome (Lowe et al., 2008; Mohler et al., 2004; Mohler et al., 2003b). This chapter will provide a general description of the ankyrin family and detail recent findings implicating key roles for ankyrin-based cellular pathways in normal cardiac function.

Ankyrins: Required for membrane protein targeting

Ankyrins are a family of ubiquitously-expressed membrane-adaptor proteins required for targeting structurally-unrelated ion channels, transporters, and cell adhesion molecules to specialized membrane domains (reviewed in (Bennett and Baines, 2001)). Human ankyrin polypeptides including ankyrin-R (for 'restricted'), ankyrin-B (for 'broad'), and ankyrin-G (for 'giant' or 'general') are encoded by three unique genes localized to human chromosomes 8p11 (*ANK1*), 4q25-27 (*ANK2*), and 10q21 (*ANK3*), respectively. While present in other metazoans including *Drosophila* (two genes *Dank1*, *Dank2*) and *Caenorhabditis elegans* (one gene, *unc-44*), ankyrins have not been identified in the genomes of lower organisms including yeast (*Saccharomyces cerevisiae,* or *Schizosaccharomyces pombe*). Canonical ankyrins (210 kDa ankyrin-R, 220 kDa ankyrin-B, and 190 kDa ankyrin-G) have four major domains including a large NH_2-terminal membrane-binding domain, a central spectrin-binding domain, a death domain, and a C-terminal regulatory domain (Figure 6).

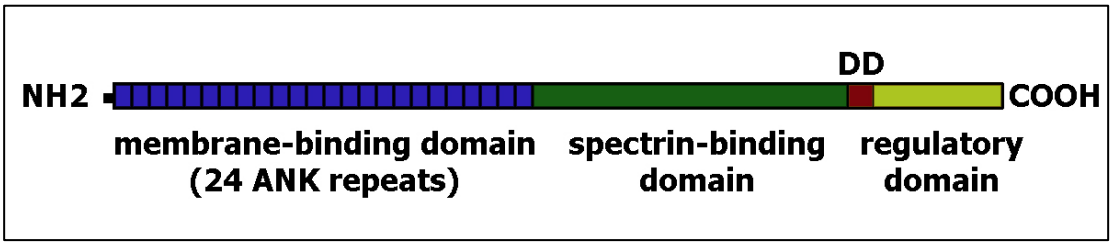
DD
NH2
COOH
membrane-binding domain
(24 ANK repeats)
spectrin-binding
domain
regulatory
domain

Figure 6.

Figure 6. Canonical ankyrin polypeptide domain organization. Ankyrins contain a NH2—terminal membrane-binding domain comprised of 24 \consecutive ANK repeats (blue), a spectrin-binding domain (green), a death domain (red), and a C-terminal regulatory domain.

The ankyrin membrane-binding domain is comprised of 24 consecutive *ANK* repeats (a 33 amino acid protein interaction domain; (Sedgwick and Smerdon, 1999). Together, these *ANK* repeats create a large super-helix which creates binding sites for a variety of structurally-diverse membrane proteins. Characterized ankyrin-binding proteins include ion channels and transporters of the plasma membrane (Na/K ATPase (Koob et al., 1988; Morrow et al., 1989), Na/Ca exchanger (Li et al., 1993), anion exchanger (Bennett and Stenbuck, 1979b; Jons and Drenckhahn, 1998), H/K ATPase (Morgans and Kopito, 1993), voltage-gated Na_v channels (Srinivasan et al., 1988), ammonium transporter (Lopez et al., 2004), and endoplasmic/ sarcoplasmic reticulum (inositol 1, 4, 5 trisphosphate receptor, ryanodine receptor; (Mohler et al., 2005a); Figure 7).

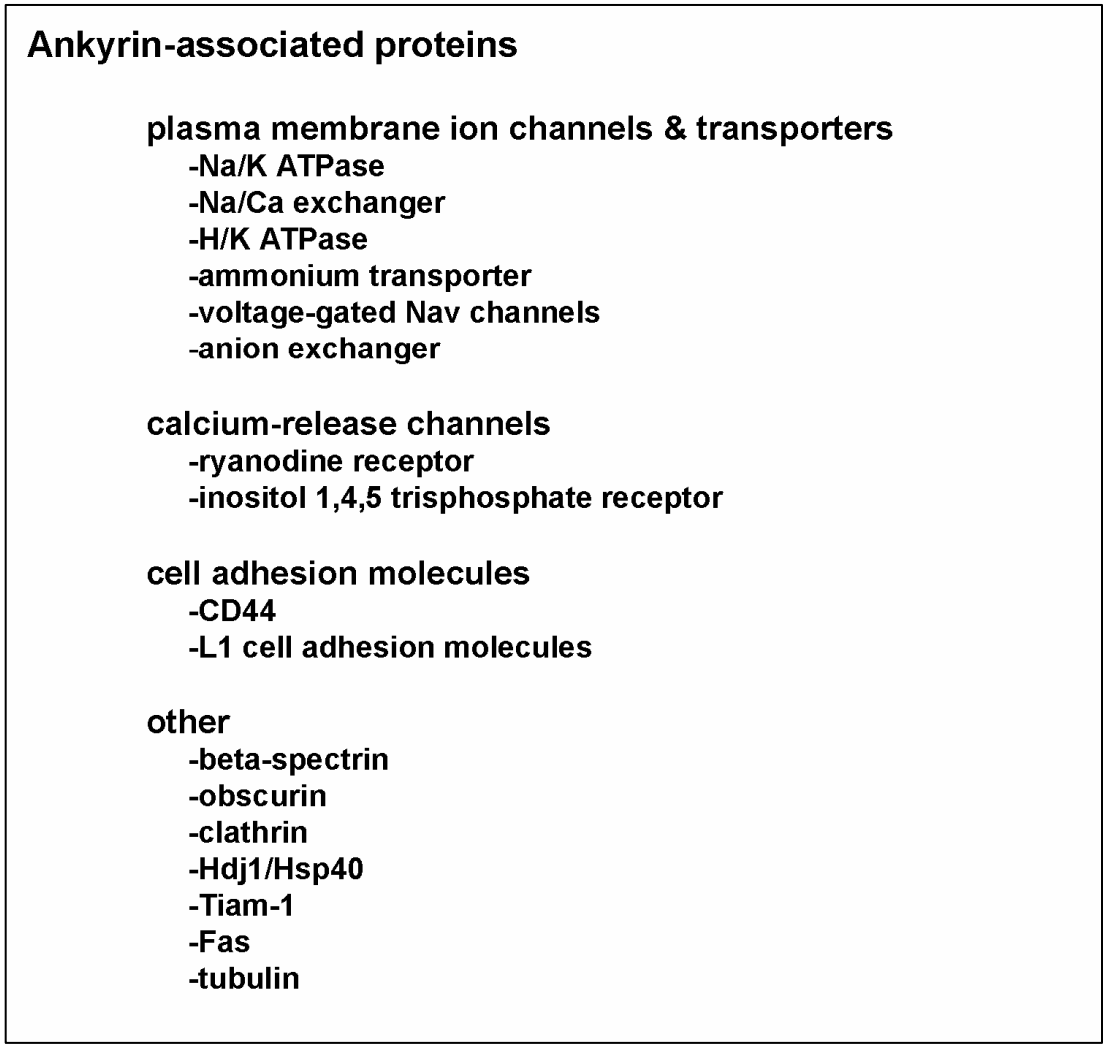
Ankyrin-associated proteins
plasma membrane ion channels & transporters
-Na/K ATPase
-Na/Ca exchanger
-H/K ATPase
-ammonium transporter
-voltage-gated Nav channels
-anion exchanger
calcium-release channels
-ryanodine receptor
-inositol 1,4,5 trisphosphate receptor
cell adhesion molecules
-CD44
-L1 cell adhesion molecules
other
-beta-spectrin
-obscurin
-clathrin
-Hdj1/Hsp40
-Tiam-1
-Fas
-tubulin

Figure 7.

Figure 7. Ankyrins associate with diverse membrane-associated, cytoskeletal, and cytosolic proteins.

The ankyrin membrane-binding domain also associates with cell adhesion molecules including L1 cell adhesion molecules (L1CAMs; (Davis and Bennett, 1994)) and CD44 adhesion molecules ((Lokeshwar et al., 1994); Figure 7). The central 62 kDa domain of ankyrin contains binding activity for the beta-spectrin family of actin-binding proteins (Bennett and Stenbuck, 1979a). Ankyrin/beta-spectrin interactions are critical for normal physiological function of multiple cell types including erythrocytes (Bennett and Baines, 2001). Identification of additional roles for this large domain is an active area of ankyrin research as recent findings suggest a key role for the C-terminus of the spectrin-binding domain in ankyrin-B-dependent function in human heart (described below). In addition to membrane-binding and spectrin-binding domains, ankyrins display a 90 amino acid death domain of unknown function (Figure 6). Based on the ability of death domain secondary structures to form low affinity homo- or hetero-dimers, this domain may be responsible for facilitating the formation of large complexes of ankyrin multimers in cellular environments where ankyrin concentrations are extremely high. Finally, canonical ankyrins express a C-terminal regulatory domain (Figure 6). This region is the most divergent between ankyrin gene products suggesting a critical role for this domain in specifying gene-specific function *in vivo*. The recent identification of nine different loss-of-function mutations in the ankyrin-B C-terminus associated with human cardiac arrhythmia (*described below*) further supports a key role for this domain for ankyrin-specific function. Based on *in vitro* experiments, ankyrin C-terminal domains have been predicted to associate *in vivo* with diverse cytoplasmic

proteins including the molecular co-chaperone Hdj1/Hsp40 (Mohler et al., 2004b) and obscurin (Bagnato et al., 2003) and the large myofibrillar protein titin (Kontrogianni-Konstantopoulos and Bloch, 2003) .

'Ankyrin-B Syndrome' A new class of cardiac arrhythmia

Autosomal-dominant type 4 long QT syndrome was first characterized in a large French kindred by Schott *et al*. in 1995 (Schott et al., 1995). Patients with this syndrome display a complex cardiac phenotype including sinus bradycardia, abnormal heart rate variability, defects in cardiac repolarization (denoted on the ECG as prolonged QT interval), and sudden cardiac death (Mohler et al., 2003). Schott et al. used the large French kindred to map the cardiac syndrome to human chromosome 4q25-27 (Schott et al., 1995), a site unique from genes previously implicated in congenital long QT syndrome. Nearly eight years later, a nucleotide variant was identified in the gene encoding ankyrin-B (*ANK2*), a non-ion channel, in affected family members of the original type 4 long QT syndrome kindred (Mohler et al., 2003). This single nucleotide transition (A-to-G transition at position 4274) was not present in non-affected family members, and was not present in a human control population which displayed normal electrocardiograms (Mohler et al., 2003). The single A4274G transition results in the change of a conserved glutamic acid-to-glycine in the C-terminus of the 220 kDa ankyrin-B spectrin-binding domain (E1425G; Figure 8).

Cardiomyocytes derived from mice heterozygous for a null mutation in ankyrin-B (ankyrin-$B^{+/-}$ mice) were utilized to determine whether the E1425G variant was an ankyrin-B loss-of-function mutation. While mice homozygous for a null mutation die shortly after birth, ankyrin-$B^{+/-}$ mice live to adulthood with ~50% reduction of 220 kDa ankyrin-B in heart (Mohler et al., 2003). Interestingly, ankyrin-$B^{+/-}$ mice share a number of common phenotypes with humans with type 4 long QT syndrome (both humans with ankyrin-B-syndrome and ankyrin-$B^{+/-}$ mice express ~50% of normal ankyrin-B) including sinus bradycardia, significant variability in heart rate, aberrant cardiac conduction (both depolarization and repolarization), stress- or exercise- induced polymorphic ventricular tachycardia, and sudden cardiac death (Mohler et al., 2003). Ankyrin-$B^{+/-}$ neonatal cardiomyocytes display approximately 50% reduction in levels of 220 kDa ankyrin-B (Mohler et al., 2002a; Mohler et al., 2003). Ankyrin-$B^{+/-}$ neonatal cardiomyocytes also exhibit significant abnormalities in spontaneous contraction rates and display abnormal cytosolic calcium transients (Mohler et al., 2003; Mohler et al., 2004d). At a molecular level, ankyrin-$B^{+/-}$ neonatal cardiomyocytes display abnormal localization and expression of Na/K ATPase, inositol 1, 4, 5 trisphosphate receptor ($InsP_3$ receptor), and Na/Ca exchanger (all ankyrin-binding proteins) while other cardiomyocyte structural proteins and ion channel/transporters (including $Na_v1.5$) are normally expressed and appropriately localized (Mohler et al., 2002b). Abnormal ankyrin-$B^{+/-}$ cardiomyocyte phenotypes, including contraction rates, calcium dynamics, and channel/transporter localizations are rescued by expression of GFP-220 kDa ankyrin-B but not GFP-190 kDa ankyrin-

G (Mohler et al., 2002a). Therefore, abnormal cellular phenotypes observed in ankyrin-B$^{+/-}$ neonatal cardiomyocytes are due to monogenic loss of ankyrin-B expression. Moreover, these results demonstrate that ankyrin-B and ankyrin-G polypeptides have non-redundant roles for ion channel and transporter targeting in heart (Mohler et al., 2002a). More importantly, these data indicated that ankyrin-B$^{+/-}$ neonatal cardiomyocyte rescue system could be used to test potential ankyrin-B loss-of-function mutations.

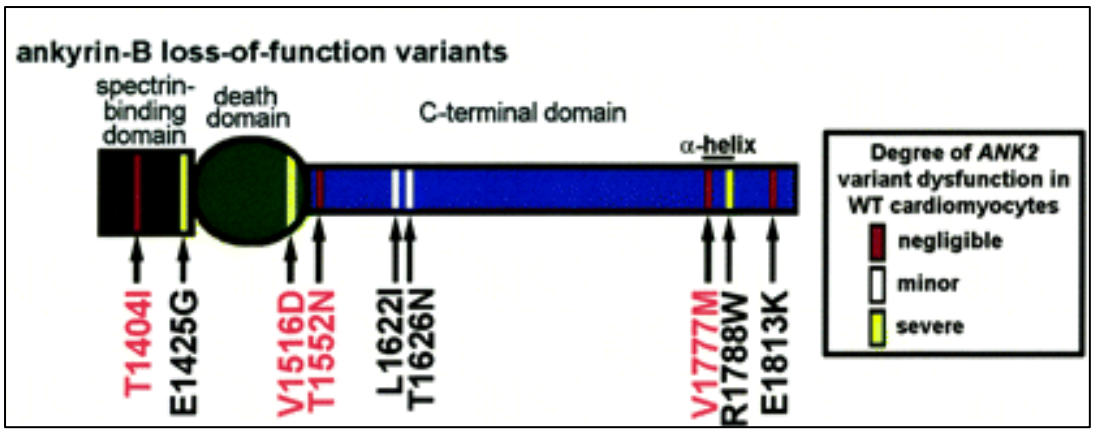
ankyrin-B loss-of-function variants
spectrin-binding domain
death domain
C-terminal domain
α-helix
T1404I
E1425G
V1516D
T1552N
L1622I
T1626N
V1777M
R1788W
E1813K
Degree of ANK2 variant dysfunction in WT cardiomyocytes
negligible
minor
severe

Figure 8.

Figure 8. Spectrum of ankyrin-B loss-of-function mutations associated with human polymorphic ventricular tachycardia. Figure from Mohler et al. *Circulation* 2007.

GFP-220kDa ankyrin-B E1425G has similar localization and expression to GFP-220 kDa ankyrin-B, and therefore likely does not represent a structural mutation (Mohler et al., 2003; Mohler et al., 2004d). However, in contrast to GFP-220 kDa ankyrin-B, expression of GFP-220 kDa ankyrin-B E1425G does not rescue abnormal spontaneous contraction rates, abnormal calcium dynamics, or abnormal ion channel and transporter localizations in ankyrin-$B^{+/-}$ cardiomyocytes (Mohler et al., 2004d). These results demonstrate that the E1425G mutation associated with cardiac arrhythmia is a loss-of-function mutation in cardiomyocytes. These data represented the first evidence for a new class of cardiac arrhythmia due to a mutation of a non-ion channel or associated subunit. Since the ankyrin-B E1425G mutation is localized near the C-terminus of the spectrin-binding domain (see Figure 8), it is unlikely to interfere with ankyrin-B binding activity for membrane proteins (binding sites in N-terminal membrane-binding domain). Therefore, this mutation may block binding of ankyrin-B to a specific regulatory protein or represent a key regulatory site for ankyrin-B-specific function (multiple potential phosphorylation sites near E1425). The molecular mechanism underlying the E1425G mutation is an active area of research by multiple ankyrin laboratories.

Since the initial identification of the E1425G ankyrin-B loss-of-function mutation, four additional loss-of-function mutations have been identified in humans with polymorphic ventricular tachycardia (Mohler et al., 2004d). Interestingly, all of these mutations are localized in the divergent ankyrin-B C-terminal regulatory domain (Figure 8; L1622I, T1626N, R1788W, E1813K)

(Mohler et al., 2004d). Like the E1425G mutation, the underlying molecular consequences of the new ankyrin-B mutations are unknown and a current focus of our lab.

Cardiomyocytes derived from adult ankyrin-$B^{+/-}$ mice display normal action potentials (Mohler et al., 2003). These results are consistent with the normal expression and localization of voltage-gated Na_v channels, K^+ channels, and voltage-gated Ca^{2+} channels in ankyrin-$B^{+/-}$ adult cardiomyocytes (Mohler et al., 2003). However, cardiomyocytes derived from adult ankyrin-$B^{+/-}$ mice display aberrant elevated calcium transients (Mohler et al., 2003). Elevations in ankyrin-$B^{+/-}$ calcium transients are explained by the reduction and abnormal localization of both Na/K ATPase and Na/Ca exchanger in these cells (Mohler et al., 2004a). Reduced Na/K ATPase expression would elevate intracellular Na^+ levels and further reduce the activity of the Na/Ca exchanger (expression already reduced in ankyrin-$B^{+/-}$ cells). Reduced Na/Ca exchanger activity reduces calcium export. Consequently, excess calcium is pumped into internal stores leading to increased sarcoplasmic reticulum calcium load and elevations in calcium transients. Elevations in calcium transients may lead to the observed early and delayed after-depolarizations and extra-systoles when ankyrin-$B^{+/-}$ cells are stimulated with isoproterenol (Mohler et al., 2004d). Therefore, ventricular arrhythmia due to ankyrin-B dysfunction in humans is likely a direct result of calcium-induced spontaneous depolarization episodes in the face of catecholaminergic stimulation.

Recently identified probands with ankyrin-B loss-of-function mutations are redefining type 4 long QT syndrome as a new cardiac syndrome distinct from classic long QT syndromes. New probands with E1425G, L1622I, T1626N, R1788W, and E1813K mutations display cardiac phenotypes similar, but not identical to the original French kindred (Mohler et al., 2004d; Zhang et al., 2004). For example, probands with ankyrin-B mutations may present with cardiac arrhythmia with sinus bradycardia, atrial fibrillation, idiopathic ventricular fibrillation, and polyphasic T waves (Mohler et al., 2004d; Zhang et al., 2004). However, unlike the original French kindred, not all probands or affected family members display significant QTc abnormalities (Mohler et al., 2004d; Schott et al., 1995; Zhang et al., 2004). While this syndrome is distinct from classic long QT syndromes, humans with ankyrin-B loss-of-function mutations may still display striking cardiac phenotypes including polymorphic ventricular tachycardia in response to emotional or physical stress, syncope, and sudden cardiac death (Zhang et al., 2004). Therefore, the most significant common clinical features of 'ankyrin-B-syndrome' are pleiotropy in the phenotype and a high rate of sudden cardiac death in the patient pedigrees.

Dysfunction in ankyrin-G-based pathways

Rhythmic contraction of the heart requires rapid and coordinated waves of depolarization. This depolarization is mediated by the activity of cardiac voltage-gated Na (Na_v channels) . $Na_v1.5$, encoded by *SCN5A*, is the major voltage-

gated Na_v channel expressed in vertebrate heart (Bezzina et al., 2001; Brugada and Brugada, 1992; Wang et al., 1995; Wedekind et al., 2001). Human mutations in $Na_v1.5$ may result in a variety of fatal inherited cardiac arrhythmias including Brugada syndrome, type 3 long QT syndrome, progressive cardiac conduction disorder (Lenègre disease) and sudden infant death syndrome (Bezzina et al., 2001; Brugada and Brugada, 1992). Ability of $Na_v1.5$ to coordinate cardiomyocyte depolarization is determined by its biophysical properties as well as its proper localization at excitable membrane domains in heart. $Na_v1.5$ biophysical properties have been a major area for molecular cardiology research for the past decade. In contrast, the identity of the molecular mechanisms and cellular pathways underlying $Na_v1.5$ targeting in heart have remained an important, but unresolved question.

Recent findings suggest that a second ankyrin-based pathway (ankyrin-G) is required for normal cardiac function (ankyrin-B and ankyrin-G are encoded by distinct genes). Specifically, ankyrin-G-dependent function may be required for $Na_v1.5$ targeting to excitable membranes in heart (Davis et al., 1996; Kordeli et al., 1995). A potential role for ankyrin-G in $Na_v1.5$ targeting in heart was first hypothesized based on the importance of ankyrin-G-based pathways for Na_v channel targeting in brain. Neuronal Na_v channel isoforms including $Na_v1.2$ and $Na_v1.6$ directly associate with ankyrin-G from brain (Flucher and Daniels, 1989; Kordeli et al., 1998; Wood and Slater, 1998). Additionally, ankyrin-G and neuronal voltage-gated Na_v channels are co-expressed at multiple excitable membrane domains including nodes of Ranvier, axon initial segments, and the

neuromuscular junction . Mice which have targeted ankyrin-G gene knock-out in the cerebellum (described in ; ankyrin-G homozygous null in cerebellum, other tissues maintain normal ankyrin-G expression) are viable, but display abnormal clustering of neuronal Na_v channel isoforms at nodes of Ranvier in peripheral nerve and axon initial segments (Jenkins and Bennett, 2001; Zhou et al., 1998). Loss of normal Na_v channel localization leads to abnormal neuronal action potentials in these mice and pronounced ataxia (Jenkins and Bennett, 2001; Zhou et al., 1998). These *in vivo* findings demonstrate that ankyrin-G-based cellular pathways are essential for Na_v channel targeting to excitable membranes of brain.

190 kDa ankyrin-G is highly expressed in ventricular cardiomyocytes, co-expressed with $Na_v1.5$ at excitable membrane domains including intercalated discs and transverse-tubules, and co-immunoprecipitates with $Na_v1.5$ from detergent-soluble extracts from heart (Mohler et al., 2004c). Direct interaction between $Na_v1.5$ and ankyrin-G requires a nine amino acid motif in the $Na_v1.5$ DII-III cytoplasmic loop (Garrido et al., 2003; Lemaillet et al., 2003). This interaction motif is nearly identical to the nine amino acid ankyrin-G-interaction motif recently identified by two independent groups (Garrido et al., 2003; Lemaillet et al., 2003; Mohler et al., 2004c).

The significance of the ankyrin-G/ $Na_v1.5$ interaction for cardiac function was established by the recent identification of a new human *SCN5A* mutation. This patient, heterozygous for an $Na_v1.5$ E1053K mutation displays Brugada syndrome, an autosomal dominant arrhythmogenic disease characterized by

right bundle branch block, ventricular arrhythmia, and risk of sudden cardiac death (Mohler et al., 2004c). Interestingly, the E1053K Brugada mutation is localized within the $Na_v1.5$ nine residue ankyrin-binding motif and eliminates ankyrin-binding activity *in vitro* (Mohler et al., 2004c).

Consistent with the loss-of-function Brugada syndrome phenotype, $Na_v1.5$ E1053K lacking ankyrin-G-binding activity is not expressed at intercalated disc or transverse-tubule membrane domains of primary ventricular cardiomyocytes (Mohler et al., 2004c). Instead, $Na_v1.5$ E1053K-positive puncta are expressed throughout the cardiomyocyte cytoplasm (Mohler et al., 2004c). One explanation for the loss of $Na_v1.5$ E1053K at the membrane surface of cardiomyocytes is that E1053K represents a structural mutation that affects $Na_v1.5$ folding and stability. However, HEK293 cells efficiently target both $Na_v1.5$ and $Na_v1.5$ E1053K to the plasma membrane (Mohler et al., 2004c). Additionally, functional experiments indicate that there is no significant difference in $Na_v1.5$ and $Na_v1.5$ E1053K current density in HEK293 cells (Mohler et al., 2004c). In addition to the abnormal targeting phenotype, $Na_v1.5$ E1053K displays abnormal channel properties when analyzed in HEK293 cells (Mohler et al., 2004c). These results suggest a potential new function for ankyrin-G for ion channel gating. This potential new role for ankyrin-G will be an obvious focus of future research. The distinct trafficking phenotypes of $Na_v1.5$ E1053K in cardiomyocytes versus HEK293 cells (epithelial-derived) suggest that Na_v targeting mechanisms are cell-type specific. Consistent with these data, previous findings demonstrate that cardiomyocytes display unique protein targeting/trafficking pathways not present

in epithelial-based cells for localization of membrane ion channels and transporters (Mohler et al., 2004c). Together, these data demonstrate that cardiac ion channel and transporter targeting must be studied in the physiological context of the cardiomyocyte.

In summary, recent results identify the first *in vivo* evidence for a cellular pathway potentially required for $Na_v1.5$ localization in heart. Human mutations that interfere with this pathway lead to loss of normal $Na_v1.5$ channel targeting, reduced I_{Na}, and risk of fatal cardiac arrhythmia (Brugada syndrome). Although largely circumstantial, these data support a potential role for an ankyrin-G–dependent pathway in $Na_v1.5$ targeting to excitable membrane domains in the heart. Therefore, we hypothesize that $Na_v1.5$ is targeted to the cardiomyocyte membrane in an ankyrin-G-dependent manner.

CHAPTER V

ANKYRIN-G IS REQUIRED FOR VOLTAGE-GATED SODIUM CHANNEL 1.5 TARGETING

Introduction

In this study, we report new data that conclusively links ankyrin-G activity and $Na_v1.5$ membrane expression and localization in cardiomyocytes. Using viral-mediated small hairpin RNA (shRNA) transfer into primary cardiomyocytes, we demonstrate that a full complement of ankyrin-G expression is required for $Na_v1.5$ expression and membrane localization. Specifically, reduced ankyrin-G expression decreases (1) total cellular $Na_v1.5$ expression, (2) efficient membrane localization, and (3) total Na^+ membrane current. We also demonstrate that although ankyrin-G is required for normal $Na_v1.5$ membrane expression, reduced ankyrin-G expression does not affect $Na_v1.5$ channel kinetics. Finally, we report the structural requirements for direct ankyrin-G–$Na_v1.5$ interactions and show that direct intermolecular interaction between these two molecules is required for efficient channel membrane localization. Together, these data identify the first clear cellular pathway for Na_v channel trafficking in the heart.

Materials and Methods

In order to test our hypothesis we had to develop a primary cardiomyocyte system with reduced ankyrin-G expression. We chose a lentiviral shRNA delivery system due to the difficulty in transducing cardiomyocyte cultures. We used neonatal cardiomyocytes for the majority of the experiments due to the amenable use of lipid-mediated transfection strategies. We also used adult cardiomyocytes to ensure the ankyrin-dependent pathway was important in adult cells. To assure that ankyrin-G expression was reduced and to assess the affect of ankyrin-G reduction on cellular protein expression we used immunoblotting and immunofluorescent confocal microscopy. Immunoelectron micrographs were generated to analyze the proximity and amount of $Na_v1.5$ associated with ankyrin-G at the membrane. We used electrophysiology to assess the functional effect of ankyrin-G reduction in cardiomyocyte cultures. We defined the sites on the ankyrin-G membrane-binding domain required to interact with $Na_v1.5$ by generating fusion proteins and performing binding studies.

shRNA targets/cDNA constructs

Ankyrin-G–specific shRNA targets were selected based on their unique sequence presence of flanking 5' AA and 3' TT nucleotides (Brummelkamp et al., 2002). Human- and rat-specific targets were conferred by three unique nucleotides located at wobble positions. The primer sequences include a nine

nucleotide linker flanked by sense and reverse complement of sense to facilitate hairpin formation and cleavage sites for Drosha (Figure 9). Primers were created (Operon), annealed, and ligated into a modified pFIV-HI-Puro lentiviral vector (System Biosciences, Inc.). The vector was modified to contain YFP driven by an independent H1PGK promoter to track transduced cells. Feline immunodeficiency viruses were titered before transduction experiments based on visual transduction of YFP (>85%) in HEK293 cells.

Ankyrin-G constructs were generated using 190-kD ankyrin-G cDNA which was cloned into pEGFPN3 (CLONTECH; Palo Alto, CA) for GFP fusion expression. GFP 190-kD ankyrin-G mutant constructs were made using Quik Change Mutagenesis (Stratagene). Loop mutations were designed to replace *ANK* repeat beta-hairpin loop tip residues with two alanines. Rescue constructs were made using GFP 190-kD ankyrin-G and *ANK* repeat mutants R14 and R15. All constructs were completely sequenced and confirmed to express protein in HEK293 cells.

Immunoblots

After viral and/or rescue treatment, cells were collected into PBS, pH 7.4. Cells were lysed using radioimmunoprecipitation assay buffer (50 mM Tris, 150 mM NaCl, 0.5% deoxycholic acid, 0.1% sodium dodecyl sulphate pH 8) containing protease inhibitor cocktail. Detergent-soluble fractions were collected after high speed centrifugation, and protein concentrations were determined

using a bicinchoninic acid protein assay kit (Thermo Fisher Scientific). Equal quantities of protein (20 µg) were analyzed by SDS-PAGE using NuPage 3-8% Tris-acetate gels (Invitrogen) and immunoblotting after transfer to nitrocellulose. Equal loading was assessed by transfer to Ponceau S and blotting with NHERF1.

Neonatal rat cardiomyocytes

Hearts were dissected from postnatal day 1 rats and placed into Ham's F10 with 1% penicillin/streptomycin. Hearts were then aspirated of remaining blood, excised from atrial tissue and transferred to 1.5ml of Ham's F10 with 1% penicillin/streptomycin with 0.05% trypsin EDTA. The hearts were then minced using extra fine scissors and forceps into ~1.0mm pieces. The diffusate was then triturated with a 1ml filtered tip ten times. The trituration step was repeated after each of two fifteen minute intervals of incubation at 37°C. Then 200µl each of collagenase (0.2mg/ml) and soybean trypsin inhibitor (2mg/ml) were added triturated and incubated for forty-five minutes at 37°C. The cell slurry was then collected and spun down at 1600 rpm for five minutes. The enzyme containing supernatant was removed and cells were resuspended in complete media (1:1 DMEM: Ham's F-10 with 1% penicillin/streptomycin and 20% fetal bovine serum. Cells were placed in 6-well tissue culture plates at one heart per well density and cultured for three hours at 37°C with 5% CO_2 and 95% humidity (Bhasin et al., 2007). This step assists in the clearance of fibroblasts from the cell cultures and enriches the proportion of cardiomyocytes to fibroblasts. After the pre-clearance

step cells are transferred to Fibronectin (50ng/ml) coated glass bottomed Mattek plates for imaging and 3.5 cm culture plates for biochemical analyses using complete medium. After eighteen hours in culture the cells are washed with serum free 1:1 DMEM/F-10 media and the media is replaced with defined media (1:1DMEM:F-10, 0.10 µg/ml insulin, 0.50 µg/ml transferrin, 0.10 nM LiCl, 0.10 nM $NaSeO_4$, and 0.01 nM thyroxine). The cells are maintained with media changes every twenty-four hours.

Adult cardiomyocytes

Myocytes were isolated from 250–300 g Sprague-Dawley rats (Grueter et al., 2006). Rats were anesthetized with 50mg/g avertin (200µl/10g intraperitoneal). Hearts were extracted and placed in Ca^{2+} free Tyrode's solution at 10°C. Fatty tissue and extraneous vasculature was removed and the aorta was affixed to perfusion cannula and perfused with calcium free Tyrode's solution for six minutes at 38°C. The Langendorff device was then switched to collagenase II/protease digestion buffer and perfused for sixteen minutes. The ventricular myocardium was then removed from the cannula, minced, and cells were then dissociated by trituration and washed with culture media. Acutely isolated cardiomyocytes were then plated at high density (~2 x 10^6 per well), infected with rat-specific ankyrin-G shRNA virus or control virus for nine hours, and maintained for twenty-two hours at 37°C before experiments.

Binding experiments

GFP 190-kD ankyrin-G and mutants were expressed in HEK293 cells and purified using affinity-purified GFP Ig coupled to protein A agarose beads. Cells were lysed in homogenization buffer (50 mM Tris HCl, 10 mM NaCl, 0.32 M sucrose, 5 mM Na EDTA, 2.5 mM Na EGTA, 1 mM PMSF, 1 mM 4-(2-aminoethyl) benzenesulfonylfluoride hydrochloride (AEBSF), 10 µg/ml leupeptin, and 10 µg/ml pepstatin) plus 1.0% Triton X-100 and 0.5% deoxycholate (Mohler et al., 2005a). The extract was centrifuged at 100,000 *g*, and the supernatant was incubated with GFP Ig coupled to protein A–Sepharose. $Na_v1.5$ DII–DIII cytoplasmic loop was subcloned into pET15b for expression and purification as a hexahistidine fusion protein. Purified proteins were incubated with GFP or control Ig coupled to protein A–Sepharose. Protein bound to each mutant GFP 190-kD ankyrin-G was eluted, analyzed by immunoblotting, normalized for relative GFP ankyrin-G expression, and compared with wild-type GFP 190-kD ankyrin-G binding.

Statistics

When appropriate, data were analyzed using a two-tailed *t* test, and $P < 0.05$ was considered significant. Values are expressed as the mean ± SD.

Virus generation

Ankyrin-G shRNAs were engineered into the pFIV lentiviral vector and packaged into viral pseudoparticles (System Biosciences, Inc.). Constructs were cotransfected with packaging plasmids (pFIV-34N and pVSV-G) into HEK293TN cells using Effectene. The HEK293FT cells were seeded the day before transfection at a density that would allow 40% confluence the day of transfection. Lipid complexes were incubated on the cells overnight and replaced with DMEM with 1% penicillin/streptomycin and 4% fetal bovine serum. The viral pseudoparticle-containing supernatant was harvested after two days in culture and concentrated using Centriplus YM-30 columns. The concentrate was stored at –80°C until used. Fresh HEK293 cells were subsequently infected with the viral pseudoparticles for nine hours and assayed for transduction, eighteen to thirty hours post-infection using confocal imaging with the argon laser set to a 514 nm excitation wavelength.

Immunostaining/confocal microscopy

Cardiomyocytes were isolated, cultured, and processed for immunofluorescence as described previously (Cunha et al., 2007; Mohler et al., 2003). Secondary antibodies included anti–rabbit and anti–mouse Igs conjugated to AlexaFluor488 or 568 (Invitrogen). Phalloidin-conjugated AlexaFluor633 was used for double-labeling experiments in Fig. 13. After secondary antibody

treatment, cells were extensively washed, covered with Vectashield imaging medium (Vector Laboratories), and coverslips (#1) were applied. Images were collected on a confocal microscope (510 Meta; Carl Zeiss, Inc.) with a 63x oil 1.40 NA or 40x oil 1.30 NA lens (pinhole equals 1.0 airy disc; Carl Zeiss, Inc.) using imaging software (release version 4.0 SP1; Carl Zeiss, Inc.). Images were collected using similar confocal protocols at room temperature. In experiments in which both AlexaFluor488 and YFP were analyzed, the emission signal from AlexaFluor488 was collected from 500 to 515 nm, and the emission from YFP was collected from 530 to 565 nm. Because YFP was only used to identify virus-positive cells (versus identifying the localization of an YFP fusion protein), we used minimal laser power and detector gain (thus the minimal YFP image resolution) to collect YFP images to prevent potential signal bleed-through to the AlexaFluor488 image, in which protein immunolocalization was crucial. For images in Figs. 11, 12, and Fig.16, the YFP image was pseudocolored. Images were imported into Photoshop CS (Adobe) for cropping and linear contrast adjustment.

Plasma membrane sheet preparation/immunoelectron microscopy

Ventricular cardiac myocytes from adult Sprague-Dawley rats were obtained as described previously (Grueter et al., 2006). Immunolabeling of the membrane sheets was performed by placing the grids on drops of primary antibody solution for 1 h on ice and rinsing six times for 5 min in PBS containing

BSA. Grids were then incubated on drops of gold-conjugated secondary antibody solution (5 nm of goat anti–rabbit diluted 1:50 or 10 nm of goat anti–mouse diluted 1:50 in PBS containing BSA; Electron Microscopy Sciences) for 1 h on ice. Grids were then rinsed three times for 5 min in PBS containing BSA followed by a 2-min fixation in 2.5% glutaraldehyde. Finally, the grids were washed for 5 min in deionized water before being allowed to air dry. Negative controls included grids labeled with secondary antibody alone. Grids were visualized on a transmission electron microscope (H-70000; Hitachi).

Antibodies

Antibodies used include anti-$Na_v1.5$ (Alomone Laboratories), anti-NCX1 (Swant), anti–connexin43 (Invitrogen), anti-$Ca_v1.2$ (Affinity BioReagents), anti-NHERF1 (Sigma-Aldrich), affinity-purified Igs against ankyrin-B, ankyrin-G, and GFP (monoclonal and polyclonal), and goat anti–rabbit AlexaFluor568 (Invitrogen).

Electrophysiology experiments

Voltage-dependent Na^+ and Ca^{+2} currents were measured using standard patch clamp techniques. Whole-cell currents were recorded with an amplifier (Axopatch 200B; MDS Analytical Technologies), and the analogue signal was filtered using an eight-pole filter (Bessel) with a bandwidth of 5 kHz and was

digitized at a sampling rate of 50 kHz. Borosilicate glass capillaries (VWR Scientific) were used to fabricate patch pipettes. Electrode resistances ranged from 1 to 1.5 MΩ, and seal resistances were 1–5 GΩ. Pipette seal resistances were compensated to >85% of the uncompensated value. The whole-cell bath solution contained 10 mM NaCl, 130 mM choline chloride, 4.5 mM KCl, 1.8 mM $CaCl_2$, 2.0 mM $MgCl_2$, 10.0 mM Hepes, and 5.5 mM glucose, pH 7.35, titrated with KOH. The pipette solution contained 130 mM CsCl, 0.5 mM $CaCl_2$, 2 mM $MgCl_2$, 5 mM Na_2ATP, 0.5 mM GTP, 5 mM EGTA, and 10 mM Hepes, pH 7.3, titrated with CsOH. All electrophysiology experiments were performed at room temperature (21–23°C).

Whole-cell voltage clamp Na^+ current data were elicited from a holding potential of –120 mV to membrane potentials ranging from –110 to 30 mV in the presence of 2.0 mM $CoCl_2$. Voltage-dependent steady-state inactivation was determined using a paired two-pulse protocol. Each conditioning voltage was paired with a control after 1.5 s. A 500-ms conditioning pulse from –120 to 20 mV in 10-mV increments was followed by a test pulse to –30 mV. The test pulse in each series was separated form the conditioning pulse by a 2-ms interval to –120 mV. The steady-state inactivation curves were constructed by normalizing currents to the maximal Na^+ current elicited from a holding potential of –120 to –30 mV for a duration of 20 ms. The resulting curve was fitted using a Boltzmann distribution equation of the form $I_{Na} = I_{Na,\,max}/ (1 + \exp ([V_m – V_{1/2}]/k))$, where V_m is the conditioning pulse voltage, $V_{1/2}$ is the voltage at half-inactivation, and k is the slope factor. The whole-cell voltage clamp protocol showing I_{Na} and I_{Ca} in Fig. 5

F was elicited using the two-pulse paradigm shown in Fig. 5 G. From a holding potential of –100 mV, I_{Na} was elicited by a 30-ms pulse to –30 mV. The membrane potential was then hyperpolarized to –70 mV for 10 ms. I_{Ca} was then elicited by a 50-ms pulse to 0 mV. This protocol allowed the simple differentiation of I_{Na} from I_{Ca} as indicated by the unique I_{Ca} and I_{Na} current signatures in Fig. 5. All presented currents were normalized for cell capacitance. Data were collected and analyzed using pCLAMP 9.0 software (MDS Analytical Technologies) and OriginPro 7.5 (OriginLab Corp.). Analysis of variance was used to compare the nominal change in current density among the means. Statistical significance is defined as $P < 0.05$.

Results

Generation of cardiomyocytes lacking ankyrin-G

We developed rat cardiomyocyte primary cultures with reduced ankyrin-G expression using lentiviral-mediated delivery of shRNA. The shRNA was designed to target all identified ankyrin-G mRNAs and was specific for rodent ankyrin-G (versus human; Fig. 9, A and B). We modified the lentiviral construct to encode YFP to enable the identification of transduced cells. A human-specific ankyrin-G shRNA was generated for control experiments (Fig. 9 A).

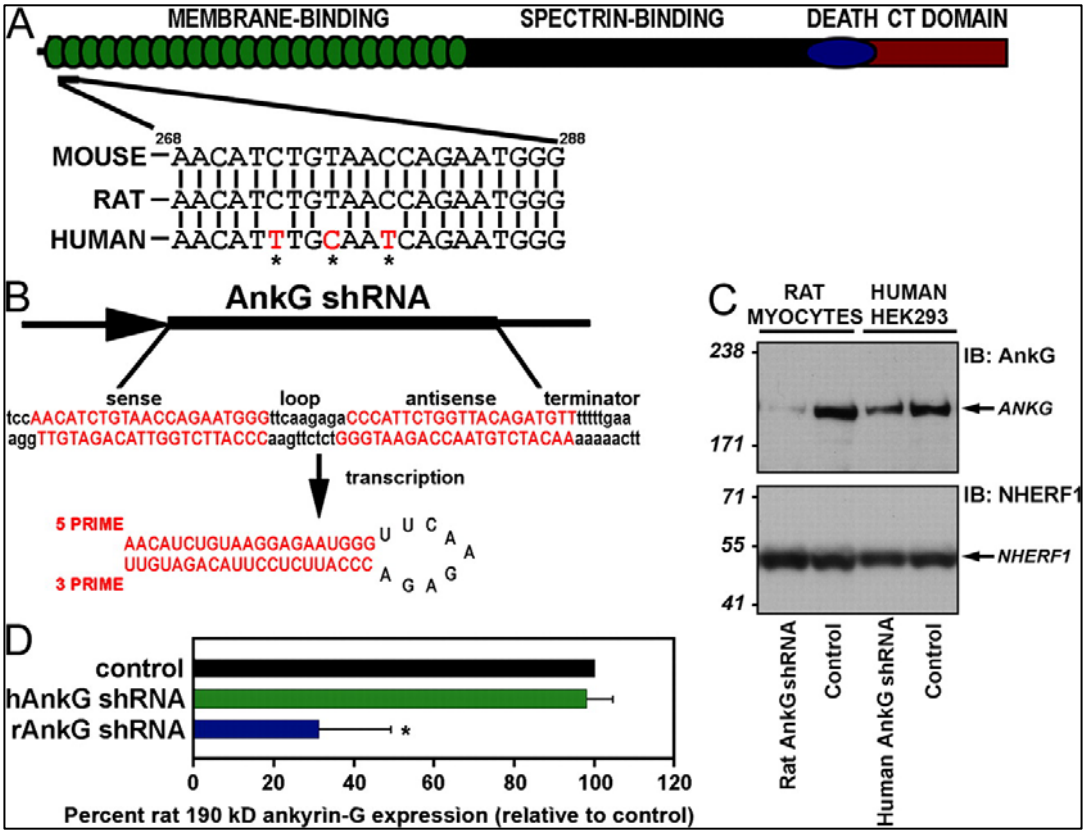
A
MEMBRANE-BINDING
SPECTRIN-BINDING
DEATH CT DOMAIN
268
288
MOUSE AACATCTGTAACCAGAATGGG
RAT AACATCTGTAACCAGAATGGG
HUMAN AACATTTGCAATCAGAATGGG
B
AnkG shRNA
sense
loop
antisense
terminator
tccAACATCTGTAACCAGAATGGGttcaagagaCCCATTCTGGTTACAGATGTTttttgaa
aggTTGTAGACATTGGTCTTACCCaagttctctGGGTAAGACCAATGTCTACAAaaaaactt
transcription
5 PRIME
AACAUCUGUAAGGAGAAUGGG
UUGUAGACAUUCCUCUUACCC
3 PRIME
U U C A A
A G A G
C
RAT MYOCYTES
HUMAN HEK293
238
171
IB: AnkG
ANKG
71
55
41
IB: NHERF1
NHERF1
Rat AnkG shRNA
Control
Human AnkG shRNA
Control
D
control
hAnkG shRNA
rAnkG shRNA
*
0
20
40
60
80
100
120
Percent rat 190 kD ankyrin-G expression (relative to control)

Figure 9.

Figure 9. Species-specific knockdown of 190-kD ankyrin-G in rat myocytes using lentiviral shRNA. (A) Domain organization of 190-kD ankyrin-G with the site of shRNA target. Rat, mouse, and human shRNA nucleotide target sequences. Note that the human 190-kD ankyrin-G target sequence has three unique nucleotides in wobble base positions (asterisks) that render this target sequence resistant to the rat shRNA. (B) The 21-nucleotide target sequence (sense) is separated by a short loop spacer sequence followed by 21 nucleotides that form the reverse complement of the target sequence. (C) Rat and human species–specific shRNAs reduce 190-kD ankyrin-G expression. Rat myocytes or human HEK293 cells were transduced with control virus, rat ankyrin-G shRNA, or human ankyrin-G shRNA. Equal quantities of protein were analyzed by immunoblotting using affinity-purified ankyrin-G Ig or an antibody to an unrelated protein, NHERF1 (loading control). Note that the rat-specific ankyrin-G shRNA effectively reduces the expression of 190-kD ankyrin-G in rat cardiomyocytes. Moreover, the expression of 190-kD ankyrin-G is reduced in HEK293 cells transduced with human-specific ankyrin-G shRNA. (D) 190-kD ankyrin-G protein levels from whole cell lysates of rat cardiomyocytes transduced with control virus, human-specific ankyrin-G shRNA virus (hAnkG shRNA), or rat-specific ankyrin-G shRNA virus (rAnkG shRNA) were analyzed by immunoblotting and quantitated. Numbers represent the mean ± SD (error bars) from four independent experiments. *, $P < 0.05$.

Rodent-specific ankyrin-G shRNA is efficient for reducing ankyrin-G expression and does not interfere with human ankyrin-G expression (Fig. 9). Introduction of rodent-specific ankyrin-G shRNA into primary rat cardiomyocytes significantly reduced ankyrin-G protein expression (Fig. 9, C and D). Likewise, human-specific ankyrin-G shRNA reduced ankyrin-G expression in human-derived HEK293 cells (Fig. 9 C). Finally, no significant decrease in ankyrin-G levels was observed in rat cardiomyocytes transduced with human-specific ankyrin-G shRNA (Fig. 9 D). Equivalent viral expression was observed in each cell system (assessed by positive YFP fluorescence).

Ankyrin-G is required for normal $Na_v1.5$ expression and localization

Rat cardiomyocytes lacking a full complement of ankyrin-G expression were used to test the role of ankyrin-G for $Na_v1.5$ expression. As shown in Fig. 9, viral transduction of ankyrin-G shRNA significantly reduces ankyrin-G expression (transduction efficiency of 80–95% based on YFP fluorescence; Fig. 10).

Moreover, a striking reduction in $Na_v1.5$ protein levels was observed in the identical cell lysates from rat-specific ankyrin-G shRNA virally transduced myocytes (Fig. 10). This reduction was specific to $Na_v1.5$, as expression differences in cardiomyocyte membrane–associated proteins, including NHERF1, connexin43, ankyrin-B, $Ca_v1.2$ (Fig. 10), SERCA2, Na/K ATPase, or Na/Ca exchanger (not depicted), were not observed.

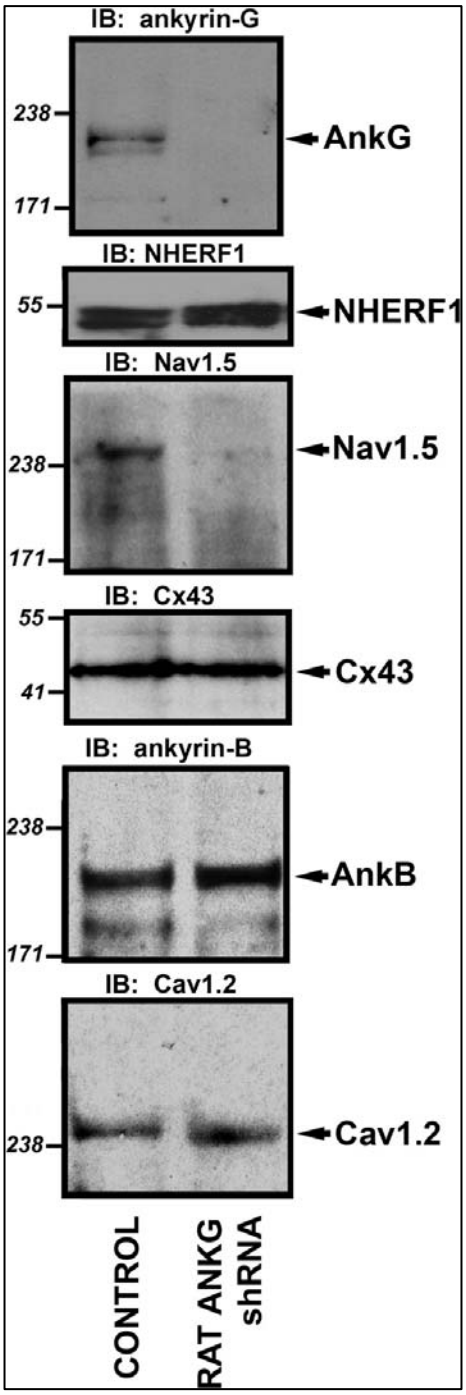
IB: ankyrin-G
238
171
AnkG
IB: NHERF1
55
NHERF1
IB: Nav1.5
238
171
Nav1.5
IB: Cx43
55
41
Cx43
IB: ankyrin-B
238
171
AnkB
IB: Cav1.2
238
Cav1.2
CONTROL
RAT ANKG shRNA

Figure 10.

Figure 10. $Na_v1.5$ expression is reduced in rat myocytes with reduced ankyrin-G expression. Neonatal cardiomyocytes were transduced with rat-specific ankyrin-G shRNA virus. After 22 h, myocytes were collected, and whole cell lysates were generated. Equal protein concentrations were analyzed by immunoblot using affinity-purified ankyrin-G Ig and $Na_v1.5$-specific antibody. In parallel, blots were probed with an unrelated Ig to ensure equal protein loading (NHERF1). Note that loss of 190-kD ankyrin-G expression in myocytes transduced with rat-specific ankyrin-G shRNA was paralleled by a significant reduction in $Na_v1.5$ expression. Reduced ankyrin-G expression did not affect the expression of ankyrin-B, connexin43, or $Ca_v1.2$. Molecular masses are expressed in kilodaltons.

The role of ankyrin-G on single cardiomyocyte $Na_v1.5$ expression was examined using immunofluorescence and confocal microscopy. In agreement with immunoblot data of cardiomyocyte populations (Fig. 10), reduced ankyrin-G expression resulted in a dramatic loss of $Na_v1.5$ cellular expression (Fig. 11 C) compared with nontransduced (Fig. 11 A), YFP-transduced (Fig. 11 B), and human-specific ankyrin-G shRNA–transduced myocytes (Fig. 11 D).

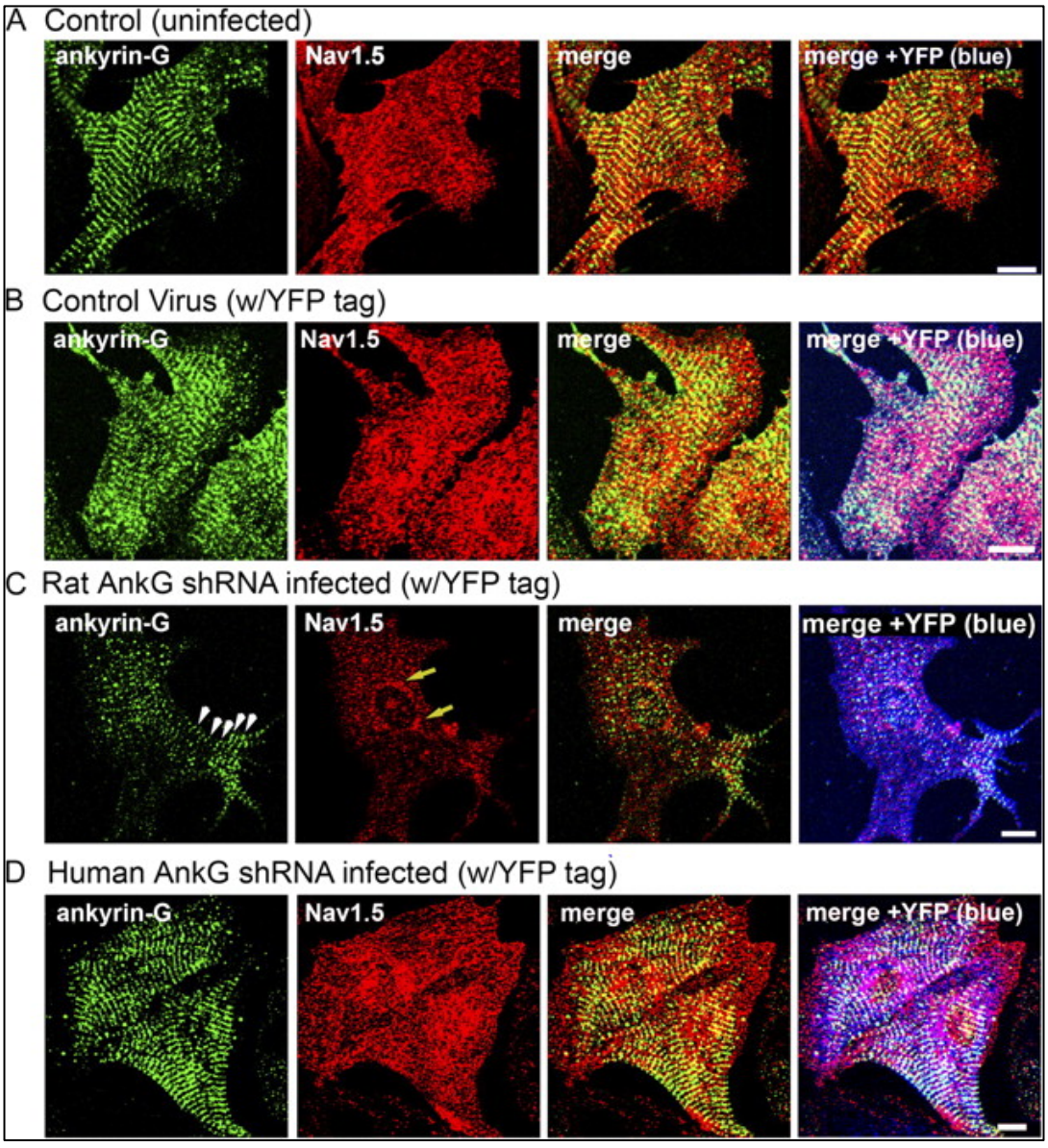
A Control (uninfected)
ankyrin-G
Nav1.5
merge
merge +YFP (blue)
B Control Virus (w/YFP tag)
ankyrin-G
Nav1.5
merge
merge +YFP (blue)
C Rat AnkG shRNA infected (w/YFP tag)
ankyrin-G
Nav1.5
merge
merge +YFP (blue)
D Human AnkG shRNA infected (w/YFP tag)
ankyrin-G
Nav1.5
merge
merge +YFP (blue)

Figure 11.

Figure 11. $Na_v1.5$ expression is reduced in single rat myocytes with reduced ankyrin-G expression. (A–D) Control myocytes (uninfected; A) and cardiomyocytes transduced with control virus (YFP alone; B), rat-specific ankyrin-G shRNA virus (C), or human-specific ankyrin-G shRNA virus (D) were immunolabeled with ankyrin-G and $Na_v1.5$-specific antibodies and imaged using identical confocal settings. Viral transduction was assessed by the presence of YFP fluorescence (pseudocolored in blue in B–D for clarity). Note that only myocytes infected with rat-specific ankyrin-G shRNA virus displayed reduced ankyrin-G expression. These myocytes consistently displayed a decreased expression of $Na_v1.5$. In fact, $Na_v1.5$ expression in myocytes with reduced ankyrin-G expression (arrowheads in C) was limited to the perinuclear region (arrows in C). Bars, 10 μm.

Specifically, $Na_v1.5$ expression appeared to only remain in the perinuclear region of cardiomyocytes lacking ankyrin-G expression (Fig. 11 C). Loss of protein localization was limited to $Na_v1.5$, as cardiomyocytes transduced with ankyrin-G shRNA displayed no difference in the expression or localization of either $Ca_v1.2$ or Na/Ca exchanger (Fig. 12).

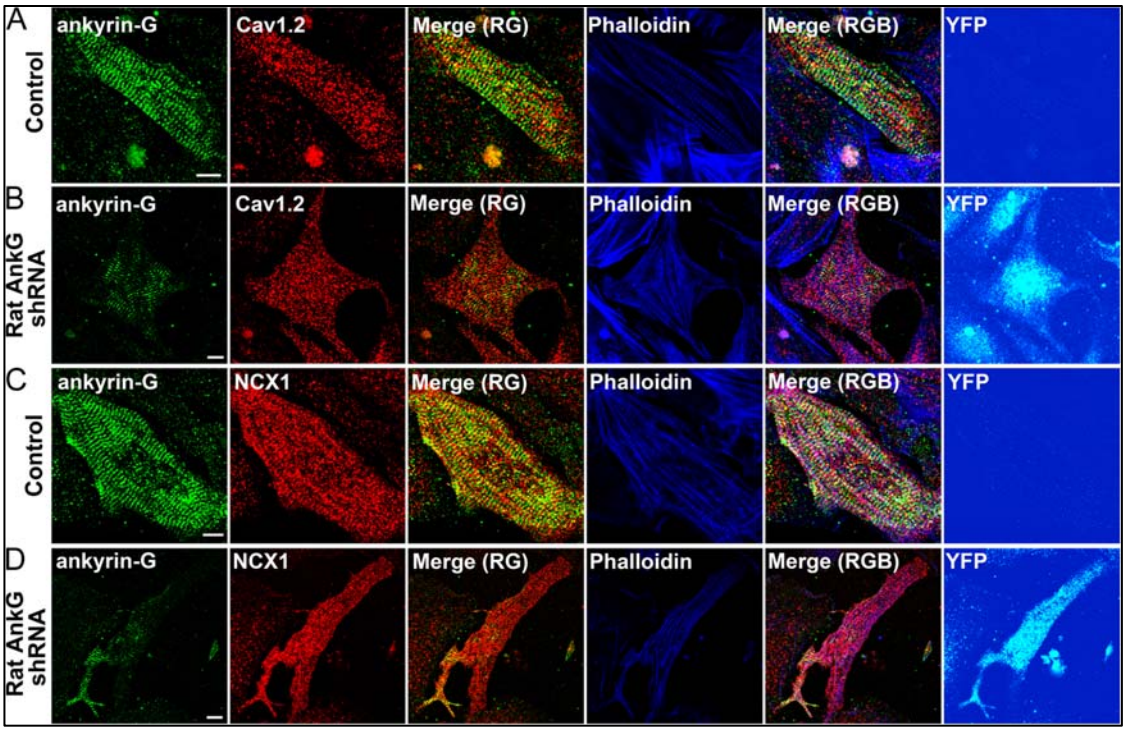
A
Control
ankyrin-G
Cav1.2
Merge (RG)
Phalloidin
Merge (RGB)
YFP
B
Rat AnkG shRNA
ankyrin-G
Cav1.2
Merge (RG)
Phalloidin
Merge (RGB)
YFP
C
Control
ankyrin-G
NCX1
Merge (RG)
Phalloidin
Merge (RGB)
YFP
D
Rat AnkG shRNA
ankyrin-G
NCX1
Merge (RG)
Phalloidin
Merge (RGB)
YFP

Figure 12.

Figure 12. Normal expression/distribution of $Ca_v1.2$ and NCX1 in cardiomyocytes lacking ankyrin-G. Control myocytes (uninfected; A and C) and cardiomyocytes transduced with rat-specific ankyrin-G shRNA virus (B and D) were immunolabeled with ankyrin-G and $Ca_v1.2$ or Na/Ca exchanger 1 (NCX1)–specific antibodies and imaged using identical confocal settings. Myocyte ultrastructure was visualized using phalloidin conjugated to AlexaFluor633 (dark blue images). Viral transduction was assessed by the presence of YFP fluorescence (pseudocolored in turquoise in the right panels of B and D). Bars, 10 μm.

Ankyrin-B is not required for $Na_v1.5$ expression in cardiomyocytes

Ankyrin-B (encoded by *ANK2*) is required for the membrane targeting of Na/Ca exchanger, $InsP_3$ receptor, and Na/K ATPase in cardiomyocytes (Mohler et al., 2005a). Ankyrin-B and -G are structurally similar and share binding activity for protein partners, including beta-spectrin and Na/K ATPase (Devarajan et al., 1994; Kizhatil and Bennett, 2004; Kizhatil et al., 2007b; Mohler et al., 2005a; Mohler et al., 2004e). We used primary cardiomyocytes from ankyrin-B–null mice to test whether ankyrin-B expression is necessary for $Na_v1.5$ membrane expression. Confocal analyses of wild-type, ankyrin-$B^{+/-}$, and ankyrin-B–null cardiomyocytes revealed no difference in $Na_v1.5$ immunolocalization (Fig. 13, A–C). Therefore, even in myocytes completely devoid of ankyrin-B expression, $Na_v1.5$ was normally expressed and properly localized. These results demonstrate that ankyrin-G (not ankyrin-B) is the physiological binding partner for $Na_v1.5$ in the heart.

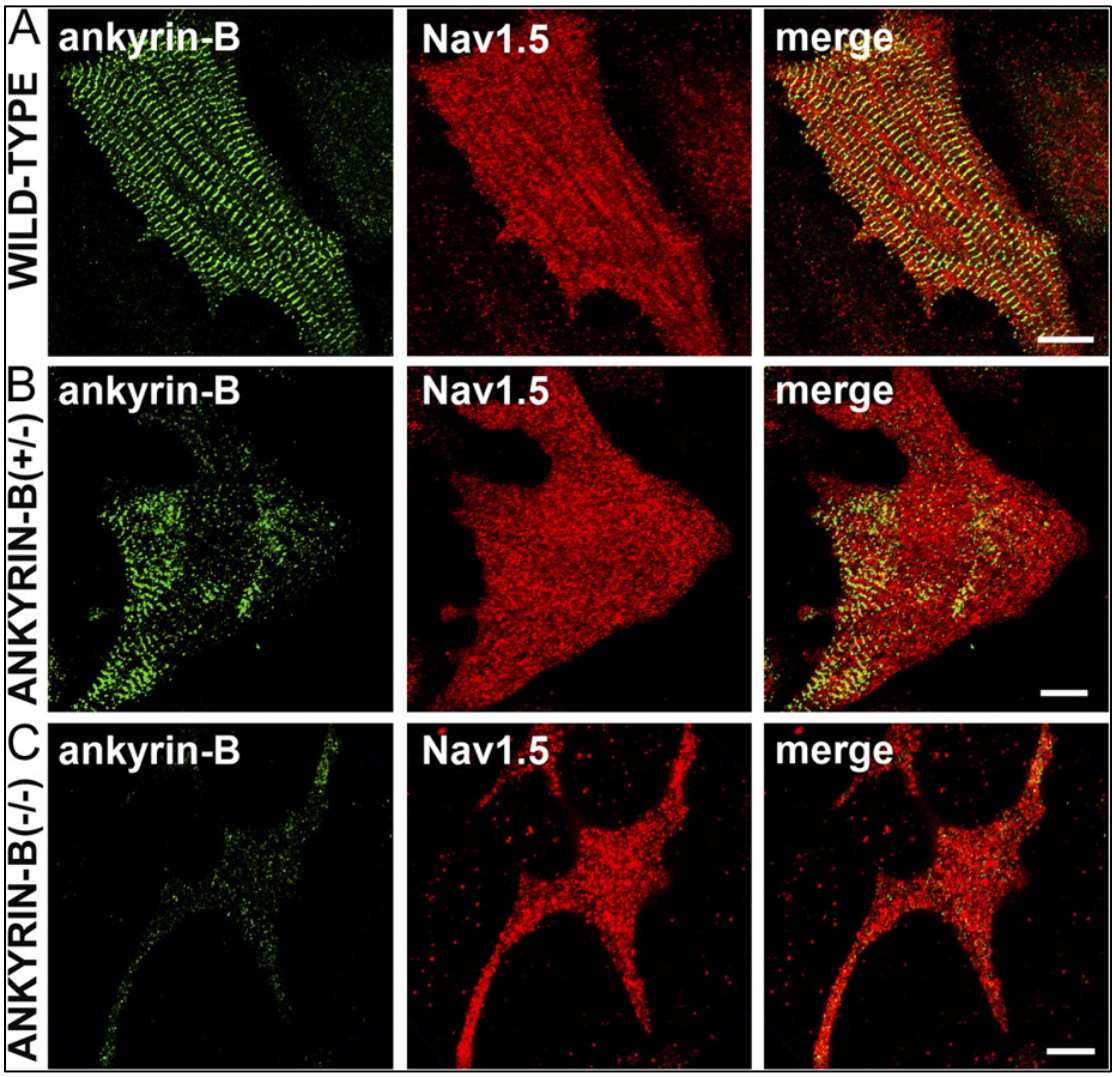
A
WILD-TYPE
ankyrin-B
Nav1.5
merge
B
ANKYRIN-B(+/-)
ankyrin-B
Nav1.5
merge
C
ANKYRIN-B(-/-)
ankyrin-B
Nav1.5
merge

Figure 13.

Figure 13. $Na_v1.5$ is normally expressed in cardiomyocytes with reduced ankyrin-B expression. Immunolocalization of ankyrin-B and $Na_v1.5$ in neonatal myocytes derived from wild-type (A), ankyrin-$B^{+/-}$ (B), and ankyrin-$B^{-/-}$ mice (C). Note that although ankyrin-B levels are reduced ~50% in ankyrin-$B^{+/-}$ myocytes and nearly 100% in ankyrin-$B^{-/-}$ cardiomyocytes, there is no reduction in $Na_v1.5$ expression/localization. Bars, 10 μm.

Ankyrin-G is required for normal $Na_v1.5$-dependent Na^+ current in cardiomyocytes

We made electrophysiological measurements to determine whether reduced ankyrin-G expression significantly affects Na_v channel membrane current density in primary cardiomyocytes (Fig. 14). Wild-type rat cardiomyocytes and cardiomyocytes transduced with human- or rat-specific ankyrin-G shRNA virus was analyzed for sodium current using whole-cell patch clamp (see Fig. 14 D [inset] for protocol).

Virally transduced cardiomyocytes were selected for electrophysiological measurements on the basis of positive YFP fluorescence. Cardiomyocytes infected with human-specific ankyrin-G shRNA virus displayed no change in peak Na^+ current compared with control (nontransduced) myocytes (note the current traces in Fig. 14 [A and B] and the current-voltage relationship in Fig. 14 D).

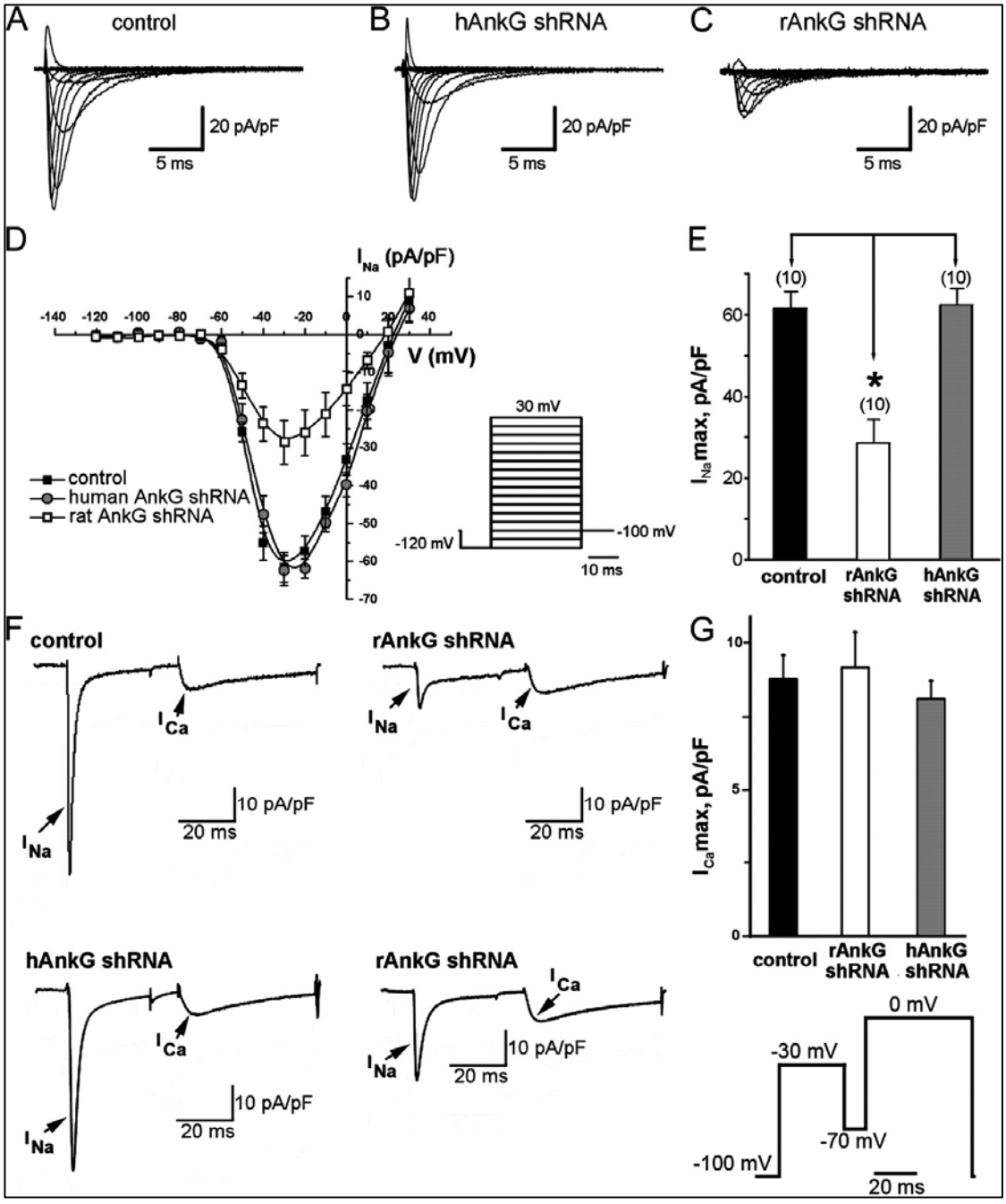
A
control
20 pA/pF
5 ms
B
hAnkG shRNA
20 pA/pF
5 ms
C
rAnkG shRNA
20 pA/pF
5 ms
D
I_Na (pA/pF)
V (mV)
control
human AnkG shRNA
rat AnkG shRNA
30 mV
-120 mV
-100 mV
10 ms
E
I_Na max, pA/pF
(10)
(10)
(10)
*
control
rAnkG shRNA
hAnkG shRNA
F
control
I_Ca
I_Na
10 pA/pF
20 ms
rAnkG shRNA
I_Na
I_Ca
10 pA/pF
20 ms
hAnkG shRNA
I_Ca
I_Na
10 pA/pF
20 ms
rAnkG shRNA
I_Ca
I_Na
10 pA/pF
20 ms
G
I_Ca max, pA/pF
control
rAnkG shRNA
hAnkG shRNA
0 mV
-30 mV
-70 mV
-100 mV
20 ms

Figure 14.

Figure 14. Reduced sodium current amplitude and current-voltage kinetics in myocytes with reduced ankyrin-G expression. Nontransduced cardiomyocytes (control) and cardiomyocytes transduced with human- (hAnkG) or rat-specific (rAnkG) shRNA virus were analyzed for $Na_v1.5$ current. (A–C) Whole-cell patch clamp sodium current traces elicited control (A; 17 pF), human ankyrin-G–specific shRNA–transduced cells (B; 18 pF), and rat-specific ankyrin-G shRNA–transduced cells (C; 16.8 pF). All cardiomyocytes displayed similar cell capacitance, and all traces are normalized for cell capacitance. (D) Mean and normalized current-voltage relationship for neonatal rat ventricular cardiomyocytes. Cardiomyocytes treated with control virus (black squares; *n* = 10), human ankyrin-G shRNA virus (gray circles; *n* = 10), and rat ankyrin-G shRNA virus (white squares; *n* = 10). (E) Normalized maximum sodium current amplitude in myocytes treated with control (black bar) and rat- (white bar) and human (gray bar)-specific ankyrin-G shRNA virus. *, $P < 0.05$. (F and G) Reduced ankyrin-G expression specifically affects cardiomyocyte sodium current. (F) Amplitude of Na^+ and Ca^{2+} current in nontransduced (control) and rat neonatal cardiomyocytes transduced with ankyrin-G species-specific shRNA viruses. Currents are elicited with the protocol shown in the inset (see Materials and methods for details). Left panels depict Na^+ and Ca^{2+} current in cardiomyocytes treated with control or human ankyrin-G–specific shRNA virus (hAnkG shRNA). Right panels display the significant decrease in I_{Na}, but not I_{Ca}, cardiomyocytes transduced with rat-specific ankyrin-G shRNA virus (rAnkG shRNA). All traces are normalized for cell capacitance. (G) Reduced ankyrin-G

(Figure 14. continued) expression leads to reduced I_{Na} but does not affect cardiomyocyte I_{Ca}. (E and G) Data are plotted as mean ± SEM (error bars; *n* = 10). Statistical difference was analyzed by analysis of variance.

In contrast, myocytes transduced with rat-specific ankyrin-G shRNA virus displayed striking decreases in peak Na^+ current density (note the traces in Fig. 14 C; currents normalized for cell capacitance). In fact, several transduced cells that completely lacked detectable Na^+ current (data not included in statistical analyses for Figs. 14 and 15; see Materials and methods) were observed.

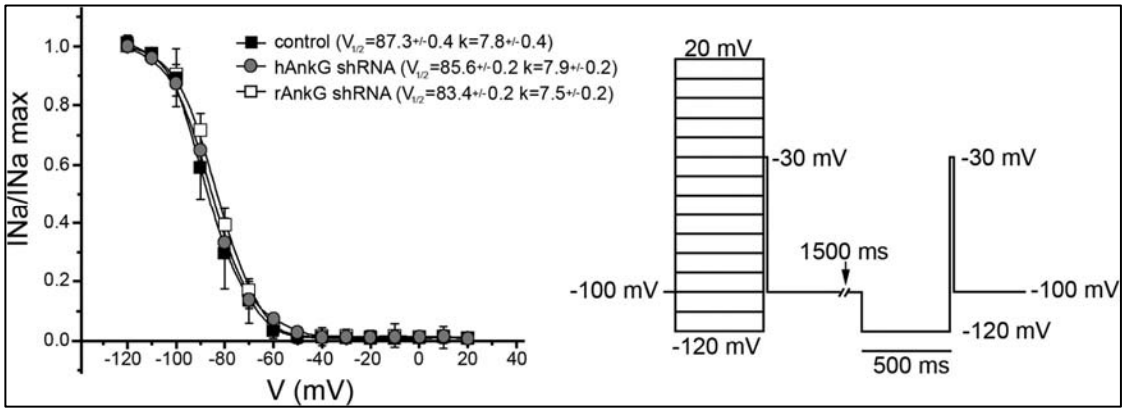
control ($V_{1/2}$=87.3+/-0.4 k=7.8+/-0.4)
hAnkG shRNA ($V_{1/2}$=85.6+/-0.2 k=7.9+/-0.2)
rAnkG shRNA ($V_{1/2}$=83.4+/-0.2 k=7.5+/-0.2)
INa/INa max
V (mV)
20 mV
-30 mV
-30 mV
1500 ms
-100 mV
-100 mV
-120 mV
-120 mV
500 ms

Figure 15.

Figure 15. Reduced ankyrin-G expression does not affect $Na_v1.5$ inactivation in primary cardiomyocytes. Superimposed $Na_v1.5$ inactivation curves obtained from neonatal rat cardiomyocytes treated with control (black squares) and species-specific (human, gray circles; rat, white squares) ankyrin-G shRNA viruses. The normalized I_{Na} plotted against preconditioning pulse potential was fitted using a Boltzmann equation. Voltage-dependent steady-state inactivation was determined using a paired two-pulse protocol. Each conditioning voltage is paired with a control after 1.5 s. A 500-ms conditioning pulse from –120 to 20 mV in 10-mV increments was followed by a test pulse to –30 mV. The test pulse in each series is separated from the conditioning pulse by a 2-ms interval to –120 mV. Each point (I_{Na}) is normalized against the amplitude of corresponding control pulse (I_{Namax}). Each point represents mean ± SEM (error bars; *n* = 5).

These functional data strongly support a role for ankyrin-G in $Na_v1.5$ membrane surface targeting in cardiomyocytes. To determine the specificity of the ankyrin-G–based cellular pathway for ion channel membrane targeting in cardiomyocytes, we evaluated the effect of reduced ankyrin-G expression on a second critical cardiomyocyte membrane current. $Ca_v1.2$-dependent calcium current (I_{Ca}) is required for normal cardiac excitability, and human $Ca_v1.2$ gene variants are associated with ventricular arrhythmia (Mohler et al., 2004d). As expected, myocytes with reduced ankyrin-G expression displayed significant reduction in peak Na^+ current amplitude (Fig. 14, F and G). However, these identical myocytes displayed peak calcium current (I_{Ca}) measurements that were unchanged from those observed in control (nontransduced) or human-specific ankyrin-G shRNA virally transduced cardiomyocytes (see Materials and methods for protocol details; Fig. 14, F and G). These data (combined with $Na_v1.5$/$Ca_v1.2$ immunoblot and immunostaining data in Figs. 10–12) establish that the cardiac ankyrin-G–targeting pathway is specific for $Na_v1.5$ channels and that loss of $Na_v1.5$ membrane expression in ankyrin-G–deficient cells is not simply the result of the general impairment of default myocyte membrane biogenesis/trafficking pathways.

$Na_v1.5$ channel inactivation is unaffected in cardiomyocytes with reduced ankyrin-G expression

Human $Na_v1.5$ Brugada Syndrome variant E1053K, which lacks ankyrin-G–binding activity, is not efficiently targeted to the cardiomyocyte intercalated disc (Mohler et al., 2004c). However, when introduced into heterologous HEK293 cells, this mutant channel is present at the plasma membrane but displays abnormalities in $Na_v1.5$ inactivation (Mohler et al., 2004c). Furthermore, similar data examining $Na_v1.2$ biophysical properties in TsA201 cells support the concept that ankyrin-G could potentially regulate the biophysical properties of Na_v channels in heterologous cells (Shirahata et al., 2006). These studies did not determine whether the inactivation of wild-type $Na_v1.5$ channels requires correct localization through ankyrin-G. Therefore, we tested whether primary cardiomyocytes with reduced ankyrin-G expression displayed abnormalities in Na_v channel inactivation. No significant difference in $Na_v1.5$ channel inactivation was observed in wild-type cardiomyocytes versus cardiomyocytes with reduced ankyrin-G expression (Fig. 14). These data demonstrate that in the physiological context of a cardiomyocyte, normal Na_v channel inactivation does not require ankyrin-G. Surprisingly, inactivation of wild-type cardiomyocyte $Na_v1.5$ is independent of physiological localization. Thus, localization controls current density but not $Na_v1.5$ inactivation. These data strongly demonstrate the critical nature of studying ankyrin biology in the appropriate physiological context.

Direct interaction between ankyrin-G and $Na_v1.5$ requires ANK repeat 14–15 beta-hairpin loop tips

We identified the structural requirements on ankyrin-G for direct $Na_v1.5$ interaction using a series of ankyrin-G *ANK* repeat mutants (Fig. 16, A–C).

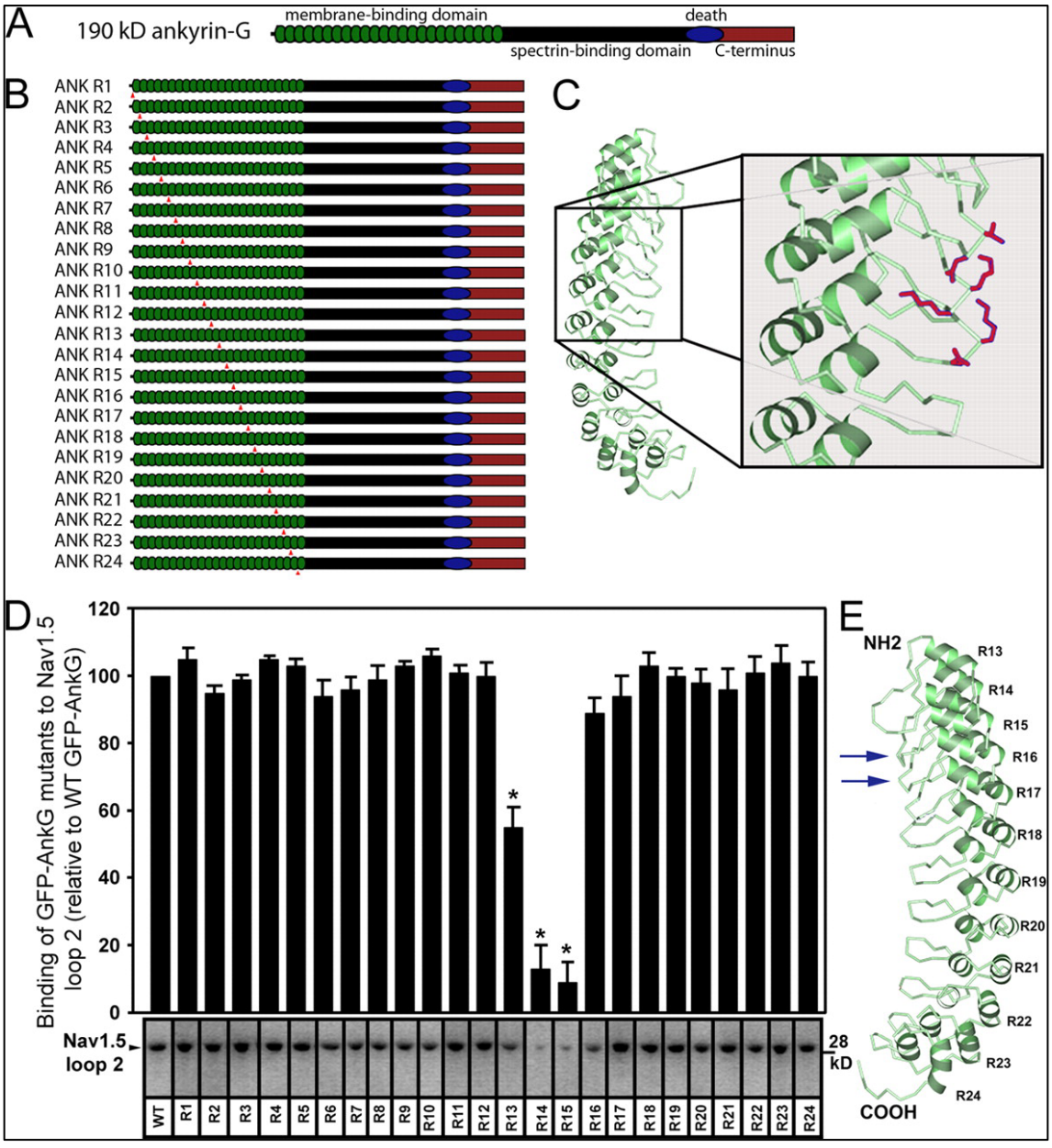
A
190 kD ankyrin-G
membrane-binding domain
death
spectrin-binding domain
C-terminus
B
ANK R1
ANK R2
ANK R3
ANK R4
ANK R5
ANK R6
ANK R7
ANK R8
ANK R9
ANK R10
ANK R11
ANK R12
ANK R13
ANK R14
ANK R15
ANK R16
ANK R17
ANK R18
ANK R19
ANK R20
ANK R21
ANK R22
ANK R23
ANK R24
C
D
Binding of GFP-AnkG mutants to Nav1.5 loop 2 (relative to WT GFP-AnkG)
120
100
80
60
40
20
0
Nav1.5 loop 2
28 kD
WT
R1
R2
R3
R4
R5
R6
R7
R8
R9
R10
R11
R12
R13
R14
R15
R16
R17
R18
R19
R20
R21
R22
R23
R24
E
NH2
COOH

Figure 16.

Figure 16. Direct interaction of ankyrin-G with $Na_v1.5$ requires two ANK repeat beta-hairpin loop tips on the ankyrin-G membrane–binding domain. (A) 190-kD ankyrin-G includes a membrane-binding domain comprised of 24 consecutive *ANK* repeats (green), a spectrin-binding domain (black), a death domain (blue), and a C-terminal domain (red). (B) *ANK* repeat mutants were engineered in the context of full-length GFP 190-kD ankyrin-G and display alanine substitutions for the two residues located at the tip of each *ANK* repeat beta-hairpin loop (red arrowheads in B and purple sites in C). (C) Crystal structure diagram of membrane-binding domain *ANK* repeats 13–24 (Michaely et al., 2002). Exposed charged residues on beta-hairpin loop tips (sites of alanine mutagenesis) are colored in purple. (D) Relative binding (compared with wild-type GFP 190-kD ankyrin-G) of GFP 190-kD ankyrin-G *ANK* repeat mutants with purified $Na_v1.5$ DII–DIII cytoplasmic domain (n = 3; *, $P < 0.05$). Binding levels are corrected for the relative expression of each GFP–ankyrin-G mutant. Error bars represent SEM. (E) $Na_v1.5$ binding sites (arrows) superimposed on the deduced crystal structure of the ankyrin-G membrane–binding domain (*ANK* repeats 13–24). Ankyrin-G membrane–binding domain structure is based on the crystal structure of *ANK* repeats 13–24 of ankyrin-R (Michaely et al., 2002).

These mutants were created based on the identification of exposed, highly accessible residues on the beta-hairpin loop tips of the ankyrin-R membrane–binding domain (repeats 13–24) crystal structure (Michaely et al., 2002) as well as the identification of membrane–protein binding sites at these sites in ankyrin-B (Cunha et al., 2007; Mohler et al., 2004b). Specifically, each of the 24 consecutive *ANK* repeats of an ankyrin membrane–binding domain fold as anti-parallel pairs of alpha-helices connected by a beta-hairpin loop. The large number of consecutive *ANK* repeats come together to form a super helix that surrounds a large central cavity (Michaely et al., 2002). Thus, these variable beta-hairpin loops are highly accessible to the solvent for potential protein interactions (Fig. 17 C). This strategy has been successfully used to map the binding sites on ankyrin-B for Na/Ca exchanger and $InsP_3$ receptor (Cunha et al., 2007; Mohler et al., 2004a).

24 individual ankyrin-G *ANK* repeat mutants were generated for binding analyses. Each ankyrin-G mutant harbored two alanine substitutions in the variable beta-hairpin loop tips connecting each pair of *ANK* repeats within the membrane-binding domain (*ANK* repeats 1–24; Fig. 16, B and C). Mutagenesis was performed in the context of GFP-tagged ankyrin-G (Mohler et al., 2004b). Mutant plasmids were completely sequenced to verify that no additional mutations were introduced during PCR amplification. Wild-type ankyrin-G and each GFP ankyrin-G mutant were expressed in HEK293 cells. Expressed proteins were immunopurified from the detergent-soluble fraction of the cells using immobilized affinity-purified GFP Ig and were incubated with purified His-

tagged $Na_v1.5$ DII–DIII cytoplasmic loop (site for ankyrin-G association on $Na_v1.5$; (Mohler et al., 2004c). The quantity of pure $Na_v1.5$ DII–DIII bound to each mutant was determined by immunoblotting using a His tag Ig. Using similar methods, the relative level of GFP–ankyrin-G mutant expression for each data point was determined. The amount of $Na_v1.5$ His-tagged DII–DIII bound to each ankyrin-G mutant was corrected for relative GFP–ankyrin-G expression in each experimental sample.

Although the majority of ankyrin-G mutants associated with $Na_v1.5$ His-tagged DII–DIII at levels similar to wild-type GFP–ankyrin-G, there was a significant reduction in DII–DIII binding to ankyrin-G mutants R13, R14, and R15 (Fig. 16, D and E). In fact, GFP–ankyrin-G mutants R14 and R15 displayed a near complete loss of $Na_v1.5$ DII–DIII binding activity in these assays. Together, our findings demonstrate that ankyrin-G–$Na_v1.5$ binding is exclusively dependent on three critical elements (two beta-hairpin loops on ankyrin-G and a nine–amino acid motif on $Na_v1.5$; (Mohler et al., 2004c).

Human ankyrin-G expression rescues abnormal $Na_v1.5$ localization

We performed rescue assays to determine whether the loss of $Na_v1.5$ localization in cardiomyocytes with reduced ankyrin-G expression was specifically caused by the monogenic loss of ankyrin-G. Rat neonatal cardiomyocytes with reduced levels of ankyrin-G and $Na_v1.5$ (as a result of the presence of rat-specific

ankyrin-G shRNA virus) were transfected with cDNA encoding human GFP–ankyrin-G. This GFP–ankyrin-G cDNA is resistant to the rat ankyrin-G shRNA (Fig. 10). As expected, shRNA-transduced cardiomyocytes displayed decreased expression and abnormal localization of $Na_v1.5$ (Fig. 17 B). In contrast, shRNA-transduced cardiomyocytes expressing human GFP–ankyrin-G cDNA displayed a $Na_v1.5$ distribution similar to wild-type cardiomyocytes (Fig. 17 C). These data demonstrate that abnormal $Na_v1.5$ localization in ankyrin-G–null cardiomyocytes can be rescued by the exogenous expression of human ankyrin-G and reinforce the critical role for ankyrin-G in the subcellular localization of $Na_v1.5$ in cardiomyocytes.

Direct ankyrin-G–$Na_v1.5$ interaction is required for $Na_v1.5$ localization

We used the aforementioned ankyrin-G rescue assay with ankyrin-G mutants that lack $Na_v1.5$-binding activity (Fig. 16) to determine whether direct ankyrin-G–$Na_v1.5$ interactions are required for $Na_v1.5$ localization in cardiomyocytes. Ankyrin-G mutants lacking $Na_v1.5$-binding activity were introduced into full-length human GFP–ankyrin-G cDNA to create human GFP–ankyrin-G R14 and R15 (both resistant to rat ankyrin-G shRNA). Cardiomyocytes with reduced ankyrin-G expression (transduced with rat ankyrin-G YFP virus) were transfected with human GFP–ankyrin-G or human ankyrin-G R14 or R15 mutant cDNAs. YFP-positive cardiomyocytes (express shRNA) were fixed and

immunostained. GFP–ankyrin-G is properly targeted in neonatal cardiomyocytes and rescues the normal expression of $Na_v1.5$ (Fig. 17 C).

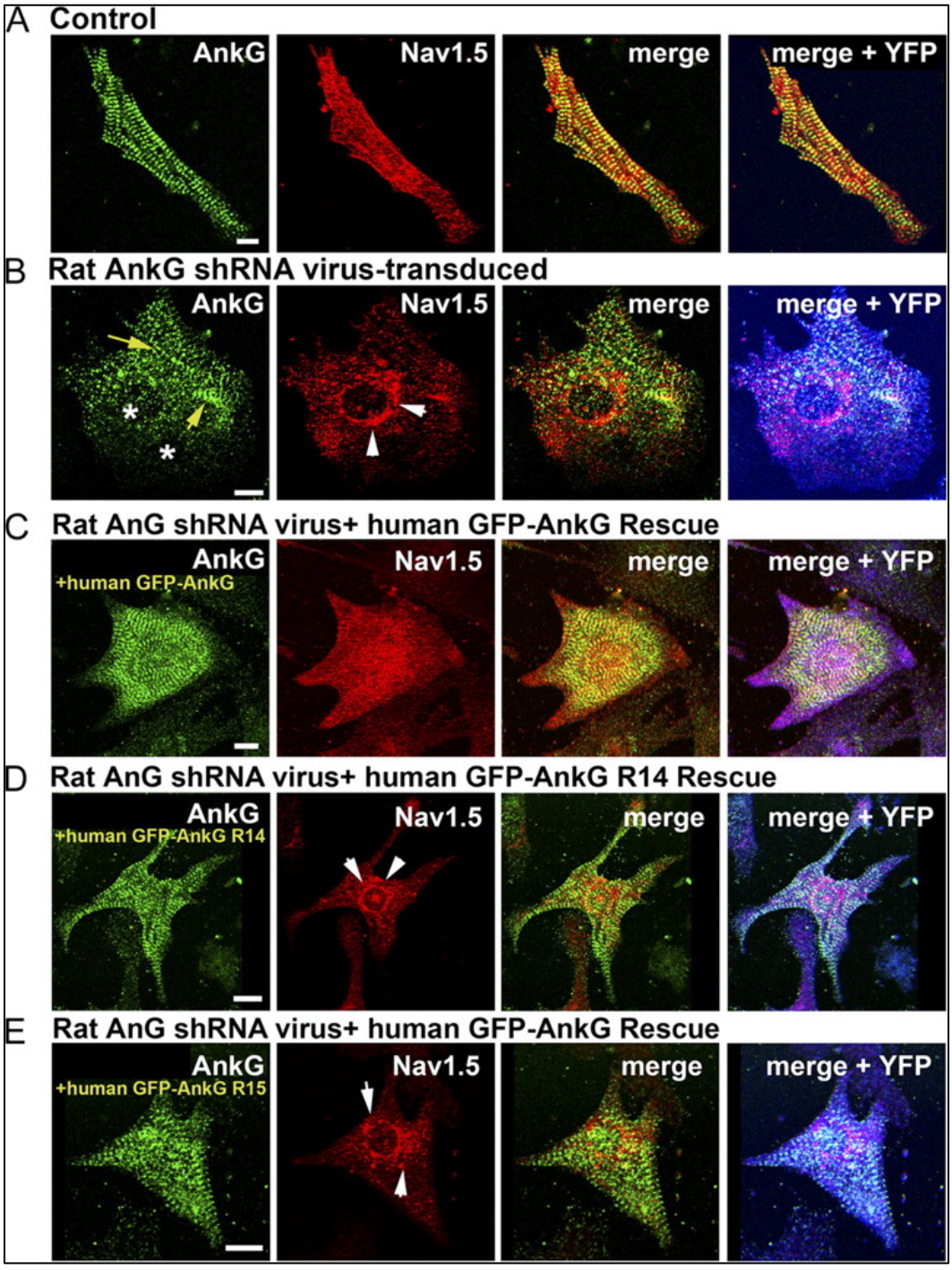
A Control
AnkG
Nav1.5
merge
merge + YFP
B Rat AnkG shRNA virus-transduced
AnkG
Nav1.5
merge
merge + YFP
C Rat AnG shRNA virus+ human GFP-AnkG Rescue
AnkG
+human GFP-AnkG
Nav1.5
merge
merge + YFP
D Rat AnG shRNA virus+ human GFP-AnkG R14 Rescue
AnkG
+human GFP-AnkG R14
Nav1.5
merge
merge + YFP
E Rat AnG shRNA virus+ human GFP-AnkG Rescue
AnkG
+human GFP-AnkG R15
Nav1.5
merge
merge + YFP

Figure 17.

Figure 17. $Na_v1.5$ targeting requires direct interaction with 190-kD ankyrin-G. (A and B) Immunolocalization of ankyrin-G and $Na_v1.5$ in control (nontransduced) and rat ankyrin-G shRNA virally transduced neonatal cardiomyocytes. Note the localization of $Na_v1.5$ in the perinuclear region of shRNA-transduced myocytes (white arrows). Yellow arrows denote remaining ankyrin-G staining in transduced myocytes, and asterisks mark sites of complete knockdown. Virally transduced myocytes in the figure are denoted by positive YFP fluorescence (pseudocolored in blue). (C) Cardiomyocytes expressing rat-specific ankyrin-G shRNA (note the blue color denoting YFP expression) were transfected with GFP-labeled human ankyrin-G cDNA and immunolabeled with $Na_v1.5$ and ankyrin-G antibodies. Note that human GFP–ankyrin-G restores the localization of $Na_v1.5$ to normal (compare $Na_v1.5$ in B and C). (D and E) GFP-human ankyrin-G mutants (R14 and R15) that lack binding activity for $Na_v1.5$ (see Fig. 17) are unable to rescue to normal the aberrant localization of $Na_v1.5$ (note perinuclear distribution; arrows) in myocytes stably transduced with rat ankyrin-G shRNA (note positive YFP fluorescence). Bars, 10 μm.

In contrast, although both GFP–ankyrin-G R14 and GFP–ankyrin-G R15 (Fig.17 D-E) were properly localized in transfected cardiomyocytes, there was no detectable rescue of $Na_v1.5$ localization as observed with wild-type human GFP–ankyrin-G (Fig. 17 C). In fact, the localization of $Na_v1.5$ in myocytes transfected with GFP–ankyrin-G R14–15 was similar to non-transfected myocytes lacking endogenous ankyrin-G expression (Fig. 17, B, D, and E). Therefore, direct association of ankyrin-G with $Na_v1.5$ is required for the membrane expression of $Na_v1.5$ in ventricular cardiomyocytes.

Ankyrin-G is required for $Na_v1.5$ expression in adult cardiomyocytes

To test whether our findings in neonatal myocytes can also be applied to adult cardiomyocytes; we performed ankyrin-G shRNA viral transduction of freshly isolated adult rat cardiomyocytes. $Na_v1.5$ expression is most pronounced at the intercalated disc of adult cardiomyocytes (see $Na_v1.5$ localization in the control myocyte; Fig. 18).

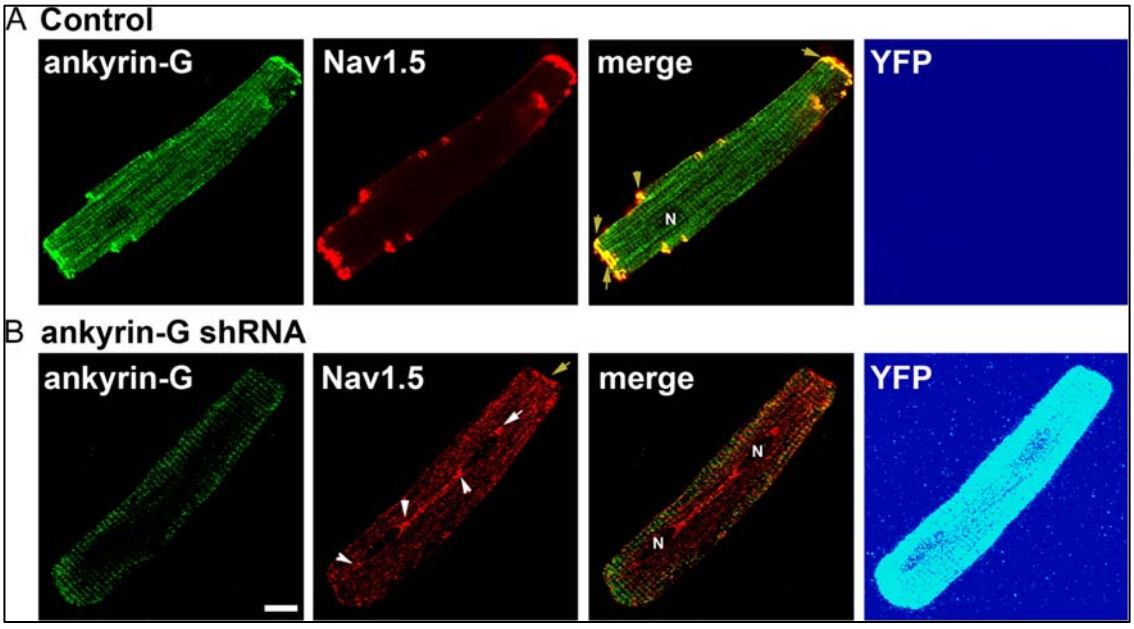
A Control
ankyrin-G
Nav1.5
merge
YFP
N
B ankyrin-G shRNA
ankyrin-G
Nav1.5
merge
YFP
N
N

Figure 18.

Figure 18. Ankyrin-G is required for normal $Na_v1.5$ expression in adult cardiomyocytes. Control (untreated) adult rat cardiomyocytes (A) and adult rat cardiomyocytes virally transduced with rat-specific ankyrin-G shRNA (B) were immunolabeled for ankyrin-G (green) and $Na_v1.5$ (red). Pseudocolor image on the right depicts positive YFP fluorescence. Yellow arrows indicate intercalated disc membrane domains (A and B). The nucleus is denoted by N. Note the predominant localization of $Na_v1.5$ at the intercalated discs in control cells (we also observed T-tubule staining in most cells). White arrows indicate the increased perinuclear localization/accumulation of $Na_v1.5$ in myocytes with reduced ankyrin-G expression (B). We observed normal localization of $Na_v1.5$ in adult cardiomyocytes treated with control (YFP alone) virus. Bar, 10 μm.

Therefore, we tested whether ankyrin-G expression is required for $Na_v1.5$ localization at the mature cardiomyocyte intercalated disc. Reduced ankyrin-G expression in adult myocytes results in the reduced membrane expression of $Na_v1.5$ (note the loss of $Na_v1.5$ intercalated disc staining in Fig. 18 B), which is consistent with results in neonatal cardiomyocytes. In fact, identical with our findings in neonatal cells, we observed that $Na_v1.5$ localized to the perinuclear region (Fig. 18 B) in adult cardiomyocytes with reduced ankyrin-G expression. These data from isolated adult cardiomyocytes further confirm the role of the ankyrin-G–based protein-targeting pathway for $Na_v1.5$ membrane expression in the heart.

Discussion

In this study, we present the first report of a cellular pathway required for Na_v channel trafficking in cardiomyocytes. We demonstrate that direct interaction of the ankyrin-G membrane–binding domain and $Na_v1.5$ DII–DIII loop is necessary for $Na_v1.5$ expression and localization at the cardiomyocyte membrane surface. Our new data provide compelling evidence that ankyrin-G–dependent targeting of $Na_v1.5$ is a fundamental requirement for cardiomyocytes and likely other excitable cells. Ankyrin polypeptides have likely coordinately evolved to regulate electrical activity in the heart by targeting key ion

channels/transporters involved in controlling the cardiac action potential. Ankyrin-G directly associates with and targets $Na_v1.5$ to the membrane surface (Fig. 19 A) to regulate inward Na^+ current and, thus, action potential initiation and cardiomyocyte depolarization.

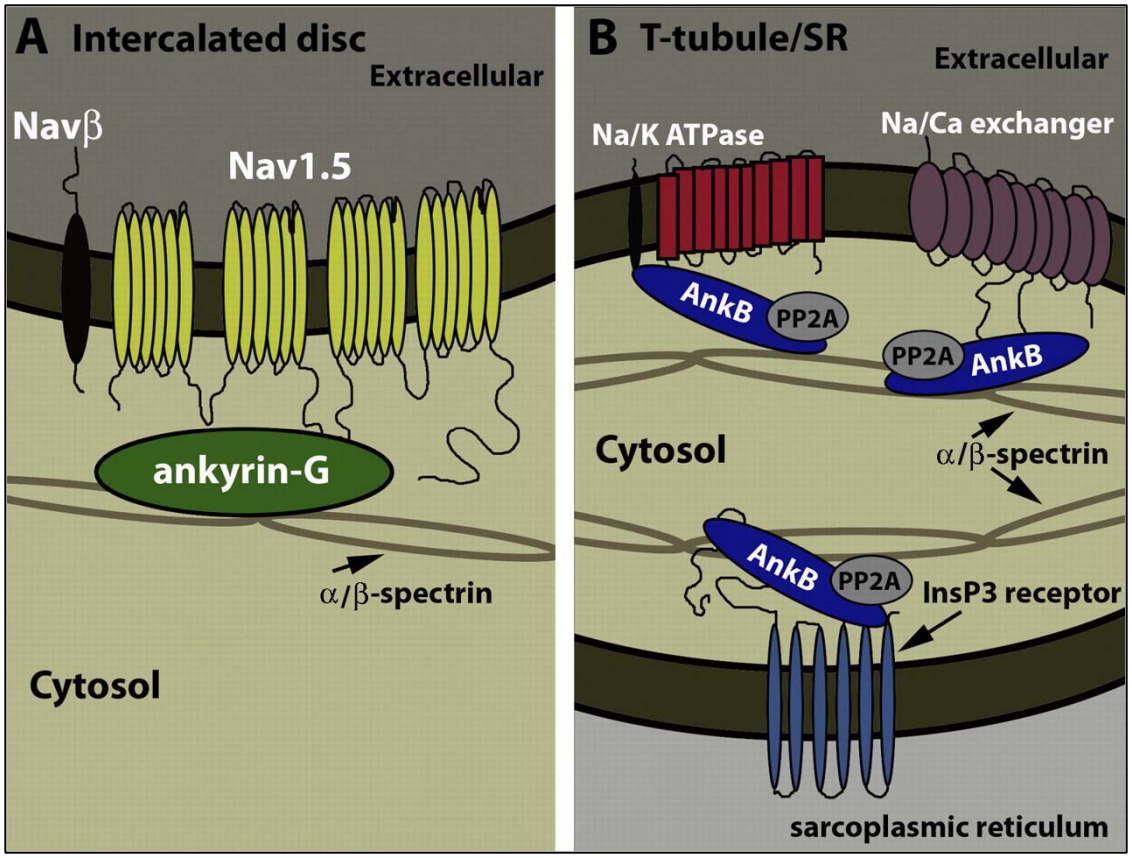
A Intercalated disc
Extracellular
Navβ
Nav1.5
ankyrin-G
α/β-spectrin
Cytosol
B T-tubule/SR
Extracellular
Na/K ATPase
Na/Ca exchanger
AnkB
PP2A
PP2A
AnkB
Cytosol
α/β-spectrin
AnkB
PP2A
InsP3 receptor
sarcoplasmic reticulum

Figure 19.

Figure 19. Ankyrin-G and ankyrin-B ion channel/transporter complexes in the heart. (A) Ankyrin-G is required for the targeting of $Na_v1.5$ to the cardiomyocyte intercalated disc. Although other $Na_v1.5$-interacting proteins have been identified, it is not yet clear whether these are present in the ankyrin-G–dependent protein complex. (B) Ankyrin-B is required for the targeting of Na/Ca exchanger and Na/K ATPase to transverse-tubule membranes in the heart. $InsP_3$ receptor targeting to the sarcoplasmic reticulum membrane requires direct interaction with ankyrin-B. Cardiac ankyrin-B protein partners also include PP2A and beta2-spectrin.

Therefore, it is not surprising that human *SCN5A* variants that disrupt ankyrin-G interactions are associated with the Brugada Syndrome (Brugada et al., 1998), a cardiac syndrome associated with reduced inward I_{Na} (for review see (Napolitano and Priori, 2006)). Clinical features of the Brugada Syndrome include fast polymorphic ventricular tachycardia typically occurring at rest or during sleep (Wilde and Priori, 2000). In contrast, ankyrin-B targets distinct ion channels and transporters with central roles in cytosolic calcium extrusion during cardiac repolarization (Cunha and Mohler, 2006; Mohler et al., 2005a; Mohler et al., 2004a; Mohler et al., 2002b; Mohler et al., 2003). Ankyrin-B (product of the *ANK2* gene) is required for targeting Na^+/Ca^{2+} exchanger, Na/K ATPase, and $InsP_3$ receptor to the transverse-tubule and sarcoplasmic reticulum in cardiomyocytes (Fig. 19 B; (Mohler et al., 2005a). In contrast to $Na_v1.5$-associated Brugada Syndrome, ventricular tachycardia and syncopal events in the ankyrin-B syndrome are most often associated with adrenergic stimulation (e.g., emotional stress and/or exercise, similar to catecholaminergic polymorphic arrhythmia; (Mohler et al., 2005a; Mohler et al., 2007; Mohler et al., 2005b; Mohler et al., 2004d; Mohler and Wehrens, 2007).

In addition to targeting ion channels in cardiomyocytes, ankyrin-B was recently shown to be required for targeting of the regulatory subunit of the PP2A complex in primary cardiomyocytes (Fig. 19 B; (Bhasin et al., 2007). This broad targeting role of ankyrin-B for both integral membrane and signaling proteins in the heart suggests that the ankyrin-G–targeting pathway may similarly facilitate the localization of additional myocyte proteins. Moreover, our new findings for

ankyrin-G in $Na_v1.5$ targeting identify an attractive, unconventional candidate disease gene for cardiac (arrhythmia and myopathy) and other excitable cell diseases.

Based on the role of ankyrin-R in the erythrocyte (Bennett and Stenbuck, 1979b), cardiac ankyrin-G may simply act as a membrane scaffold to link integral membrane proteins (such as $Na_v1.5$) with the underlying actin- and spectrin-based cytoskeleton. In support of this role, we observe a significant level of $Na_v1.5$ clustering on the plasma membrane surface with ankyrin-G as assessed by immunoelectron microscopy of cardiomyocyte membrane sheets (Fig. 20).

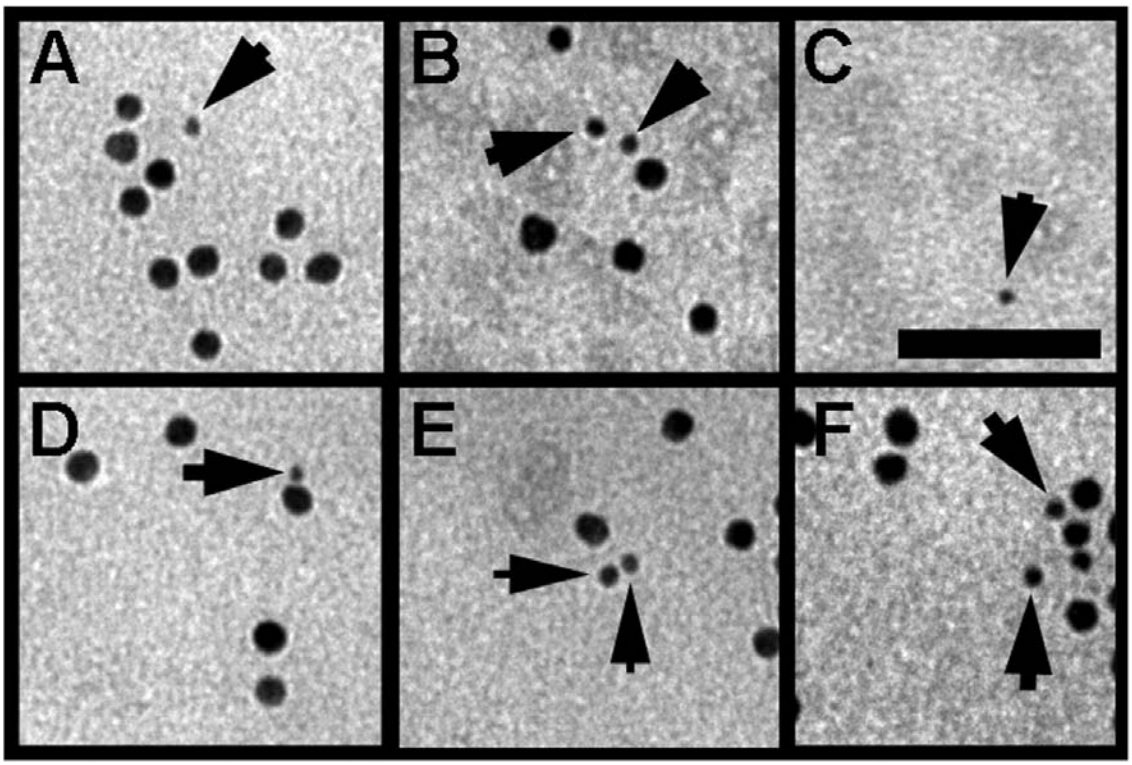

Figure 20.

Figure 20. $Na_v1.5$ is clustered at the cardiomyocyte membrane surface with ankyrin-G. Immunogold electron microscopy of adult rat ventricular cardiomyocyte plasma membrane sheets. Anti–ankyrin-G Ig particles (10 nm gold) and anti-$Na_v1.5$ Ig particles (5 nm gold; arrows) are found in clusters at the plasma membrane. The majority of $Na_v1.5$-positive gold particles were clustered in proximity (<10 nm) to ankyrin-G–positive gold particles (see A, B, and D–F). However, we also observed a small fraction of $Na_v1.5$-positive particles that were physically isolated from ankyrin-G (C). Membrane sheets labeled with gold-conjugated secondary antibodies (negative control) were clear of any gold particles (not depicted). Bar, 50 nm.

Alternatively, ankyrin-G may play an active role in the cellular trafficking of $Na_v1.5$ to specific membrane domains. In theory, ankyrin-G could have multiple roles in both trafficking and stabilization/retention of $Na_v1.5$ channels in the heart. Although these findings are beyond the scope of this study, elucidating the specific cellular roles of ankyrin polypeptides in excitable cells is an obvious future goal in the field. An interesting finding in these studies was the peri-nuclear accumulation of $Na_v1.5$ in myocytes lacking ankyrin-G (Figures 11 and 17). In fact, we consistently observed this peri-nuclear $Na_v1.5$, albeit at a reduced level even in untreated wild-type myocytes. Therefore, based on our data, we hypothesized that this compartment represented the site of ankyrin-G function for the trafficking of $Na_v1.5$ to the cardiomyocyte plasma membrane. To address this hypothesis, we prepared primary neonatal myocytes and evaluated the localization of $Na_v1.5$ in by co-labeling with a variety of membrane and subcellular organelle markers (e.g. ER, Golgi, Trans-Golgi, endosome). As shown in the upper panels of Figure 21, $Na_v1.5$ is clearly organized at both plasma membrane and underlying peri-nuclear sites. In regard to the subcellular distribution of $Na_v1.5$, we observed significant co-localization with markers of the early endosome compartment (Figure 21. B). In contrast, while there was apparent co-distribution of $Na_v1.5$ with TGN and other Golgi markers at low magnification, stringent high magnification analyses of the cells revealed juxtaposed $Na_v1.5$ positive staining with these markers (Figure 21. A and C). Therefore, these preliminary results suggest that $Na_v1.5$ accumulates in a peri-nuclear endosomal compartment preceding it's trafficking to the plasma membrane. Moreover, our findings suggest that $Na_v1.5$ accumulates in this compartment in the absence of ankyrin-

G. Future experiments will be necessary to further characterize this trafficking pathway for $Na_v1.5$ in the context of the primary myocyte.

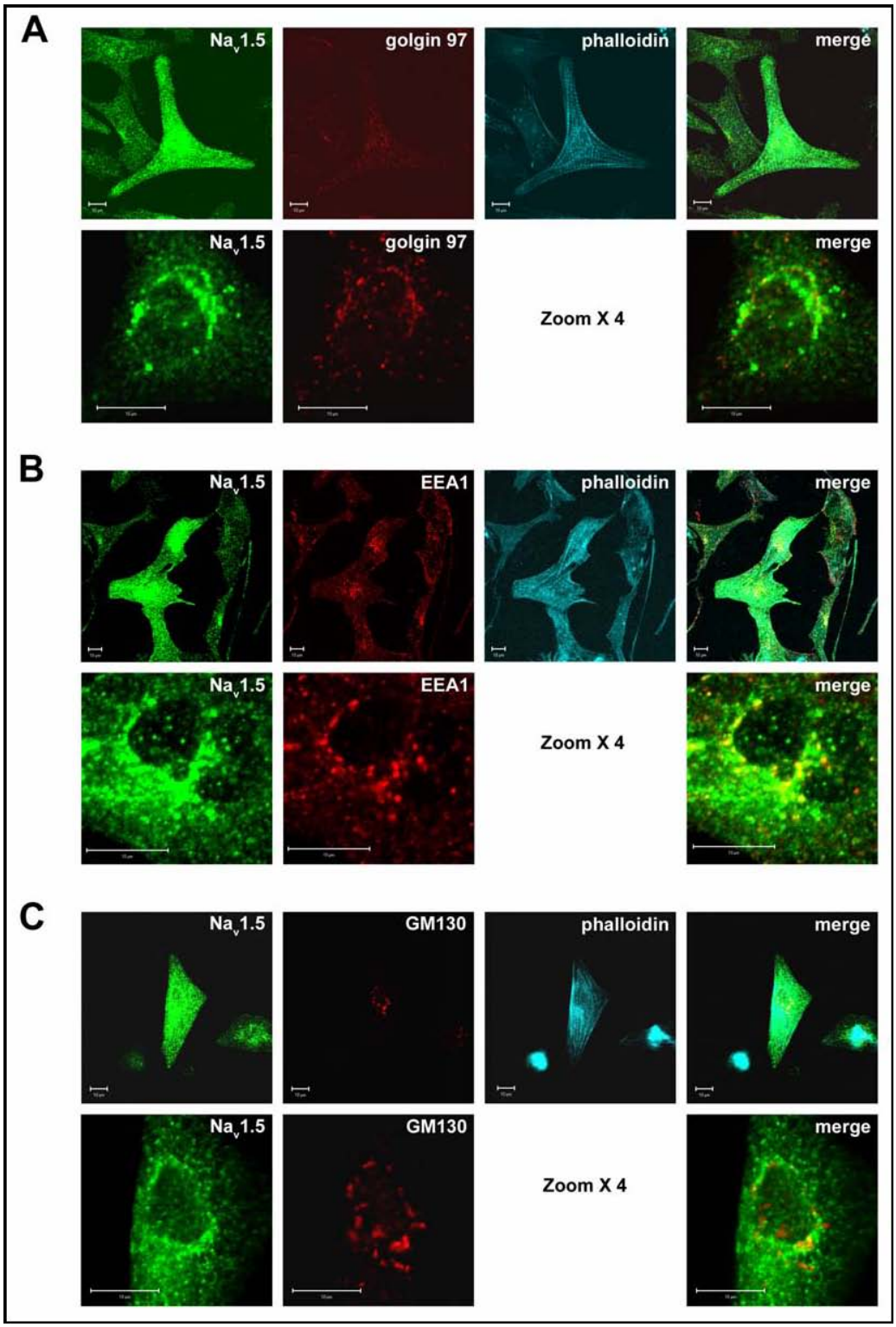
A
Na$_v$1.5
golgin 97
phalloidin
merge
Na$_v$1.5
golgin 97
Zoom X 4
merge
B
Na$_v$1.5
EEA1
phalloidin
merge
Na$_v$1.5
EEA1
Zoom X 4
merge
C
Na$_v$1.5
GM130
phalloidin
merge
Na$_v$1.5
GM130
Zoom X 4
merge

Figure 21.

Figure 21. Localization of $Na_v1.5$ at the plasma membrane and perinuclear subcellular membrane compartment in untreated neonatal cardiomyocytes. (A) Immunolocalization of $Na_v1.5$, F-actin (phalloidin), and the cis-Golgi marker golgin 97 at the plasma membrane focal plane (upper panels), lower panels show localization of $Na_v1.5$ and golgin 97 in/near the peri-nuclear Golgi compartment. (B) Immunolocalization of $Na_v1.5$ and the early endosome marker EEA1 at the plasma membrane focal plane (upper panels), lower panels show localization of $Na_v1.5$ and EEA1 in the early endosomal peri-nuclear compartment. Notice the significant amount of signal overlap of $Na_v1.5$ and EEA1 in merged images. (C) Immunolocalization of $Na_v1.5$, F-actin (phalloidin), and the trans-Golgi marker GM130 (upper panels), lower panels show localization of $Na_v1.5$ and GM130 in/near the trans-Golgi compartment.

Our electrophysiological measurements illustrate the importance of studying ankyrin–membrane protein interactions in the physiological context of a native cell. Our previous work suggested that $Na_v1.5$ E1053K lacking ankyrin-G–binding activity displayed minor yet significant abnormalities in activation and inactivation when expressed in HEK293 cells (Mohler et al., 2004c). However, when expressed in native cardiomyocytes, these biophysical abnormalities were inconsequential, as the majority of the channel lacked sufficient targeting information to even reach the plasma membrane (Mohler et al., 2004c). Our new findings demonstrate that in myocytes lacking ankyrin-G, the small number of residual $Na_v1.5$ channels that reach the plasma membrane have effectively normal biophysical characteristics. These findings are in contrast to a recent publication that demonstrated abnormal inactivation gating of $Na_v1.2$ in TsA201 cells (modified HEK293 cell) lacking ankyrin-G (Shirahata et al., 2006). Our new data suggest that these measurements should be re-evaluated in the context of a neuron.

Cardiomyocytes have clearly evolved unique channel trafficking pathways for the precise localization of specific ion channels to unique cardiomyocyte membrane domains. For example, although $Na_v1.5$, $K_v4.2$, and connexin 43 are concentrated at the intercalated disc (Barry et al., 1995; Kanter et al., 1992; Maier et al., 2004; Mohler et al., 2004c) Kir2.1, Kir2.3, and $Ca_v1.2$ are primarily localized to transverse-tubule membranes (Carl et al., 1995; Melnyk et al., 2002; Sun et al., 1995). Moreover, significant populations of KvLQT1, ERG, minK, MiRP, Na/Ca exchanger, and Na/K ATPase are found at transverse-tubule and

peripheral sarcolemma membranes (Frank et al., 1992; Kieval et al., 1992; McDonough et al., 1996; Pond et al., 2000; Rasmussen et al., 2004; Wu et al., 2006). Finally, high resolution imaging techniques have revealed unique transverse-tubule membrane domains that further segregate cardiac ion channel signaling complexes (Scriven et al., 2000). Clearly, the molecular and structural characteristics of cardiac membrane domains represent a central feature for the regulation of local ion channel pathways and represent a relatively unexplored field in cell biology.

Ankyrin-based ion channel trafficking pathways have unique roles in specific cells. Recently, Pan and colleagues demonstrated the requirement of ankyrin-G association for the targeting of KCNQ2 and KCNQ3 (encode axonal M currents responsible for stabilizing neuronal resting potential) to axon initial segments. Specifically, ankyrin-G cerebellar-specific null mice display loss of KCNQ2/3 clustering at axonal initial segments (Pan et al., 2006). Moreover, the ankyrin-G–binding motif originally described in $Na_v1.2$ and $Na_v1.5$ (Garrido et al., 2003; Lemaillet et al., 2003; Mohler et al., 2004c) is present in the C-terminal domain of KCNQ2/3 and is required for neuronal KCNQ2/3 targeting (Chung et al., 2006; Pan et al., 2006; Rasmussen et al., 2007). Interestingly, although nearly structurally identical, KCNQ1 (cardiac KvLQT1) lacks the C-terminal ankyrin-G–binding motif (Pan et al., 2006; Rasmussen et al., 2007). Consistent with this data, ankyrin-G and KCNQ1 are differentially targeted in ventricular cardiomyocytes (Mohler et al., 2004c; Rasmussen et al., 2004). Therefore, these data strongly suggest that ankyrin-based pathways operate in a cell type–specific

manner. Furthermore the molecular mechanisms that target ankyrins are undefined and warrant further investigation.

In summary, our new findings show that ankyrin-G is the physiological binding partner for $Na_v1.5$ in cardiomyocytes. Loss of direct interaction between ankyrin-G and $Na_v1.5$ results in abnormal $Na_v1.5$ channel localization in primary cardiomyocytes. Moreover, the loss of ankyrin-G expression affects $Na_v1.5$ expression, membrane localization, and, therefore, whole cell $Na_v1.5$ activity. Based on recent ankyrin findings in the brain (Lencesova et al., 2004; Mohler and Bennett, 2005), heart (Kanter et al., 1992; Maier et al., 2004), and skeletal muscle (Kontrogianni-Konstantopoulos et al., 2004; Kontrogianni-Konstantopoulos et al., 2006), our new findings likely represent only the first component of a larger ankyrin-G macromolecular signaling complex at cardiomyocyte excitable membrane domains.

CHAPTER VI

FUTURE DIRECTIONS

Ankyrin-based trafficking pathways are vital for the normal expression of ion channels, transporters, cell adhesion molecules, and signaling proteins in several different cells (Cunha and Mohler, 2006; Kline and Mohler, 2006; Mohler et al., 2005b). Our findings demonstrate that the proper localization and function of voltage-gated sodium channels in striated muscle is controlled by an ankyrin-G-based cellular pathway (Lowe et al., 2008). While these data have provided new insight into the molecular mechanisms governing $Na_v1.5$ trafficking in excitable cells, a number of exciting questions remain unaddressed. For example, while we have determined that ankyrin-G is required for $Na_v1.5$ targeting to the plasma membrane, the molecular basis of ankyrin-G trafficking is unknown. Additionally, based on the role of ankyrins in other tissues for the biogenesis of membrane domains (e.g. epithelial membrane formation, initial segment development), does ankyrin-G play a similar role in the cardiomyocyte for membrane development? Moreover, once at the plasma membrane, what are the other components of the ankyrin-G-based intercalated disc complex? Finally, how is ankyrin-G regulated in the cardiomyocyte, and what defines ankyrin-G specificity (versus other ankyrins) for protein interactions *in vivo*?

Targeting of ankyrins

An ankyrin-G-dependent pathway targets $Na_v1.5$ (Lowe et al., 2008). However, to date, the pathways involved in the targeting of ankyrin-G are unknown. Based on findings from a number of mammalian tissues, as well data from *Drosophila* and *C. elegans*, we hypothesize that ankyrin-G trafficking in cardiomyocytes will be dictated by a combination of both plasma membrane cell adhesion molecule and cytoskeletal element activity (Dubreuil, 2006; Dubreuil et al., 1997; Dubreuil et al., 2000; Hammarlund et al., 2000; Hammarlund et al., 2007; Komada and Soriano, 2002).

A number of cell adhesion molecules have been demonstrated to target ankyrins. Specifically, ankyrins associate with cell adhesion molecules including CD44 (Kalomiris and Bourguignon, 1988; Lokeshwar et al., 1994), E-cadherin (Kizhatil et al., 2007a), and L1-cell adhesion molecule family molecules (L1CAM, NrCAM, neurofascin, NgCAM, CHLI) (Ango et al., 2004; Davis et al., 1993; Dubreuil and Yu, 1994; Dzhashiashvili et al., 2007; Hortsch et al., 1998; Martin et al., 2008; Zhou et al., 1998). Investigation of mouse node of Ranvier formation and development identified L1CAM members neurofascin-186 (NF-186) and neuron-glia related cell adhesion molecule (NrCAM) as the first molecules to establish protein clustering at nascent nodes (Lambert et al., 1997; Schafer, 2006). Specifically, NF-186 signals the recruitment of ankyrin-G in the central and peripheral nervous system (Schafer, 2006). The ligand for NF-186 is termed

gliomedin, which can induce Na_V channel clustering in cultures of neurons without Schwann cells (Eshed et al., 2005).

In addition to cell adhesion molecules, cytoskeletal elements including titin (Kontrogianni-Konstantopoulos and Bloch, 2003), tubulin (Davis and Bennett, 1984), obscurin (Bagnato et al., 2003), and beta-spectrin (Bennett, 1979) have been implicated in the membrane localization of ankyrin polypeptides. In erythrocytes, beta spectrin has a critical role for ankyrin-R membrane targeting (Bennett and Baines, 2001; Tse et al., 1990; Tse et al., 1991). Mice lacking beta spectrin display loss of ankyrin-R at the plasma membrane resulting in spherocytosis (Bodine et al., 1984; Greenquist et al., 1978). Human beta spectrin mutations affect ankyrin-R expression in the red blood cell and result in a similar human spherocytosis phenotype (Delaunay et al., 1996; Hassoun and Palek, 1996). In the central nervous system, mice lacking beta-IV spectrin display loss of ankyrin-G at axon initial segments and nodes of Ranvier (Komada and Soriano, 2002). Finally, in polarized epithelial cells, loss of beta-II spectrin affects ankyrin-G membrane localization resulting in abnormal lateral membrane formation (see below)(Kizhatil et al., 2007b). In contrast to these findings for ankyrin-G, recent findings from our lab suggest that beta-II spectrin is not required for ankyrin-B targeting in cardiomyocytes (Mohler et al., 2004e). Together, these findings suggest that both membrane and cytoskeletal elements may prove critical for ankyrin-G targeting to the cardiomyocyte intercalated disc. Future experiments using our neonatal and adult myocyte systems will be valuable to characterize these pathways as well as intracellular trafficking

systems (Rabs, Bves, ARFs, myosins, etc) for ankyrin-G (Du et al., 2008; Grosshans et al., 2006; Myers and Casanova, 2008; Sartore et al., 1981; Smith et al., 2008).

Ankyrins are critical for the establishment of membrane domains

In addition to roles in protein targeting, ankyrin-G may play an additional critical role in the development of the cardiomyocyte intercalated disc membrane domain. Data from cerebellar-specific ankyrin-G knockout mice, siRNA-treated human bronchial epithelial cells, and siRNA-injected mouse embryos support the necessity of ankyrin-G in membrane development (Kizhatil et al., 2007a; Kizhatil et al., 2007b). In the central nervous system, ankyrin-G is critical for the development of the AIS and node of Ranvier (Jenkins and Bennett, 2001; Zhang and Bennett, 1998). Specifically, mice lacking ankyrin-G in the cerebellum display decreased thickness of the molecular layer (Jenkins and Bennett, 2001; Zhang and Bennett, 1998; Zhou et al., 1998). Loss of molecular layer thickness and electrogenic properties in ankyrin-G null Purkinje neurons is thought to lead to cell degeneration that results in 60% fewer cells, when compared to littermate controls (Zhou et al., 1998).

In polarized epithelial cells, loss of ankyrin-G results in loss of lateral membrane, that subsequently increases cross-sectional area and reduces the height of the cells, changing the cells from columnar to squamous morphology (Kizhatil and Bennett, 2004). Loss of ankyrin-G also disrupts *de novo* biogenesis

of epithelial cell membranes following cytokinesis, as evidenced by a dramatic increase in binucleate cells (Kizhatil and Bennett, 2004). Bennett and colleagues have also suggested that the ankyrin-G pathway is critical for organizing the E-cadherin complex at sites of cell-cell contact in epithelial cells (Kizhatil and Bennett, 2004). Moreover, recent experiments show that ankyrin-G is required for exit of E-cadherin from the Trans-Golgi network, accumulation of E-cadherin at sites of cell-cell contact, and the process of compaction in mouse embryos (Kizhatil et al., 2007a). Relevant to the cardiomyocyte, ankyrin-G was recently reported to bind to N-cadherin, a protein critical for the development and maintenance of the intercalated disc (Kizhatil et al., 2007a; Oxford et al., 2007; Zuppinger et al., 2000). Interestingly, developmental abnormalities and/or disruption of intercalated disc structure have been linked to severe cardiac diseases, including dilated cardiomyopathies, cardiac-conduction disease, and cardiac hypertrophy (Awad et al., 2008; Li et al., 2008; Oxford et al., 2007; Perriard et al., 2003; Saffitz, 2005; van Tintelen et al., 2007).

Together, these data suggest that ankyrin-G could play a significant role in cardiac development at the level of compaction in the blastocyst, phospholipid accumulation in the membrane, and/or formation of specialized excitable cell membranes including the intercalated disc. The development of a cardiac-specific ankyrin-G null model mouse system will be critical to evaluate the role of ankyrin-G in cardiac development and mature myocyte membrane maintenance and function. Finally, $Na_v1.5$ itself appears to be important as a developmental checkpoint for the cardiomyocyte (Papadatos et al., 2002). For example, fetal

Scn5a null mice display severe structural heart defects, abnormal cardiac contractility, and undergo autolysis by embryonic day 12 (Papadatos et al., 2002). Thus, ankyrin-G-dependent and downstream elements appear to play important roles in development and will be important topics for future research.

Ankyrin-based signaling complex

$Na_v1.5$ is a key component of the ankyrin-G-based intercalated disc protein complex (Lowe et al., 2008; Maier et al., 2004; Mohler et al., 2004c). An obvious future direction is to identify other critical structural (see above) and signaling components of this ankyrin-G complex. For example, the phosphorylation state of $Na_v1.5$ is clearly important for the function of the channel (Abriel, 2007; Wagner et al., 2006). We hypothesize that ankyrin-G may play a role in coordinating local $Na_v1.5$ phospho-regulation. There are several kinases thought to modulate the activity of $Na_v1.5$ including protein kinase A (PKA) (Baba et al., 2004; Hallaq et al., 2006; Murray et al., 1997), Ca^{2+}/calmodulin-dependent kinase II delta-c ($CaMKII_{delta-c}$) (Wagner et al., 2006), protein kinase C (PKC) (Wagner et al., 2006), adenosine monophosphate-activated protein kinase (AMPK) (Arad et al., 2007; Light et al., 2003), and Src-family tyrosine kinases (including Fyn) (Ahern et al., 2005).

$Na_v1.5$ has been identified as a target of PKA signaling in myocytes (Baba et al., 2004; Murray et al., 1997). Specifically, beta-adrenergic activation drives the up regulation of cellular cyclic AMP and increases the activity of PKA. This

increase in PKA has been linked with forward trafficking of $Na_v1.5$ to the plasma membrane (Baba et al., 2004; Hallaq et al., 2006). It will interesting in future studies to determine whether ankyrin-G plays a role in this specific trafficking pathway, or whether this pathway is more closely related to the proposed caveolae-based membrane trafficking system .

In addition to PKA signaling, recent studies identified that CaMKII can directly bind and phosphorylate $Na_v1.5$ (Wagner et al., 2006). In cells that over-express $CaMKII_{delta-c}$, there was a Ca^{2+}-dependent shift of inactivation to hyperpolarized potentials, the recovery from inactivation was slowed, and the cells displayed an increase in persistent I_{Na} (Abriel, 2007; Wagner et al., 2006). These biophysical modifications were rate-dependent and therefore could lead to a Brugada syndrome phenotype at rapid heart rates, or an LQT3 phenotype at slow heart rates (Abriel, 2007; Wagner et al., 2006). Interestingly, $CaMKII_{delta-c}$ is up regulated in patients with heart failure and therefore may lead to rate-dependent arrhythmias in diseased patients (Abriel, 2007; Wagner et al., 2006).

PKC-dependent phosphorylation of $Na_v1.5$ is hypothesized to reduce the ability of the channel to conduct current and shifts steady state inactivation to more hyperpolarized potentials (Murray et al., 1997; Wagner and Maier, 2006). Previous data suggested that PKC activity can lead to a down regulation of $Na_v1.5$ at the membrane surface (Murray et al., 1997). However, the role of PKC-dependent activity in normal physiological function and $Na_v1.5$ surface expression remains to be clearly demonstrated.

The role of protein tyrosine kinases (various growth factors and Src family kinases) is very important in the regulation of ion channel biophysics (Ahern et al., 2005). For example, Fyn (discussed in Chapter III) is a potential member of a local $Na_v1.5$ signaling complex that causes a positive shift in the threshold of inactivation (Ahern et al., 2005). The positive shift in inactivation due to co-expression of constitutively active Fyn in HEK293 cells that stably express $Na_v1.5$ can lead to persistent I_{Na} (Ahern et al., 2005). Given the diverse set of kinases discussed above, another interesting family of proteins to consider as part of the local signaling complex of $Na_v1.5$ are protein phosphatases. The phosphatases PTPH1 (Davis et al., 2001) and PP2A (Bhasin et al., 2007) were discussed in Chapters III and V.

The potential modulatory activity of proteins known to organize multiple-component signaling complexes (including ion channels and kinases) such as clathrin and caveolin-3 are also potentially relevant for the ankyrin-G complex (Abriel, 2007). Clathrin is a well characterized component of several signaling complexes such as lipid rafts and a known binding partner of ankyrins (Maguy et al., 2006; Tombler et al., 2006). The specific physiological contribution of caveolae remain a topic of investigation due to the broad spectrum of ion channels and signaling proteins thought to be active partners in the caveolar-compartment of myocytes (Abriel, 2007; Baba et al., 2004; Cusdin et al., 2008; Palygin et al., 2008).

Together, these data set the stage for future experiments to further evaluate local signaling pathways that control $Na_v1.5$. Based on the linkage of

the number of signaling pathways with $Na_v1.5$, it will be interesting in future experiments to determine the role of ankyrin-G in recruiting and organizing signaling pathways at local membrane domains in myocytes. Moreover, it will be important to determine if other phospho-targets including ion channels, transporters, cytoskeletal elements, and/or signaling molecules are modulated by ankyrin-G in the myocyte.

Regulation of ankyrin-based activity

Ankyrin-based pathways play critical physiological roles in excitable and non-excitable cells. However, little is known regarding the regulation of the ankyrins themselves. Moreover, little is known regarding the mechanisms that determine specificity between ankyrin isoforms. Combinations of biochemical- and cell-based analyses have gleaned what little we know about these transcriptional, translational, and post-translational pathways.

Targeted analysis of *ANK1* gene regulation has revealed the promoter and transcription elements necessary for ankyrin-R expression (Gallagher et al., 2000). Promoter variants of *ANK1* block binding of TATA-binding protein that results in disruption of TFIID complex assembly and aberrant transcription (Gallagher et al., 2005). Further analyses into ankyrin-R expression revealed that alternative exon usage is used for the transcription of ankyrin-R in the brain (Gallagher et al., 1997). Analysis of small ankyrin-1 (links myofibrils with the SR) revealed that expression is driven by a muscle-specific promoter, further

supporting tissue-specific expression of ankyrin isoforms (Birkenmeier et al., 1998; Gallagher and Forget, 1998; Zhou et al., 1997).

Translational mechanisms further regulate ankyrin expression by demonstrating tissue-specific spliced forms of *ANK1* (Gallagher et al., 1997). Subsequent analyses demonstrate that there are several splice forms of *ANK1* and that splicing of the regulatory domain results in altered function of the protein product (Gallagher et al., 1997; Lambert and Bennett, 1993; Lambert et al., 1990; Lux et al., 1990b). Ankyrin-G is also alternatively spliced in a tissue-specific manner, and within the regulatory domain (Hopitzan et al., 2005). Similar to ankyrin-R, ankyrin-G was discovered to maintain two alternative start sites for translation (Peters et al., 1995). Finally, alternate length polyadenylation signals were discovered as another modulator of translation in ankyrin-R (Gallagher et al., 1997).

The first evidence for post-translational modification of ankyrin came from studies of the neuronal isoforms of ankyrin-G (Zhang and Bennett, 1996). The neuronal isoforms that localize to the nodes of Ranvier are post-translationally-modified by O-linked N-acetylglucosamine within a serine-rich insert in the regulatory domain (Zhang and Bennett, 1996). There is also a high concentration of potential phospho-regulation sites between the spectrin-binding and membrane–binding domain (Peters et al., 1995). Although there is incomplete evidence that these motifs are phosphorylated *in vivo*, the charged structures and salt sensitivity of ankyrin polypeptides, suggests that phosphorylation may dramatically affect the tertiary folding of the protein (Abdi et

al., 2006; Davis et al., 1989; Hall and Bennett, 1987; Michaely and Bennett, 1993; Michaely and Bennett, 1995a; Peters et al., 1995). Recent studies have identified the importance of inhibitor of kappa-B kinase ($IKK_{alpha/beta}$) activity and the localized accumulation of phosphorylated-inhibitor of kappa-B (pIKb) in establishment of the AIS (Sanchez-Ponce et al., 2008). Inhibition of this pathway eliminated the accumulation of ankyrin-G and $Na_v1.5$ at the AIS (Sanchez-Ponce et al., 2008). These data suggest the potential modulation of the ankyrin-G-pathway by phospho-proteins that are downstream of several signaling pathways. However, the specific molecular mechanism of pIKb modulation of ankyrin-G and whether this pathway is required for accumulation of ankyrin-G and $Na_v1.5$ at the intercalated disc in cardiomyocytes has not been defined.

Structural and biochemical analysis of the membrane-binding domain has determined that protein folding is also critical for ankyrin function (Davis et al., 1989; Michaely and Bennett, 1993; Michaely and Bennett, 1995a). Specifically, the binding sites for anion exchanger on ankyrin-R membrane-binding domain are along a non-contiguous stretch of residues (Davis et al., 1989). Further analysis of how the anion exchanger is bound by ankyrin-R revealed that the tertiary structure of the membrane-binding domain was as important as the primary residue sequence (Michaely and Bennett, 1993; Michaely and Bennett, 1995b). Although these studies provided important clues about what determines specificity of the membrane-binding domain for binding proteins, the high degree of residue conservation between ankyrin isoforms still require exploration to address the question of ankyrin isoform specificity. For example, the localization

of the Na^+/K^+ ATPase is ankyrin-G-dependent in kidney, but surprisingly ankyrin-B-dependent in cardiomyocytes, even though both isoforms readily associate with the pump *in vitro* and are expressed in the respective tissues (Gallagher et al., 1997; Mohler et al., 2002a; Thevananther et al., 1998).

The first clues for domain specificity and intermolecular interactions of ankyrin isoforms came from studies of ankyrin-R that demonstrated that an alternatively spliced fragment associated with the longer isoform (ankyrin-R 2.2) and modulated the availability of the isoform to bind spectrin and the anion exchanger (Gallagher et al., 1997; Lambert and Bennett, 1993; Lambert et al., 1990; Lux et al., 1990a). Subsequent studies for intermolecular interactions with ankyrins identified that obscurin (see above) and the heat-shock protein Hsp40 can bind the carboxy-terminal domain of ankyrin-B (Kontrogianni-Konstantopoulos et al., 2003; Mohler et al., 2004b). Analyses done to determine the specificity of ankyrin-B versus ankyrin–G protein domains (Membrane-binding, Spectrin-binding, Carboxy-terminal (MSC)) showed that the carboxy-terminal domain of ankyrin-B has regulatory properties for protein-protein interactions and membrane targeting (localization of $InsP_3$ and RyR)(Mohler et al., 2002a). However, the specific regulatory properties of ankyrin-G in heart are the target of future experiments. Recent mutagenesis experiments of the carboxy-terminal domain in ankyrin-B have identified a unique domain in ankyrin-B that is critical for cardiac function (Abdi et al., 2006). These experiments identified a large non-homologous region between ankyrin-B and ankyrin-G that has intramolecular regulatory activity (Abdi et al., 2006). Specifically, a region

within the carboxy-terminal domain binds the membrane-binding domain and changes the conformation and availability of the molecule (Abdi et al., 2006). Moreover, biochemical and structural studies of ankyrin polypeptides show that the charged residues are likely to impart structural modification after changes in charge (phosphorylation) or hydrophobicity (Abdi et al., 2006; Davis and Bennett, 1994; Davis et al., 1991; Hall and Bennett, 1987; Michaely and Bennett, 1993; Michaely and Bennett, 1995a, b; Mohler et al., 2004b). These conformational changes may have functional significance in modulating signaling complex activity, associated ion channel gating and/or specialized membrane domain conformation. Together, these data demonstrate several pathways to investigate the intricate regulation of ankyrin-G activity and expression. Future experiments designed to evaluate the domain-specific regulation of ankyrin-G will be vitally important in understanding ankyrin-G-dependent pathways in cardiomyocytes.

REFERENCES

Abdi, K.M., Mohler, P.J., Davis, J.Q., and Bennett, V. (2006). Isoform specificity of ankyrin-B: A site in the divergent c-terminal domain is required for intramolecular association. J Biol Chem *281*, 5741-5749.

Abriel, H. (2007). Roles and regulation of the cardiac sodium channel $Na_v1.5$: Recent insights from experimental studies. Cardiovasc Res *76*, 381-389.

Abriel, H., and Kass, R.S. (2005). Regulation of the voltage-gated cardiac sodium channel $Na_v1.5$ by interacting proteins. Trends in Cardiovascular Medicine *15*, 35.

Agarkova, I., and Perriard, J.-C. (2005). The M-band: an elastic web that crosslinks thick filaments in the center of the sarcomere. Trends in Cell Biology *15*, 477.

Ahern, C.A., Zhang, J.-F., Wookalis, M.J., and Horn, R. (2005). Modulation of the cardiac sodium channel $Na_v1.5$ by Fyn, a Src family tyrosine kinase. Circ Res *96*, 991-998.

Ango, F., di Cristo, G., Higashiyama, H., Bennett, V., Wu, P., and Huang, Z.J. (2004). Ankyrin-based subcellular gradient of Neurofascin, an immunoglobulin family protein, directs GABAergic innervation at Purkinje axon initial segment. Cell *119*, 257.

Antzelevitch, C., Brugada, P., Borggrefe, M., Brugada, J., Brugada, R., Corrado, D., Gussak, I., LeMarec, H., Nademanee, K., Perez Riera, A.R.*, et al.* (2005). Brugada syndrome: report of the second consensus conference. Circulation *111*, 659 - 670.

Arad, M., Seidman, C.E., and Seidman, J.G. (2007). AMP-Activated Protein Kinase in the heart: Role during health and disease. Circ Res *100*, 474-488.

Awad, M.M., Calkins, H., and Judge, D.P. (2008). Mechanisms of Disease: molecular genetics of arrhythmogenic right ventricular dysplasia/cardiomyopathy. Nat Clin Pract Cardiovasc Med *5*, 258.

Baba, S., Dun, W., and Boyden, P.A. (2004). Can PKA activators rescue Na^+ channel function in epicardial border zone cells that survive in the infarcted canine heart? Cardiovasc Res *64*, 260-267.

Bagnato, P., Barone, V., Giacomello, E., Rossi, D., and Sorrentino, V. (2003). Binding of an ankyrin-1 isoform to obscurin suggests a molecular link between the sarcoplasmic reticulum and myofibrils in striated muscles. J Cell Biol *160*, 245-253.

Balser, J.R. (2001). The cardiac sodium channel: Gating function and molecular pharmacology. Journal of Molecular and Cellular Cardiology *33*, 599.

Barry, D.M., Trimmer, J.S., Merlie, J.P., and Nerbonne, J.M. (1995). Differential expression of voltage-gated K^+ channel subunits in adult rat heart : Relation to functional K^+ channels? Circ Res *77*, 361-369.

Bennett, V. (1979). Immunoreactive forms of human erythrocyte ankyrin are present in diverse cells and tissues. Nature *281*, 597.

Bennett, V., and Baines, A.J. (2001). Spectrin and ankyrin-based pathways: Metazoan inventions for integrating cells into tissues. Physiol Rev *81*, 1353-1392.

Bennett, V., and Stenbuck, P.J. (1979a). Identification and partial purification of ankyrin, the high affinity membrane attachment site for human erythrocyte spectrin. J Biol Chem *254*, 2533-2541.

Bennett, V., and Stenbuck, P.J. (1979b). The membrane attachment protein for spectrin is associated with band 3 in human erythrocyte membranes. Nature *280*, 468.

Bers, D.M. (2001). Excitation-Contraction Coupling and Cardiac Contractile Force, Second edn (Kluwer Academic Publishers).

Bers, D.M. (2002). Cardiac excitation-contraction coupling. Nature *415*, 198.

Bers, D.M., and Despa, S. (2006). Cardiac myocytes Ca^{2+} and Na^+ regulation in normal and failing hearts. Journal of Pharmacological Sciences *100*, 315.

Bezzina, C.R., Rook, M.B., and Wilde, A.A. (2001). Cardiac sodium channel and inherited arrhythmia syndromes. Cardiovasc Res *49*, 257-271.

Bhasin, N., Cunha, S.R., Mudannayake, M., Gigena, M.S., Rogers, T.B., and Mohler, P.J. (2007). Molecular basis for PP2A regulatory subunit B56 alpha targeting in cardiomyocytes. Am J Physiol Heart Circ Physiol *293*, H109-119.

Birkenmeier, C.S., Sharp, J.J., Gifford, E.J., Deveau, S.A., and Barker, J.E. (1998). An alternative first exon in the distal end of the erythroid ankyrin gene leads to production of a small isoform containing an NH2-terminal membrane anchor. Genomics *50*, 79.

Bodine, D.M., Birkenmeier, C.S., and Barker, J.E. (1984). Spectrin deficient inherited hemolytic anemias in the mouse: Characterization by spectrin synthesis and mRNA activity in reticulocytes. Cell *37*, 721.

Brugada, J., and Brugada, P. (1995). Right bundle branch block, ST segment elevation and sudden cardiac death. Symptomatic, asymptomatic and intermittent forms. Journal of the American College of Cardiology *25*, 93A.

Brugada, J., Brugada, R., and Brugada, P. (1998). Right bundle-branch block and ST-segment elevation in leads V1 through V3: a marker for sudden death in patients without demonstrable structural heart disease. Circulation *97*, 457 - 460.

Brugada, P., and Brugada, J. (1992). Right bundle branch block, persistent ST segment elevation and sudden cardiac death: a distinct clinical and electrocardiographic syndrome. A multicenter report. J Am Coll Cardiol *20*, 1391 - 1396.

Brummelkamp, T.R., Bernards, R., and Agami, R. (2002). A system for stable expression of short interfering RNAs in mammalian cells. Science *296*, 550-553.

Carl, S.L., Felix, K., Caswell, A.H., Brandt, N.R., Ball, W.J., Jr., Vaghy, P.L., Meissner, G., and Ferguson, D.G. (1995). Immunolocalization of sarcolemmal dihydropyridine receptor and sarcoplasmic reticular triadin and ryanodine receptor in rabbit ventricle and atrium. J Cell Biol *129*, 673-682.

Catterall, W.A., Goldin, A.L., and Waxman, S.G. (2005). International Union of Pharmacology. XLVII. Nomenclature and structure-function relationships of voltage-gated sodium channels. Pharmacol Rev *57*, 397-409.

Chen, C., Bharucha, V., Chen, Y., Westenbroek, R.E., Brown, A., Malhotra, J.D., Jones, D., Avery, C., Gillespie, P.J., Kazen-Gillespie, K.A.*, et al.* (2002). Reduced sodium channel density, altered voltage dependence of inactivation, and increased susceptibility to seizures in mice lacking sodium channel beta2-subunits. Proceedings of the National Academy of Sciences of the United States of America *99*, 17072-17077.

Chopra, N., Kannankeril, P.J., Yang, T., Hlaing, T., Holinstat, I., Ettensohn, K., Pfeifer, K., Akin, B., Jones, L.R., Franzini-Armstrong, C.*, et al.* (2007). Modest reductions of cardiac calsequestrin increase sarcoplasmic reticulum Ca^{2+} leak independent of luminal Ca^{2+} and trigger ventricular arrhythmias in mice. Circ Res *101*, 617-626.

Chung, H.J., Jan, Y.N., and Jan, L.Y. (2006). Polarized axonal surface expression of neuronal KCNQ channels is mediated by multiple signals in the KCNQ2 and KCNQ3 C-terminal domains. Proceedings of the National Academy of Sciences *103*, 8870-8875.

Cunha, S.R., Bhasin, N., and Mohler, P.J. (2007). Targeting and stability of Na/Ca exchanger 1 in cardiomyocytes requires direct interaction with the membrane adaptor ankyrin-B. J Biol Chem *282*, 4875-4883.

Cunha, S.R., and Mohler, P.J. (2006). Cardiac ankyrins: Essential components for development and maintenance of excitable membrane domains in heart. Cardiovasc Res *71*, 22-29.

Curran, M.E., Splawski, I., Timothy, K.W., Vincen, G.M., Green, E.D., and Keating, M.T. (1995). A molecular basis for cardiac arrhythmia: HERG mutations cause long QT syndrome. Cell *80*, 795.

Cusdin, F.S., Clare, J.J., and Jackson, A.P. (2008). Trafficking and cellular distribution of voltage-gated sodium channels. Traffic *9*, 17-26.

Danowski, B.A., Imanaka-Yoshida, K., Sanger, J.M., and Sanger, J.W. (1992). Costameres are sites of force transmission to the substratum in adult rat cardiomyocytes. J Cell Biol *118*, 1411-1420.

Davis, J., Davis, L., and Bennett, V. (1989). Diversity in membrane binding sites of ankyrins. Brain ankyrin, erythrocyte ankyrin, and processed erythrocyte ankyrin associate with distinct sites in kidney microsomes. J Biol Chem *264*, 6417-6426.

Davis, J.Q., and Bennett, V. (1984). Brain ankyrin. A membrane-associated protein with binding sites for spectrin, tubulin, and the cytoplasmic domain of the erythrocyte anion channel. J Biol Chem *259*, 13550-13559.

Davis, J.Q., and Bennett, V. (1994). Ankyrin binding activity shared by the neurofascin/L1/NrCAM family of nervous system cell adhesion molecules. J Biol Chem *269*, 27163-27166.

Davis, J.Q., Lambert, S., and Bennett, V. (1996). Molecular composition of the node of Ranvier: identification of ankyrin- binding cell adhesion molecules neurofascin (mucin+/third FNIII domain-) and NrCAM at nodal axon segments. J Cell Biol *135*, 1355-1367.

Davis, J.Q., McLaughlin, T., and Bennett, V. (1993). Ankyrin-binding proteins related to nervous system cell adhesion molecules: candidates to provide transmembrane and intercellular connections in adult brain. J Cell Biol *121*, 121-133.

Davis, L.H., Otto, E., and Bennett, V. (1991). Specific 33-residue repeat(s) of erythrocyte ankyrin associate with the anion exchanger. J Biol Chem *266*, 11163-11169.

Davis, M.J., Wu, X., Nurkiewicz, T.R., Kawasaki, J., Gui, P., Hill, M.A., and Wilson, E. (2001). Regulation of ion channels by protein tyrosine phosphorylation. Am J Physiol Heart Circ Physiol *281*, H1835-1862.

Delaunay, J., Alloisio, N., Morle, L., Baklouti, F., Dalla Venezia, N., Maillet, P., and Wilmotte, R. (1996). Molecular genetics of hereditary elliptocytosis and hereditary spherocytosis. Annales de Genetique *39*, 209-221.

Delisle, B.P., Anson, B.D., Rajamani, S., and January, C.T. (2004). Biology of cardiac arrhythmias: Ion channel protein trafficking. Circ Res *94*, 1418-1428.

Devarajan, P., Scaramuzzino, D.A., and Morrow, J.S. (1994). Ankyrin binds to two distinct cytoplasmic domains of Na,K-ATPase alpha subunit. Proceedings of the National Academy of Sciences of the United States of America *91*, 2965-2969.

Dobson, G.P. (2003). On being the right size: heart design, mitochondrial efficiency, and lifespan potential. Clinical and Experimental Pharmacology and Physiology *30*, 590-597.

Du, A., Sanger, J.M., and Sanger, J.W. (2008). Cardiac myofibrillogenesis inside intact embryonic hearts. Developmental Biology *318*, 236.

Dubreuil, R. (2006). Functional links between membrane transport and the spectrin cytoskeleton. Journal of Membrane Biology *211*, 151.

Dubreuil, R.R., Maddux, P.B., Grushko, T.A., and Macvicar, G.R. (1997). Segregation of two spectrin isoforms: Polarized membrane-binding sites direct polarized membrane skeleton assembly. Mol Biol Cell *8*, 1933-1942.

Dubreuil, R.R., Wang, P., Dahl, S., Lee, J., and Goldstein, L.S.B. (2000). Drosophila beta-spectrin functions independently of alpha-spectrin to polarize the Na,K ATPase in epithelial cells. J Cell Biol *149*, 647-656.

Dubreuil, R.R., and Yu, J. (1994). Ankyrin and beta-spectrin accumulate independently of alpha-spectrin in Drosophila. Proceedings of the National Academy of Sciences of the United States of America *91*, 10285-10289.

Dzhashiashvili, Y., Zhang, Y., Galinska, J., Lam, I., Grumet, M., and Salzer, J.L. (2007). Nodes of Ranvier and axon initial segments are ankyrin G-dependent domains that assemble by distinct mechanisms. J Cell Biol *177*, 857-870.

Endoh, M. (2006). Signal transduction and Ca^{2+} signaling in intact myocardium. Journal of Pharmacological Sciences *100*, 525.

Eshed, Y., Feinberg, K., Poliak, S., Sabanay, H., Sarig-Nadir, O., Spiegel, I., Bermingham, J.J.R., and Peles, E. (2005). Gliomedin mediates Schwann cell-axon interaction and the molecular assembly of the nodes of Ranvier. Neuron *47*, 215.

Flucher, B.E., and Daniels, M.P. (1989). Distribution of Na^{+} channels and ankyrin in neuromuscular junctions is complementary to that of acetylcholine receptors and the 43 kd protein. Neuron *3*, 163.

Frank, J.S., Mottino, G., Reid, D., Molday, R.S., and Philipson, K.D. (1992). Distribution of the Na^{+}/Ca^{2+} exchange protein in mammalian cardiac myocytes: An immunofluorescence and immunocolloidal gold-labeling study. J Cell Biol *117*, 337-345.

Gallagher, P.G., and Forget, B.G. (1998). An alternate promoter directs expression of a truncated, muscle-specific isoform of the human ankyrin-1 gene. J Biol Chem *273*, 1339-1348.

Gallagher, P.G., Nilson, D.G., Wong, C., Weisbein, J.L., Garrett-Beal, L.J., Eber, S.W., and Bodine, D.M. (2005). A dinucleotide deletion in the ankyrin promoter alters gene expression, transcription initiation and TFIID complex formation in hereditary spherocytosis. Hum Mol Genet *14*, 2501-2509.

Gallagher, P.G., Romana, M., Tse, W.T., Lux, S.E., and Forget, B.G. (2000). The human ankyrin-1 gene is selectively transcribed in erythroid cell lines despite the presence of a housekeeping-like promoter. Blood *96*, 1136-1143.

Gallagher, P.G., Tse, W.T., Scarpa, A.L., Lux, S.E., and Forget, B.G. (1997). Structure and organization of the human ankyrin-1 Gene. Basis for complexity of pre-mRNA processing. J Biol Chem *272*, 19220-19228.

Garrido, J.J., Giraud, P., Carlier, E., Fernandes, F., Moussif, A., Fache, M.P., Debanne, D., and Dargent, B. (2003). A targeting motif involved in sodium channel clustering at the axonal initial segment. Science *300*, 2091-2094.

Greenquist, A.C., Shohet, S.B., and Bernstein, S.E. (1978). Marked reduction of spectrinin hereditary spherocytosis in the common house mouse. Blood *51*, 1149-1155.

Grosshans, B.L., Ortiz, D., and Novick, P. (2006). Rabs and their effectors: Achieving specificity in membrane traffic. Proceedings of the National Academy of Sciences *103*, 11821-11827.

Grueter, C.E., Abiria, S.A., Dzhura, I., Wu, Y., Ham, A.-J.L., Mohler, P.J., Anderson, M.E., and Colbran, R.J. (2006). L-type Ca^{2+} channel facilitation mediated by phosphorylation of the beta-subunit by CaMKII. Molecular Cell *23*, 641.

Hall, T.G., and Bennett, V. (1987). Regulatory domains of erythrocyte ankyrin. Journal of Biological Chemistry *262*, 10537-10545.

Hallaq, H., Yang, Z., Viswanathan, P.C., Fukuda, K., Shen, W., Wang, D.W., Wells, K.S., Zhou, J., Yi, J., and Murray, K.T. (2006). Quantitation of protein kinase A-mediated trafficking of cardiac sodium channels in living cells. Cardiovasc Res *72*, 250-261.

Hammarlund, M., Davis, W.S., and Jorgensen, E.M. (2000). Mutations in beta-spectrin disrupt axon outgrowth and sarcomere structure. J Cell Biol *149*, 931-942.

Hammarlund, M., Jorgensen, E.M., and Bastiani, M.J. (2007). Axons break in animals lacking {beta}-spectrin. J Cell Biol *176*, 269-275.

Hassoun, H., and Palek, J. (1996). Hereditary spherocytosis: a review of the clinical and molecular aspects of the disease. Blood Reviews *10*, 129.

Hopitzan, A.A., Baines, A.J., Ludosky, M.-A., Recouvreur, M., and Kordeli, E. (2005). Ankyrin-G in skeletal muscle: Tissue-specific alternative splicing contributes to the complexity of the sarcolemmal cytoskeleton. Experimental Cell Research *309*, 86.

Hortsch, M., Homer, D., Malhotra, J.D., Chang, S., Frankel, J., Jefford, G., and Dubreuil, R.R. (1998). Structural requirements for outside-in and inside-out signaling by Drosophila neuroglian, a member of the L1 family of cell adhesion molecules. J Cell Biol *142*, 251-261.

Jenkins, S.M., and Bennett, V. (2001). Ankyrin-G coordinates assembly of the spectrin-based membrane skeleton, voltage-gated sodium channels, and L1 CAMs at Purkinje neuron initial segments. J Cell Biol *155*, 739-746.

Jespersen, T., Gavillet, B., van Bemmelen, M.X., Cordonier, S., Thomas, M.A., Staub, O., and Abriel, H. (2006). Cardiac sodium channel Nav1.5 interacts with and is regulated by the protein tyrosine phosphatase PTPH1. Biochemical and Biophysical Research Communications *348*, 1455.

Jons, T., and Drenckhahn, D. (1998). Anion exchanger 2 (AE2) binds to erythrocyte ankyrin and is colocalized with ankyrin along the basolateral plasma membrane of human gastric parietal cells. Eur J Cell Biol *75*, 232-236.

Kahlig, K.M., Misra, S.N., and George, A.L., Jr. (2006). Impaired inactivation gate stabilization predicts increased persistent current for an epilepsy-associated SCN1A mutation. J Neurosci *26*, 10958-10966.

Kalomiris, E.L., and Bourguignon, L.Y. (1988). Mouse T lymphoma cells contain a transmembrane glycoprotein (GP85) that binds ankyrin. J Cell Biol *106*, 319-327.

Kanter, H.L., Saffitz, J.E., and Beyer, E.C. (1992). Cardiac myocytes express multiple gap junction proteins. Circ Res *70*, 438-444.

Keating, M., Atkinson, D., Dunn, C., Timothy, K., Vincent, G.M., and Leppert, M. (1991). Linkage of a cardiac arrhythmia, the long QT syndrome, and the Harvey ras-1 gene. Science *252*, 704-706.

Kieval, R.S., Bloch, R.J., Lindenmayer, G.E., Ambesi, A., and Lederer, W.J. (1992). Immunofluorescence localization of the Na-Ca exchanger in heart cells. Am J Physiol Cell Physiol *263*, C545-550.

Kizhatil, K., and Bennett, V. (2004). Lateral membrane biogenesis in human bronchial epithelial cells requires 190-kDa ankyrin-G. J Biol Chem *279*, 16706-16714.

Kizhatil, K., Davis, J.Q., Davis, L., Hoffman, J., Hogan, B.L.M., and Bennett, V. (2007a). Ankyrin-G Is a molecular partner of E-cadherin in epithelial cells and early embryos. J Biol Chem *282*, 26552-26561.

Kizhatil, K., Yoon, W., Mohler, P.J., Davis, L.H., Hoffman, J.A., and Bennett, V. (2007b). Ankyrin-G and beta2-spectrin collaborate in biogenesis of lateral membrane of human bronchial epithelial cells. J Biol Chem *282*, 2029-2037.

Kline, C.F., and Mohler, P.J. (2006). Weighing in on molecular anchors: the role of ankyrin polypeptides in human arrhythmia. Expert Review of Cardiovascular Therapy *4*, 477-485.

Komada, M., and Soriano, P. (2002). betaIV-spectrin regulates sodium channel clustering through ankyrin-G at axon initial segments and nodes of Ranvier. J Cell Biol *156*, 337-348.

Kontrogianni-Konstantopoulos, A., and Bloch, R.J. (2003). The hydrophilic domain of small ankyrin-1 interacts with the two N-terminal immunoglobulin domains of titin. J Biol Chem *278*, 3985-3991.

Kontrogianni-Konstantopoulos, A., Catino, D.H., Strong, J.C., Randall, W.R., and Bloch, R.J. (2004). Obscurin regulates the organization of myosin into A bands. Am J Physiol Cell Physiol *287*, C209-217.

Kontrogianni-Konstantopoulos, A., Catino, D.H., Strong, J.C., Sutter, S., Borisov, A.B., Pumplin, D.W., Russell, M.W., and Bloch, R.J. (2006). Obscurin modulates the assembly and organization of sarcomeres and the sarcoplasmic reticulum. FASEB J *20*, 2102-2111.

Kontrogianni-Konstantopoulos, A., Jones, E.M., van Rossum, D.B., and Bloch, R.J. (2003). Obscurin is a ligand for small ankyrin 1 in skeletal muscle. Mol Biol Cell *14*, 1138-1148.

Koob, R., Zimmermann, M., Schoner, W., and Drenckhahn, D. (1988). Colocalization and coprecipitation of ankyrin and Na^+,K^+-ATPase in kidney epithelial cells. Eur J Cell Biol *45*, 230-237.

Kordeli, E., Lambert, S., and Bennett, V. (1995). Ankyrin-G. A new ankyrin gene with neural-specific isoforms localized at the axonal initial segment and node of Ranvier. J Biol Chem *270*, 2352-2359.

Kordeli, E., Ludosky, M.A., Deprette, C., Frappier, T., and Cartaud, J. (1998). Ankyrin-G is associated with the postsynaptic membrane and the sarcoplasmic reticulum in the skeletal muscle fiber. J Cell Sci *111*, 2197-2207.

Lambert, S., and Bennett, V. (1993). Postmitotic expression of ankyrin-R and beta-spectrin in discrete neuronal populations of the rat brain. J Neurosci *13*, 3725-3735.

Lambert, S., Davis, J.Q., and Bennett, V. (1997). Morphogenesis of the node of Ranvier: Co-clusters of ankyrin and ankyrin-binding integral proteins define early developmental intermediates. J Neurosci *17*, 7025-7036.

Lambert, S., Yu, H., Prchal, J.T., Lawler, J., Ruff, P., Speicher, D., Cheung, M.C., Kan, Y.W., and Palek, J. (1990). cDNA sequence for human erythrocyte ankyrin. Proceedings of the National Academy of Sciences of the United States of America *87*, 1730-1734.

Lange, S., Ehler, E., and Gautel, M. (2006a). From A to Z and back? Multicompartment proteins in the sarcomere. Trends in Cell Biology *16*, 11-18.

Lehnart, S.E., Ackerman, M.J., Benson, D.W., Jr., Brugada, R., Clancy, C.E., Donahue, J.K., George, A.L., Jr., Grant, A.O., Groft, S.C., January, C.T.*, et al.* (2007). Inherited Arrhythmias: A National Heart, Lung, and Blood Institute and Office of Rare Diseases Workshop Consensus Report About the Diagnosis, Phenotyping, Molecular mechanisms, and Therapeutic approaches for primary cardiomyopathies of gene mutations affecting ion channel function. Circulation *116*, 2325-2345.

Lemaillet, G., Walker, B., and Lambert, S. (2003). Identification of a conserved ankyrin-binding motif in the family of sodium channel alpha-subunits. J Biol Chem *278*, 27333-27339.

Lencesova, L., O'Neill, A., Resneck, W.G., Bloch, R.J., and Blaustein, M.P. (2004). Plasma membrane-cytoskeleton-endoplasmic reticulum complexes in neurons and astrocytes. J Biol Chem *279*, 2885-2893.

Li, J., Levin, M.D., Xiong, Y., Petrenko, N., Patel, V.V., and Radice, G.L. (2008). N-cadherin haploinsufficiency affects cardiac gap junctions and arrhythmic susceptibility. Journal of Molecular and Cellular Cardiology *44*, 597.

Li, Z.P., Burke, E.P., Frank, J.S., Bennett, V., and Philipson, K.D. (1993). The cardiac Na^+/Ca^{2+} exchanger binds to the cytoskeletal protein ankyrin. J Biol Chem *268*, 11489-11491.

Light, P.E., Wallace, C.H.R., and Dyck, J.R.B. (2003). Constitutively active Adenosine Monophosphate-activated Protein Kinase regulates voltage-gated sodium channels in ventricular myocytes. Circulation *107*, 1962-1965.

Liu, C.-j., Dib-Hajj, S.D., Renganathan, M., Cummins, T.R., and Waxman, S.G. (2003). Modulation of the cardiac sodium channel $Na_v1.5$ by Fibroblast Growth Factor Homologous Factor 1B. J Biol Chem *278*, 1029-1036.

Locke, I., G.R., Ackerman, M.J., Zinsmeister, A.R., Thapa, P. and Farrugia, G. (2006). Gastrointestinal symptoms in families of patients with an SCN5A-encoded cardiac channelopathy: Evidence of an intestinal channelopathy. The American Journal of Gastroenterology *101*, 1299-1304.

Lokeshwar, V.B., Fregien, N., and Bourguignon, L.Y. (1994). Ankyrin-binding domain of CD44(GP85) is required for the expression of hyaluronic acid-mediated adhesion function. J Cell Biol *126*, 1099-1109.

Lopez-Santiago, L.F., Meadows, L.S., Ernst, S.J., Chen, C., Malhotra, J.D., McEwen, D.P., Speelman, A., Noebels, J.L., Maier, S.K.G., Lopatin, A.N.*, et al.* (2007). Sodium channel Scn1b null mice exhibit prolonged QT and RR intervals. Journal of Molecular and Cellular Cardiology *43*, 636.

Lopez, C., Metral, S., Eladari, D., Drevensek, S., Gane, P., Chambrey, R., Bennett, V., Cartron, J.-P., Le Van Kim, C., and Colin, Y. (2004). The ammonium transporter RhBG : Requirement of a tyrosine-based signal and ankyrin-G for basolateral targeting and membrane anchorage in polarized kidney epithelial cells. J Biol Chem, M413351200.

Lowe, J.S., Palygin, O., Bhasin, N., Hund, T.J., Boyden, P.A., Shibata, E., Anderson, M.E., and Mohler, P.J. (2008). Voltage-gated Nav channel targeting in the heart requires an ankyrin-G dependent cellular pathway. J Cell Biol *180*, 173-186.

Lux, S.E., John, K.M., and Bennett, V. (1990a). Analysis of cDNA for human erythrocyte ankyrin indicates a repeated structure with homology to tissue-differentiation and cell-cycle control proteins. Nature *344*, 36-42.

Lux, S.E., Tse, W.T., Menninger, J.C., John, K.M., Harris, P., Shalev, O., Chilcote, R.R., Marchesi, S.L., Watkins, P.C., and Bennett, V. (1990b). Hereditary spherocytosis associated with deletion of human erythrocyte ankyrin gene on chromosome 8. Nature *345*, 736-739.

Maguy, A., Hebert, T.E., and Nattel, S. (2006). Involvement of lipid rafts and caveolae in cardiac ion channel function. Cardiovasc Res *69*, 798-807.

Maier, S.K.G., Westenbroek, R.E., McCormick, K.A., Curtis, R., Scheuer, T., and Catterall, W.A. (2004). Distinct subcellular localization of different sodium channel alpha- and beta- subunits in single ventricular myocytes from mouse heart. Circulation *109*, 1421-1427.

Malhotra, J.D., Thyagarajan, V., Chen, C., and Isom, L.L. (2004). Tyrosine-phosphorylated and nonphosphorylated sodium channel beta1 subunits are differentially localized in cardiac myocytes. J Biol Chem *279*, 40748-40754.

Martin, P.-M., Carnaud, M., del Cano, G.G., Irondelle, M., Irinopoulou, T., Girault, J.-A., Dargent, B., and Goutebroze, L. (2008). Schwannomin-Interacting Protein-1 isoform IQCJ-SCHIP-1 is a late component of nodes of Ranvier and axon initial segments. J Neurosci *28*, 6111-6117.

McDonough, A.A., Zhang, Y., Shin, V., and Frank, J.S. (1996). Subcellular distribution of sodium pump isoform subunits in mammalian cardiac myocytes. Am J Physiol Cell Physiol *270*, C1221-1227.

Melnyk, P., Zhang, L., Shrier, A., and Nattel, S. (2002). Differential distribution of $K_{ir}2.1$ and $K_{ir}2.3$ subunits in canine atrium and ventricle. Am J Physiol Heart Circ Physiol *283*, H1123-1133.

Michaely, P., and Bennett, V. (1993). The membrane-binding domain of ankyrin contains four independently folded subdomains, each comprised of six ankyrin repeats. J Biol Chem *268*, 22703-22709.

Michaely, P., and Bennett, V. (1995a). The ANK repeats of erythrocyte ankyrin form two distinct but cooperative binding sites for the erythrocyte anion exchanger. J Biol Chem *270*, 22050-22057.

Michaely, P., and Bennett, V. (1995b). Mechanism for binding site diversity on ankyrin. J Biol Chem *270*, 31298-31302.

Michaely, P., Tomchick, D.R., Machius, M., and Anderson, R.G.W. (2002). Crystal structure of a 12 ANK repeat stack from human ankyrinR. The EMBO Journal *21*, 6387.

Mohler, P.J., and Bennett, V. (2005). Defects in ankyrin-based cellular pathways in metazoan physiology. Front Biosci *10*, 2832-2840.

Mohler, P.J., Davis, J.Q., and Bennett, V. (2005a). Ankyrin-B coordinates the Na/K ATPase, Na/Ca exchanger, and $InsP_3$ receptor in a cardiac T-Tubule/SR microdomain. PLoS Biology *3*, e423.

Mohler, P.J., Davis, J.Q., Davis, L.H., Hoffman, J.A., Michaely, P., and Bennett, V. (2004a). Inositol 1,4,5-trisphosphate receptor localization and stability in neonatal cardiomyocytes requires interaction with ankyrin-B. J Biol Chem *279*, 12980-12987.

Mohler, P.J., Gramolini, A.O., and Bennett, V. (2002a). The ankyrin-B c-terminal domain determines activity of ankyrin-B/G chimeras in rescue of abnormal Inositol 1,4,5-trisphosphate and ryanodine receptor distribution in ankyrin-B (-/-) neonatal cardiomyocytes. J Biol Chem *277*, 10599-10607.

Mohler, P.J., Gramolini, A.O., and Bennett, V. (2002b). Ankyrins. J Cell Sci *115*, 1565-1566.

Mohler, P.J., Healy, J.A., Xue, H., Puca, A.A., Kline, C.F., Rand Allingham, R., Kranias, E.G., Rockman, H.A., and Bennett, V. (2007). Ankyrin-B Syndrome: enhanced cardiac function balanced by risk of cardiac death and premature senescence. PLoS ONE *2*, e1051.

Mohler, P.J., Hoffman, J.A., Davis, J.Q., Abdi, K.M., Kim, C.R., Jones, S.K., Davis, L.H., Roberts, K.F., and Bennett, V. (2004b). Isoform specificity among ankyrins: An amphipathic alpha-helix in the divergent regulatory domain of ankyrin-B interacts with the molecular co-chaperone Hdj1/Hsp40. J Biol Chem *279*, 25798-25804.

Mohler, P.J., Lowe, J.S., and Banks, S. (2005b). Dysfunction in ankyrin-based cellular pathways and human cardiac arrhythmia. Future Cardiology *1*, 363-371.

Mohler, P.J., Rivolta, I., Napolitano, C., LeMaillet, G., Lambert, S., Priori, S.G., and Bennett, V. (2004c). $Na_v1.5$ E1053K mutation causing Brugada syndrome blocks binding to ankyrin-G and expression of $Na_v1.5$ on the surface of cardiomyocytes. Proceedings of the National Academy of Sciences of the United States of America *101*, 17533-17538.

Mohler, P.J., Schott, J.J., Gramolini, A.O., Dilly, K.W., Guatimosim, S., duBell, W.H., Song, L.S., Haurogne, K., Kyndt, F., Ali, M.E.*, et al.* (2003). Ankyrin-B mutation causes type 4 long-QT cardiac arrhythmia and sudden cardiac death. Nature *421*, 634-639.

Mohler, P.J., Splawski, I., Napolitano, C., Bottelli, G., Sharpe, L., Timothy, K., Priori, S.G., Keating, M.T., and Bennett, V. (2004d). A cardiac arrhythmia syndrome caused by loss of ankyrin-B function. Proceedings of the National Academy of Sciences of the United States of America *101*, 9137-9142.

Mohler, P.J., and Wehrens, X.H.T. (2007). Mechanisms of human arrhythmia syndromes: Abnormal cardiac macromolecular interactions. Physiology *22*, 342-350.

Mohler, P.J., Yoon, W., and Bennett, V. (2004e). Ankyrin-B targets beta2-spectrin to an intracellular compartment in neonatal cardiomyocytes. J Biol Chem *279*, 40185-40193.

Morgans, C.W., and Kopito, R.R. (1993). Association of the brain anion exchanger, AE3, with the repeat domain of ankyrin. J Cell Sci *105*, 1137-1142.

Morrow, J.S., Cianci, C.D., Ardito, T., Mann, A.S., and Kashgarian, M. (1989). Ankyrin links fodrin to the alpha subunit of Na,K-ATPase in Madin-Darby canine kidney cells and in intact renal tubule cells. J Cell Biol *108*, 455-465.

Murray, K.T., Hu, N., Daw, J.R., Shin, H.-G., Watson, M.T., Mashburn, A.B., and George, A.L., Jr. (1997). Functional effects of Protein Kinase C activation on the human cardiac Na^+ channel. Circ Res *80*, 370-376.

Myers, K.R., and Casanova, J.E. (2008). Regulation of actin cytoskeleton dynamics by Arf-family GTPases. Trends in Cell Biology *18*, 184.

Napolitano, C., and Priori, S.G. (2006). Brugada syndrome. Orphanet J Rare Dis *1*, 35.

Nerbonne, J.M., and Kass, R.S. (2005). Molecular physiology of cardiac repolarization. Physiol Rev *85*, 1205-1253.

Ohtsuki, I., and Morimoto, S. (2008). Troponin: Regulatory function and disorders. Biochemical and Biophysical Research Communications *369*, 62.

Oxford, E.M., Everitt, M., Coombs, W., Fox, P.R., Kraus, M., Gelzer, A.R.M., Saffitz, J., Taffet, S.M., Moïse, N.S., and Delmar, M. (2007). Molecular composition of the intercalated disc in a spontaneous canine animal model of arrhythmogenic right ventricular dysplasia/cardiomyopathy. Heart Rhythm *4*, 1196.

Palygin, O.A., Pettus, J.M., and Shibata, E.F. (2008). Regulation of caveolar cardiac sodium current by a single $G_s$alpha histidine residue. Am J Physiol Heart Circ Physiol *294*, H1693-1699.

Pan, Z., Kao, T., Horvath, Z., Lemos, J., Sul, J.-Y., Cranstoun, S.D., Bennett, V., Scherer, S.S., and Cooper, E.C. (2006). A common ankyrin-G-based mechanism retains KCNQ and Na_v channels at electrically active domains of the axon. J Neurosci *26*, 2599-2613.

Papadatos, G.A., Wallerstein, P.M., Head, C.E., Ratcliff, R., Brady, P.A., Benndorf, K., Saumarez, R.C., Trezise, A.E., Huang, C.L., Vandenberg, J.I.*, et al.* (2002). Slowed conduction and ventricular tachycardia after targeted disruption of the cardiac sodium channel gene Scn5a. Proc Natl Acad Sci U S A *99*, 6210-6215.

Park, D.S., Woodman, S.E., Schubert, W., Cohen, A.W., Frank, P.G., Chandra, M., Shirani, J., Razani, B., Tang, B., Jelicks, L.A.*, et al.* (2002). Caveolin-1/3 double-knockout mice are viable, but lack both muscle and non-muscle caveolae, and develop a severe cardiomyopathic phenotype. Am J Pathol *160*, 2207-2217.

Perriard, J.-C., Hirschy, A., and Ehler, E. (2003). Dilated cardiomyopathy: A disease of the intercalated disc? Trends in Cardiovascular Medicine *13*, 30.

Peters, L.L., John, K.M., Lu, F.M., Eicher, E.M., Higgins, A., Yialamas, M., Turtzo, L.C., Otsuka, A.J., and Lux, S.E. (1995). Ank3 (epithelial ankyrin), a widely distributed new member of the ankyrin gene family and the major ankyrin in kidney, is expressed in alternatively spliced forms, including forms that lack the repeat domain. J Cell Biol *130*, 313-330.

Petty, M.A., and Lo, E.H. (2002). Junctional complexes of the blood-brain barrier: permeability changes in neuroinflammation. Progress in Neurobiology *68*, 311.

Plaster, N.M., Tawil, R., Tristani-Firouzi, M., Canún, S., Bendahhou, S., Tsunoda, A., Donaldson, M.R., Iannaccone, S.T., Brunt, E., Barohn, R.*, et al.* (2001). Mutations in $K_{ir}2.1$ cause the developmental and episodic electrical phenotypes of Andersen's Syndrome. Cell *105*, 511-519.

Pond, A.L., Scheve, B.K., Benedict, A.T., Petrecca, K., Van Wagoner, D.R., Shrier, A., and Nerbonne, J.M. (2000). Expression of distinct ERG proteins in rat, mouse, and human heart. Relation to functional I_{Kr} channels. J Biol Chem *275*, 5997-6006.

Priori, S.G., Bloise, R., and Crotti, L. (2001a). The long QT syndrome. Europace *3*, 16-27.

Priori, S.G., Napolitano, C., Gasparini, M., Pappone, C., Della Bella, P., Giordano, U., Bloise, R., Giustetto, C., De Nardis, R., Grillo, M.*, et al.* (2002). Natural history of Brugada syndrome: insights for risk stratification and management. Circulation *105*, 1342-1347.

Priori, S.G., Napolitano, C., Tiso, N., Memmi, M., Vignati, G., Bloise, R., Sorrentino, V., and Danieli, G.A. (2001b). Mutations in the cardiac ryanodine receptor gene (hRyR2) underlie catecholaminergic polymorphic ventricular tachycardia. Circulation *103*, 196-200.

Rasmussen, H.B., Frokjar-Jensen, C., Jensen, C.S., Jensen, H.S., Jorgensen, N.K., Misonou, H., Trimmer, J.S., Olesen, S.-P., and Schmitt, N. (2007). Requirement of subunit co-assembly and ankyrin-G for M-channel localization at the axon initial segment. J Cell Sci, jcs.03396.

Rasmussen, H.B., Moller, M., Knaus, H.-G., Jensen, B.S., Olesen, S.-P., and Jorgensen, N.K. (2004). Subcellular localization of the delayed rectifier K^+ channels KCNQ1 and ERG1 in the rat heart. Am J Physiol Heart Circ Physiol *286*, H1300-1309.

Roberts, E. (2006). GABAergic malfunction in the limbic system resulting from an aboriginal genetic defect in voltage-gated Na^+ channel SCN5A is proposed to give rise to susceptibility to schizophrenia. Advances in Pharmacology *54*, 119-145.

Roden, D.M., Balser, J.R., George Jr, A.L., and Anderson, M.E. (2002). Cardiac ion channels. Annual Review of Physiology *64*, 431-475.

Royer, A., van Veen, T.A.B., Le Bouter, S., Marionneau, C., Griol-Charhbili, V., Leoni, A.-L., Steenman, M., van Rijen, H.V.M., Demolombe, S., Goddard, C.A.*, et al.* (2005). Mouse model of SCN5A-linked hereditary Lenegre's disease: Age-related conduction slowing and myocardial fibrosis. Circulation *111*, 1738-1746.

Rubart, M., and Zipes, D.P. (2005). Mechanisms of sudden cardiac death. The Journal of Clinical Investigation *115*, 2305-2315.

Saffitz, J.E. (2005). The pathology of sudden cardiac death in patients with ischemic heart disease--arrhythmology for anatomic pathologists. Cardiovascular Pathology *14*, 195-203.

Sanchez-Ponce, D., Tapia, M., Muñoz, A., and Garrido, J.J. (2008). New role of IKK[alpha]/[beta] phosphorylated I[kappa]B[alpha] in axon outgrowth and axon initial segment development. Molecular and Cellular Neuroscience *37*, 832.

Sartore, S., Gorza, L., Pierobon Bormioli, S., Dalla Libera, L., and Schiaffino, S. (1981). Myosin types and fiber types in cardiac muscle. I. Ventricular myocardium. J Cell Biol *88*, 226-233.

Schafer, D.P., Custer, A.W., Shrager, P., and Rasband, M.N. (2006). Early events in node of Ranvier formation during myelination and remyelination in the PNS. Neuron Glia Biology *2*, 69-79.

Schott, J.J., Charpentier, F., Peltier, S., Foley, P., Drouin, E., Bouhour, J.B., Donnelly, P., Vergnaud, G., Bachner, L., Moisan, J.P.*, et al.* (1995). Mapping of a gene for long QT syndrome to chromosome 4q25-27. Am J Hum Genet *57*, 1114-1122.

Schram, G., Pourrier, M., Melnyk, P., and Nattel, S. (2002). Differential distribution of cardiac ion channel expression as a basis for regional specialization in electrical function. Circ Res *90*, 939-950.

Scriven, D.R.L., Dan, P., and Moore, E.D.W. (2000). Distribution of proteins implicated in excitation-contraction coupling in rat ventricular myocytes. Biophys J *79*, 2682-2691.

Seda, M., Pinto, F.M., Wray, S., Cintado, C.G., Noheda, P., Buschmann, H., and Candenas, L. (2007). Functional and molecular characterization of voltage-gated sodium channels in uteri from nonpregnant rats. Biol Reprod *77*, 855-863.

Sedgwick, S.G., and Smerdon, S.J. (1999). The ankyrin repeat: a diversity of interactions on a common structural framework. Trends in Biochemical Sciences *24*, 311.

Shirahata, E., Iwasaki, H., Takagi, M., Lin, C., Bennett, V., Okamura, Y., and Hayasaka, K. (2006). Ankyrin-G regulates inactivation gating of the neuronal sodium channel, $Na_v1.6$. J Neurophysiol *96*, 1347-1357.

Smith, T.K., Hager, H.A., Francis, R., Kilkenny, D.M., Lo, C.W., and Bader, D.M. (2008). Bves directly interacts with GEFT, and controls cell shape and movement through regulation of Rac1/Cdc42 activity. Proceedings of the National Academy of Sciences *105*, 8298-8303.

Splawski, I., Shen, J., Timothy, K.W., Lehmann, M.H., Priori, S., Robinson, J.L., Moss, A.J., Schwartz, P.J., Towbin, J.A., Vincent, G.M.*, et al.* (2000). Spectrum

of mutations in Long-QT Syndrome genes : KVLQT1, HERG, SCN5A, KCNE1, and KCNE2. Circulation *102*, 1178-1185.

Splawski, I., Timothy, K.W., Sharpe, L.M., Decher, N., Kumar, P., Bloise, R., Napolitano, C., Schwartz, P.J., Joseph, R.M., Condouris, K.*, et al.* (2004). $Ca_V1.2$ calcium channel dysfunction causes a multisystem disorder including arrhythmia and autism. Cell *119*, 19-31.

Srinivasan, Y., Elmer, L., Davis, J., Bennett, V., and Angelides, K. (1988). Ankyrin and spectrin associate with voltage-dependent sodium channels in brain. Nature *333*, 177.

Strege, P.R., Ou, Y., Sha, L., Rich, A., Gibbons, S.J., Szurszewski, J.H., Sarr, M.G., and Farrugia, G. (2003). Sodium current in human intestinal interstitial cells of Cajal. Am J Physiol Gastrointest Liver Physiol *285*, G1111-1121.

Sun, X.H., Protasi, F., Takahashi, M., Takeshima, H., Ferguson, D.G., and Franzini-Armstrong, C. (1995). Molecular architecture of membranes involved in excitation-contraction coupling of cardiac muscle. J Cell Biol *129*, 659-671.

Thevananther, S., Kolli, A.H., and Devarajan, P. (1998). Identification of a novel ankyrin isoform (AnkG190) in kidney and lung that associates with the plasma membrane and binds alpha -Na,K-ATPase. J Biol Chem *273*, 23952-23958.

Tombler, E., Cabanilla, N.J., Carman, P., Permaul, N., Hall, J.J., Richman, R.W., Lee, J., Rodriguez, J., Felsenfeld, D.P., Hennigan, R.F.*, et al.* (2006). G protein-induced trafficking of voltage-dependent calcium channels. J Biol Chem *281*, 1827-1839.

Tse, W.T., Lecomte, M.C., Costa, F.F., Garbarz, M., Feo, C., Boivin, P., Dhermy, D., and Forget, B.G. (1990). Point mutation in the beta-spectrin gene associated with alpha I/74 hereditary elliptocytosis. Implications for the mechanism of spectrin dimer self-association. Journal of Clinical Investigation *86*, 909-916.

Tse, W.T., Menninger, J.C., Yang-Feng, T.L., Francke, U., Sahr, K.E., Lux, S.E., Ward, D.C., and Forget, B.G. (1991). Isolation and chromosomal localization of a novel nonerythroid ankyrin gene. Genomics *10*, 858-866.

van Tintelen, J.P., Hofstra, R.M., Wiesfeld, A.C., van den Berg, M.P., Hauer, R.N., and Jongbloed, J.D. (2007). Molecular genetics of arrhythmogenic right ventricular cardiomyopathy: Emerging horizon? Current Opinion in Cardiology *22*, 185-192.

Wagner, S., Dybkova, N., Rasenack, E.C., Jacobshagen, C., Fabritz, L., Kirchhof, P., Maier, S.K., Zhang, T., Hasenfuss, G., Brown, J.H.*, et al.* (2006). Ca^{2+}/calmodulin-dependent protein kinase II regulates cardiac Na^+ channels. Journal of Clinical Investigation *116*, 3127-3138.

Wagner, S., and Maier, L.S. (2006). Modulation of cardiac Na^+ and Ca^{2+} currents by CaM and CaMKII. Journal of Cardiovascular Electrophysiology *17 Suppl 1*, S26-S33.

Wang, Q., Curran, M.E., Splawski, I., Burn, T.C., Millholland, J.M., VanRaay, T.J., Shen, J., Timothy, K.W., Vincent, G.M., de Jager, T.*, et al.* (1996). Positional cloning of a novel potassium channel gene: KVLQT1 mutations cause cardiac arrhythmias. Nat Genet *12*, 17.

Wang, Q., Shen, J., Splawski, I., Atkinson, D., Li, Z., Robinson, J.L., Moss, A.J., Towbin, J.A., and Keating, M.T. (1995). SCN5A mutations associated with an inherited cardiac arrhythmia, long QT syndrome. Cell *80*, 805 - 811.

Watanabe, H., Koopmann, T.T., Le Scouarnec, S., Yang, T., Ingram, C.R., Schott, J.J., Demolombe, S., Probst, V., Anselme, F., Escande, D.*, et al.* (2008). Sodium channel beta1 subunit mutations associated with Brugada syndrome and cardiac conduction disease in humans. Journal of Clinical Investigation *118*, 2260-2268.

Wedekind, H., Smits, J.P.P., Schulze-Bahr, E., Arnold, R., Veldkamp, M.W., Bajanowski, T., Borggrefe, M., Brinkmann, B., Warnecke, I., Funke, H.*, et al.* (2001). De Novo mutation in the SCN5A gene associated with early onset of sudden infant death. Circulation *104*, 1158-1164.

Westermann, M., Steiniger, F., and Richter, W. (2005). Belt-like localisation of caveolin in deep caveolae and its re-distribution after cholesterol depletion. Histochemistry and Cell Biology *123*, 613.

Wilde, A.A.M., and Priori, S.G. (2000). Brugada syndrome and sudden death. Eur Heart J *21*, 1483-.

Wood, S.J., and Slater, C.R. (1998). Beta-spectrin is colocalized with both voltage-gated sodium channels and ankyrin-G at the adult rat neuromuscular junction. J Cell Biol *140*, 675-684.

Wu, L., Yong, S.L., Fan, C., Ni, Y., Yoo, S., Zhang, T., Zhang, X., Obejero-Paz, C.A., Rho, H.-J., Ke, T.*, et al.* (2008). Identification of a new co-factor, MOG1, required for the full function of cardiac sodium channel $Na_v1.5$. J Biol Chem *283*, 6968-6978.

Wu, X., Zhang, T., Bossuyt, J., Li, X., McKinsey, T.A., Dedman, J.R., Olson, E.N., Chen, J., Brown, J.H., and Bers, D.M. (2006). Local $InsP_3$-dependent perinuclear Ca^{2+} signaling in cardiac myocyte excitation-transcription coupling. J Clin Invest *116*, 675-682.

Yu, F., and Catterall, W. (2003). Overview of the voltage-gated sodium channel family. Genome Biology *4*, 207.